

**UC Davis**

**UC Davis Electronic Theses and Dissertations**

**Title**

Functional Evaluation of Cell-Based Carriers for the Encapsulation, Targeted Delivery, Controlled Release and Biotransformation of Bioactives

**Permalink**

<https://escholarship.org/uc/item/9qt7g99j>

**Author**

Dou, Fang

**Publication Date**

2021

Peer reviewed|Thesis/dissertation

Functional Evaluation of Cell-Based Carriers for the Encapsulation, Targeted Delivery,  
Controlled Release and Biotransformation of Bioactives

By

FANG DOU  
DISSERTATION

Submitted in partial satisfaction of the requirements for the degree of

DOCTOR OF PHILOSOPHY

in

Food Science

in the

OFFICE OF GRADUATE STUDIES

of the

UNIVERSITY OF CALIFORNIA

DAVIS

Approved:

---

Nitin Nitin, Chair

---

Stephanie R. Dungan

---

Selina C. Wang

Committee in Charge

2021

## Acknowledgement

*The best moments in our lives ... usually occur if a person's body or mind is stretched to its limits in a voluntary effort to accomplish something difficult and worthwhile.*

*- Mihaly Csikszentmihalyi*

I would like to express great gratitude to my school, my mentors, friends and family who supported me through this journey and made completing my doctorate degree possible.

I would be remiss not to acknowledge University of California, Davis for all the support and fellowships that allowed me to learn and explore in the fields of my interest and for the opportunities that facilitated my professional and personal development.

I own my deepest appreciation to my advisor, Dr. Nitin Nitin. His vision, expertise and mentorship carried me through this journey of academic achievements and personal growth. Working with Dr. Nitin truly has been a pivotal experience that shaped my values and characters. Without his guidance, persistence, unwavering support and trust, this work would not exist.

I would like to thank Dr. Stephanie Dungan and Dr. Selina Wang for serving on my dissertation committee. Their prompt support and kind suggestions have enabled me to complete this dissertation as a piece of work that I will remain proud of for life.

My warmest thank you to my dearest Davis friends who made this journey colorful. Dr. Kang Huang, Dr. Maha Alshehab, Dr. Stephen Young and many others who have educated and supported me during my time in Davis and beyond.

Last but not least, I would like to thank my family with all my heart. I own everything I have, and I am to my mother and my father.

## Abstract

Microbial cells and the derivative structures have the potential to efficiently encapsulate, protect and controlled release a diversity of bioactive and liable compounds. The cell carriers with unique structural and compositional properties could potentially possess functional properties such as binding with target sites and transforming the compounds *in situ*. Whilst extensive studies have been carried out to develop synthetic and chemical encapsulation carriers, the natural microbial structures have had limited applications as microcarriers.

The primary goal of this study is to evaluate the encapsulation and delivery functionalities of cell carriers. Yeast cells, yeast cell wall particles (YCWPs) and bacterial cells were selected as model microcarriers. Encapsulation of model phenolic compounds was carried out using an established pressure-assisted technology. Overall, we hypothesize that the cell-based carriers are able to encapsulate and effectively protect diverse profiles of bioactive chemicals and bind to target delivery sites. In addition, live cells will transform the encapsulated compounds with the intrinsic metabolic activities and deliver the functional metabolites *in situ*.

In order to characterize the encapsulation and delivery of model bioactive compounds using cell carriers and explore their *ex-vivo* binding properties with target biological sites, yeast cells and YCWPs were applied as model microcarriers, and pathogenic biofilms and dermal tissue were used as model delivery sites. Scanning electron microscopy was employed to study the cell structural integrity after encapsulation. Confocal laser scanning microscopy and *in-vivo* fluorescence macro-imaging were applied to visualize the cellular localization of encapsulated substances and the binding affinity between the microcarrier and the target sites respectively. Quantitative understandings of the encapsulation efficiency, antimicrobial performance and

transdermal delivery were furthered with spectrophotometry coupled with microbiological protocols and HPLC analysis.

To understand the cell carriers' encapsulation of complex mixtures of compounds from crude materials, bacterial cells were selected as the model cell carrier to encapsulate phytochemicals from plant juices. Oxidative stability of encapsulated compounds under thermal treatment has also been monitored over time and measured using spectrophotometry.

In addition, this study also evaluated a novel delivery mechanism using live cell carriers. The viability and metabolomic response of cell carriers after encapsulation, transformation of the target compound and delivery of produced metabolites were elucidated using liquid chromatography coupled with tandem mass spectrometry.

The results of this study demonstrated that the cell carriers can bind to target cells and tissues such as pathogenic biofilms and skin surfaces, which facilitated the antimicrobial treatment and transdermal delivery of bioactive compounds. The microcarriers were able to encapsulate complex profiles of phenolic compounds and protect the compounds against degradation from heat and oxidation for an extended period of time. Moreover, live cell carriers were able to maintain viability after the encapsulation process and produce target metabolites from encapsulated compounds with deranged metabolic activities.

In summary, the results of this research demonstrated that cell-based carriers are a promising class of new emerging microencapsulation systems with a wide range of applications. Furthermore, the project was the first to investigate live cell carriers as an active encapsulation and delivery system that can transform target substances *in situ*. Future studies could further the development of novel cell-based encapsulation carriers with enhanced functionalities and target modifications leveraging the unique and intrinsic properties of microorganism.

# Chapter 1

## Introduction

### 1.1 Microencapsulation using cell-based carriers

#### 1.1.1 Definition encapsulation

Developed approximately 70 years ago, microencapsulation technology is a process that packages solid, liquid, or gaseous materials in micron-scale structures that can both contain the material and also release the content at a controlled rate under specific conditions (Desai and Park, 2005). The main objective of the encapsulation is often to protect the core or coated material from adverse conditions, such as oxygen, heat, pH, light, and moisture (Desai and Park, 2005; Shahidi and Han, 1993). Diverse classes of compounds including antioxidants, flavoring, coloring or aromatic agents, chemicals with undesirable flavors and nutraceuticals have been encapsulated as a core content in microparticles (Bernard F. Gibbs, 1999).

Microencapsulation techniques can be classified into two groups based on the type of carrier structures: (1) physical, chemical or physio-chemical methods that form the carrier structures during the encapsulation process (Ozkan et al., 2019); and (2) microencapsulation process that utilizes pre-formed cells and the derivative structures. In the first technique, the shell materials in the microparticles, also called coating or wall material, can be made of pure material or a mixture of sugars, gums, proteins, polysaccharides, lipoids and synthetic polymers (Fang and Bhandari, 2010). In the second method, pre-formed carriers such as cell-based microcapsules eliminate the structure formation process and can provide additional functionalities such as binding with target

delivery sites and biotransformation of encapsulated substances. These features can be advantageous for certain biomedical and food applications. The cell-based delivery systems will be further discussed in the following section.

## **1.1.2 Overview of cell-based encapsulation carriers**

### 1.1.2.1 Definition of cell-based carriers

Cell based encapsulation carriers can be defined as delivery systems that are based on cells and their derivative products, such as yeast and yeast cell wall particles (YCWPs) (Ciamponi et al., 2012; Dadkhodazade et al., 2018; Young et al., 2020), bacterial cells (Li et al., 2018) and mammalian cells including erythrocytes (a.k.a. red blood cells), stem cells and other cells and extracellular vesicles (Lanao et al., 2020; Li et al., 2018). These systems can be applied in diverse fields such as food and nutrition (Dadkhodazade et al., 2018), biomedicine (Lanao et al., 2020; Li et al., 2018), cosmetics, and antimicrobial treatments (Dou et al., 2021). Among others, microbial cell carriers have been considered as convenient and functional micro-vehicles for bioactive compounds due to their abundance, low production cost, and their structural and compositional versatility compared to synthetic particles and colloidal systems, as described in the following sections (Lipke and Ovalle, 1998; Paramera et al., 2011).

### 1.1.2.2 Yeast-cell based encapsulation carrier

#### 1.1.2.2.1 Introduction and applications

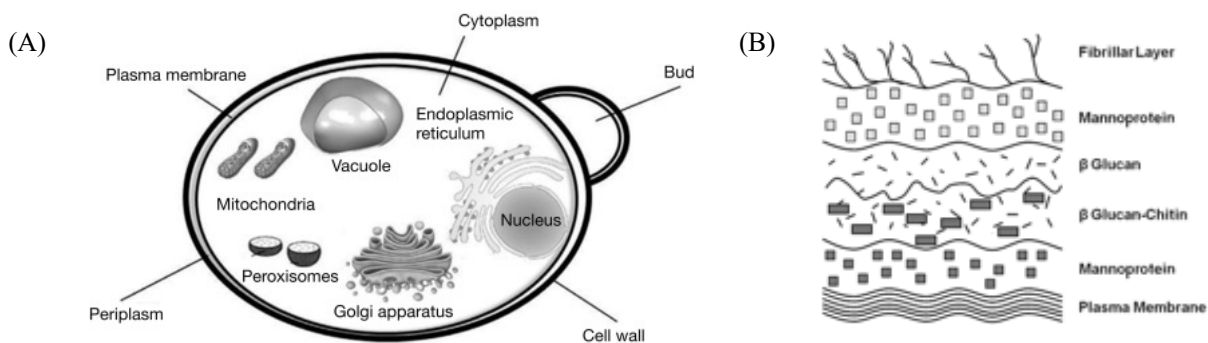


**Figure 1.1.** Schematic diagrams of (A) yeast cell (Tofalo and Suzzi, 2016), and (B) architecture of yeast cell wall (Stewart, 2017)

Yeasts are eukaryotic, single-celled microorganisms classified as members of the fungus kingdom. As one of the most thoroughly studied eukaryotic microorganisms, the yeast species *Saccharomyces cerevisiae* has been used for fermentation in baking and alcohol production for thousands of years (Legras et al., 2007). *S. cerevisiae*, also known as “baker’s yeast” is “generally recognized as safe” by the U.S. Food and Drug Administration as a food substance, and has been widely applied in food, medicine, cosmetics and agrochemical products. Besides its essential role in its native form, the yeast cell’s potential to function as a microcapsule for the encapsulation of phytochemicals and micronutrients has been evaluated in various studies including the encapsulation of 1) phenolics and other micronutrients, e.g. limonene (Errenst et al., 2021), resveratrol (Shi et al., 2008), curcumin (Young et al., 2017), and vitamin D<sub>3</sub> (Dadkhodazade et al., 2018); 2) hydrophobic animal and plant extracts, e.g. fish oil (Czerniak et al., 2015), and oregano essential oil (Dimopoulos et al., 2021); and 3) hydrophilic plant extracts and anthocyanins, e.g. *Hibiscus sabdariffa* (Nguyen et al., 2018). The yeast cell’s function as an excellent encapsulating wall material has been accredited to its physical structure and chemical properties, which will be discussed in the following section.



#### 1.1.2.2.2 Structural composition of cell wall and membrane

In *S. cerevisiae* cells, the cell wall makes up 15 to 30% of the dry weight of the cell (Orlean, 1997) and 25 to 50% of the volume (Lipke and Ovalle, 1998). The walls are mostly composed of mannoprotein, fibrous  $\beta$ -1,3-glucan, branched  $\beta$ -1,6-glucan, and a small amount of chitin.  $\beta$ -1,3-glucan-chitin complex forms the fibrous scaffold of the wall, and  $\beta$ -1,6-glucan links the components of the inner and outer walls (Lipke and Ovalle, 1998). On the outer surface of the wall are mannoproteins, which are extensively O and N glycosylated (Nobel et al., 1990). Chitin as a minor component contributes to the structural integrity of the wall (Nakhaee Moghadam et al., 2019) and insolubility of the fibers (Lipke and Ovalle, 1998). These components are covalently linked to form macromolecular complexes, which are assembled to form the intact wall (Orlean, 1997). The stoichiometry and molecular interactions between the components are yet to be comprehensively characterized.

The lattice-like cell wall structure played an important role both enabling and constraining the yeast-cell-based encapsulation process. The mechanical strength of the cellular structure enabled the carrier to stay intact through the process of encapsulation, storage and application (Young and Nitin, 2019). Furthermore, the stable structures better protected the encapsulated molecules from the environment such as heat, oxygen and UV radiation, as compared to structures that easily lapse during application. On the other hand, compounds needed to pass through the porous wall to get into the cell carrier. The yeast cell wall therefore restricted the transport and posed a physical barrier for encapsulation. For example, mannoproteins were shown to be densely packed and limited wall permeability (Nobel et al., 1990; Orlean, 1997). Therefore, the cell wall provided mechanical strength and protected the core compounds while constraining the size of the molecules that can diffuse freely into the cell.

The plasma membrane is a fluid bilayer structure composed mostly of phospholipids and ergosterols, which help separate the cytoplasm from the outside environment. It was proposed that acting as a liposome, the phospholipid membrane is the major permeability barrier for a target encapsulated molecule. (Paramera et al., 2011). The **cell envelope**, composed of the cell wall and plasma membrane, thus modulates the encapsulation process depending on the molecular size, shape and polarity of the target compounds (Bishop et al., 1998). Previous research has shown that substances with a molecular radius smaller than 0.81 nm or molecular weight lower than 620 Da could easily penetrate through the yeast cell wall and membrane of intact yeast cells (Scherrer et al., 1974). Other studies indicated that encapsulation yield will be higher when the molecular weight and octanol-water partition coefficients (log P value) were in the range 200–1000 g/mol and 2.0–6.0, respectively (Svenson, 2006).

While the mechanism of the encapsulation process has yet to be fully understood, researchers have hypothesized a process of four successive stages. (1) Compounds of varied hydrophobicity first coat and adsorb on the cell wall surface: the absorption of hydrophilic compounds has been observed in previous studies (Aksu, 2005), while hydrophobic compounds were proposed to form oil droplets and an “oily” layer on the yeast surface (Coradello and Tirelli, 2021). (2) Compounds permeate through the cell wall: this stage is often considered to be based on passive diffusions (Coradello and Tirelli, 2021) and as the rate-determining step of encapsulation (Stirke et al., 2019). (3) Compounds permeate through the cell membrane: the membrane acts as the “sink” that stabilizes the target compounds, and eventually loses integrity with increasing amount of incorporated compounds. (4) Other membranous structures in the yeast cytoplasm replace the cell membrane as the “sink” for the exogenous compounds. More experimental evidence is required to confirm the mechanistic hypothesis; however, the process could consist of absorption and permeation through the cell wall, followed by the insertion and disruption of

the cell membrane, which ultimately leads to the distribution of the encapsulated compounds within the cell (Coradello and Tirelli, 2021).

#### 1.1.2.2.3 Intracellular content

Naturally, the yeast cell contains a nucleus, vacuoles, mitochondria, the endoplasmic reticulum and a number of vesicular bodies to perform various physiological functions (Tofalo and Suzzi, 2016). As described in the previous section, the subcellular structures might help contain and stabilize the encapsulated compounds. For example, non-polar lipids including triacylglycerols and steryl esters are stored in so-called lipid particles as a biologically inert form for fatty acids and sterols in *S. cerevisiae* and other eukaryotes (Grillitsch et al., 2011). These lipid particles/droplets could act as natural reservoirs to associate with and accumulate hydrophobic compounds of interest intracellularly in the encapsulation process. Similarly, other subcellular structures including DNA, mitochondria and other lipid-membrane-based organelles have also shown affinity to bind a variety of bioactive compounds (Naoi et al., 2019; Sun et al., 2008).

In addition, yeast cells manage oxidative stress that resulted from metabolism or fermentation with several endogenous antioxidant systems. For instance, the naturally-occurring antioxidants in yeast might include superoxide dismutases, catalases and glutathione (Jakubowski, 2000), which have shown robust antioxidant capacity (Fakruddin et al., 2017) and thermal stability (Pradhan et al., 2000). These cellular constituents, therefore, could potentially help stabilize and protect liable molecules from oxidation during the encapsulation and application process.

#### 1.1.2.2.4 Yeast cell wall particles (YCWPs)

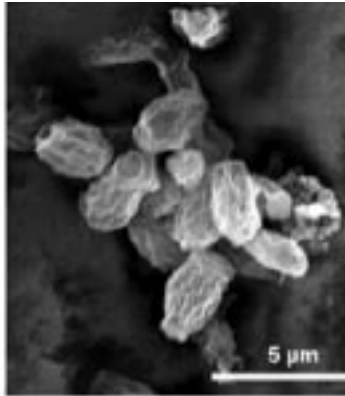


**Figure 1.2.** SEM image of freeze-dried YCWPs (Huang et al., 2019)

In addition to leveraging the natural form of the yeast cells, studies have suggested removing part of the cytosol to create voids that can be filled with encapsulated materials (Soto and Ostroff, 2008). Often these encapsulating materials require additional stabilizers to improve retention in YCWPs (Jakubowski, 2000). YCWPs are partially hollow microparticles that are derived from the cell walls of yeast cells. The particles retained the cross-linked  $\beta$ -glucan layer and other key cell wall components of the yeast cells such as chitin and protein (Li et al., 2020; Osumi, 1998). Specifically, YCWPs consist of two classes: glucan particles and glucan mannan particles. Preparation of the YCWPs require heating the yeast cells with concentrated base and acid followed by repeated washing cycles (suspending and centrifuging) (Soto and Ostroff, 2008). This chemically aggressive process is widely applied to remove the subcellular content in the yeast cell and might alter the natural properties of the yeast cell wall as the permeation barrier, which might in turn affect the encapsulation and release kinetics of the encapsulated compounds in the microcarrier (Young and Nitin, 2019).

### 1.1.2.3 Bacteria-based encapsulation carrier

#### 1.1.2.3.1 Introduction and applications

Bacteria constitute a large domain of prokaryotic microorganisms, inhabiting ubiquitously on earth in symbiotic and parasitic relationships with human beings. Over the past two decades, probiotic strains' health benefits transmitted through the gastrointestinal tract, such as immunomodulation, antagonistic and antimutagenic functionalities (Forestier et al., 2001; Lopez et al., 2008; Tiptiri-Kourpeti et al., 2016), have been increasingly uncovered with scientific research. Despite extensive research focused on the microorganism, limited studies in the current literature have looked into leveraging bacterial cells as a novel encapsulation carrier.

#### 1.1.2.3.2 Cellular structure

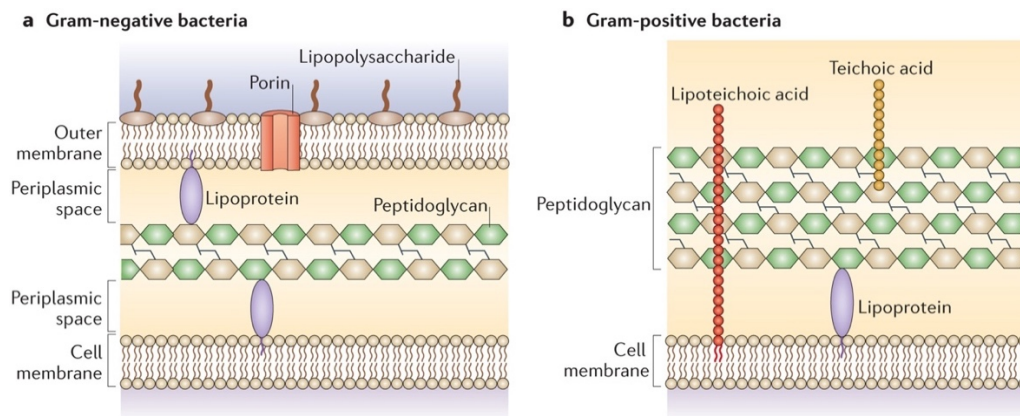


**Figure 1.3.** Cell wall structure of Gram-negative bacteria, Gram-positive bacteria  
(Brown et al., 2015)

Similar to the yeast cell, bacteria cells are also mechanically supported by the cell wall structure. The principal surface structure of both Gram-positive and Gram-negative bacteria is the cell wall peptidoglycans, which are highly cross-linked peptide chains in Gram-positive cells

and partially cross-linked in Gram-negative cells. Specifically, the cell wall of Gram-positive bacteria is mainly composed of a thick layer of peptidoglycan with other cell wall polymers attached, whereas Gram-negative bacteria is surrounded with a thin layer of peptidoglycan with an outer membrane structure composed of lipopolysaccharides (Salton and Kim, 1996). Located inside the cell wall, bacterial plasma membranes are primarily composed of proteins and phospholipids. Enclosed by the cell envelope, membrane-based vesicular structures and intracellular components are present in the cytoplasm (Salton and Kim, 1996).

Based on the current understanding of the yeast cell carrier, the presence of bacterial cell envelope and subcellular components indicate that bacteria could potentially be applied as a novel encapsulation carrier. Similarly with the yeast cells, bacteria possess intracellular content with antioxidant capacity such as glutathione and other lipid and protein components (Aguilar-Toalá et al., 2019), which would potentially protect encapsulated compounds against oxidation. Moreover, probiotic strains might provide additional health benefits from the probiotic carrier itself, as immense research has demonstrated *in-vitro* and *in-vivo* functionalities of active and inactivated probiotics (Forestier et al., 2001; Galdeano and Perdigón, 2006; Lopez et al., 2008). However, current understanding of bacterial microcarriers and the application of this microencapsulation system is limited. Further investigation into the physiochemical structure of the carriers and factors influencing the encapsulation process is still needed.

#### 1.1.2.4 Other cell-based carriers

In addition to microorganisms like yeast and bacteria, mammalian cells such as erythrocytes, stem cells and extracellular vesicles have also been used for encapsulation and drug delivery in a wide range of applications. These mammalian cells have many unique advantages for *in-vivo* injection, such as long life-span in circulation, targeted release, and natural membrane-binding properties (Sun et al., 2017; Weber et al., 2010). However, mass production of these carriers is

intrinsically limited by the availability of the source material (Sun et al., 2017). To overcome this program, synthetic materials that mimic the mammalian cells have been increasingly developed and might represent another direction for cell-based encapsulation carriers (Doshi et al., 2009; Lee et al., 2008; Yoo et al., 2011).

## **1.2 Methods of encapsulation into cell-based carriers**

### **1.2.1 Passive infusion**

The primary goal of microencapsulation in cell-based carriers is to allow actives to pass through the cell envelope and remain within the cell. Encapsulation techniques that are based on passive-diffusion have been widely applied due to its easy set-up and convenient procedures. The process typically involves mixing the aqueous suspension of the cells with the compounds of interest and incubating, usually with agitation and elevated temperature, for an extended period of time (i.e. hours). This process allows the compounds to partition into the cell barrier and into the intracellular compartments. The rate of permeation depends on the size, shape and polarity of the compounds as well as the microcapsule. It has been proposed that the size and shape of microcapsules are structurally optimal for diffusion of small molecules.

Additional permeability control on the capsules can be achieved by modifying the barrier properties of the cell envelope. For example, a pretreatment of the cells by autolysis or plasmolysis is commonly applied to increase yeast cell permeability, by disrupting the cell membrane and cell wall while the cell wall still retains the cellular shape. Plasmolysis is a process in which cells lose water and cell content in hypertonic solutions, which usually involves incubating cell carriers with a plasmolyzing agent such as NaCl or ethyl acetate (Czerniak et al., 2015). Other pretreatments include the use of surfactants and cell wall hydrolysis enzymes such as  $\beta$ -glucanase (Czerniak et al., 2015). These treatments have been shown to modify cell membrane fluidity and cell wall composition (Paramera et al., 2011), and as the result facilitate

the encapsulation process, increase the encapsulation rate, and affect the release kinetics for hydrophobic as well as hydrophilic compounds (Dimopoulos et al., 2021; Shi et al., 2007). The passive diffusion, however, is still limited by the required extended incubation time and heating, which is detrimental to heat liable bioactives and leads to suboptimal encapsulation results.

### **1.2.2 Non-thermal processes to increase cell permeability**

Several non-thermal processes have been applied to assist microencapsulation by increasing cell permeability (Dimopoulos et al., 2021). For instance, high pressure homogenization is commonly used for cell permeabilization. During the process, the pressure of the cell carrier suspension is raised up to 1000 bar and dispensed through a valve assembly to disrupt the cell structure and thereby increase cellular permeability (Kleinig and Middelberg, 1998, p. 1). Pulsed electric field (PEP) treatment is another process that can increase cellular permeability. During PEP treatment at a moderate electric field, the transmembrane potential of the cell membranes increases, and pores are formed on the membrane (Stirke et al., 2019)

To date, these permeabilization techniques have not been widely applied for encapsulation, and their improvements in the encapsulation efficiencies and impact on the release kinetics need to be thoroughly investigated. In addition, these techniques still involve elevated temperature or prolonged treatment, encapsulation and incubation process.

### **1.2.3 Vacuum infusion**

Applying vacuum infusion to assist encapsulation into cell carriers has recently emerged as a quick, efficient encapsulation technique. In this approach, cell carriers are mixed with the solution of interested compound(s), and the suspension would undergo vacuum treatment followed by incubation and washing steps to achieve infusion and remove excess compound. Specifically, cell carriers suspended in the solution of target compounds with a ratio of water and organic solvent are contained in vacuum bags and placed inside the vacuum chamber of a



commercial vacuum sealing machine. The machine lowers the pressure in the chamber to 99% vacuum (~1.0 kPa) and holds the low-pressure environment for 5 s before sealing the bag under the vacuum. The sealed samples are then be placed in dark at room temperature for 10 min to allow for incubation. Samples were then decanted into centrifuge tubes and washed by multiple cycles of centrifuge using organic solvent and ultrapurified water. (Dou et al., 2021; Huang et al., 2019; Young et al., 2017; Young and Nitin, 2019)

This rapid, non-thermal encapsulation process has shown to enhance encapsulation efficiency and yield in cell-based carriers when compared to traditional passive diffusion-based methods (Young et al., 2017). The exact mechanisms for its effectiveness have not been confirmed. It was proposed that the performance enhancement can be attributed to the rapid evaporation of the optimal solvent of the bioactive compound during the negative-pressure treatment, which leads to a concentration of the bioactives, and potentially expedites partitioning of the bioactives into the cells (Young et al., 2017). This research was primarily conducted with yeast cell carriers and YCWPs. The use of other microbial carriers such as bacterial cells has yet to be explored.

### **1.3 Characteristics of cell-based encapsulation systems**

#### **1.3.1 Encapsulation efficiency**

A high encapsulation efficiency is usually desirable with microencapsulation systems, and reflects the ability of a microencapsulation carrier in conjunction with the encapsulation technique to capture and load the carrier with target bioactive compounds. Encapsulation efficiency (EE, %) is usually defined as:

$$EE (\%) = \frac{C_E}{C_T} \times 100\%,$$

where  $C_E$  is the encapsulated content of the target compound(s) in the microcarriers, and  $C_T$  is the original content (total mass) of the target compound(s) in total before encapsulation. Factors

that affect encapsulation efficiencies for synthetic polymer-based carriers with chemical and/or physical methods have been summarized in the literature (Jyothi et al., 2010). For the cell-based encapsulation carriers, factors include the biochemical composition and structure of the cell carrier, hydrophobicity of the compounds and the encapsulation medium, and the parameters of the encapsulation process that might interact with and impact the loading efficiency. For example, it has been observed that with yeast-cell based encapsulation, EE of curcumin from a vacuum-based infusion process was three times of the EE of simple passive diffusion (Young et al., 2017). In that study, Young *et al.* also observed that differences in ethanol % in the encapsulation medium, vacuum pressure applied during encapsulation, and hydrophobicity of the compounds all led to different encapsulation efficacy. Specifically, the author proposed that the EE of the vacuum infusion technique is dependent on ethanol concentration, partition coefficient (influenced by the compound hydrophobicity), and the vacuum effects. The partition coefficient describes the equilibrium ratio of the concentration of compounds dissolved in one phase versus another. EE increased with an increase in ethanol concentration during passive diffusion, which was proposed to be a function of partition coefficient. When the yeast cell provides a more hydrophobic environment compared to the hydrophilic medium, hydrophobic compounds would partition into the yeast cells more favorably. However, the trend was different under vacuum infusion, which might be caused by the rapid evaporation of ethanol. Consistent with the theory discussed previously, Young *et al.* proposed that the evaporation increased the local concentration of bioactives on the cell surface, which might facilitate the absorption and permeation through the cell wall. This was confirmed based on the observation that a higher level of vacuum (i.e., lower pressure) led to higher EE.

### **1.3.2 Protection of the core compounds**

One of the most important objectives of the microencapsulation process is to conserve the functional properties of the target bioactive compounds from adverse environmental conditions. Past studies have indicated a protective effect of the cell-based carriers in limiting the oxidation of encapsulated bioactives, and its advantages in overcoming some of the limitations of synthetic chemical carriers that require the addition of exogenous antioxidants. For example, Young *et al.* compared thermal and oxidative stabilities of encapsulated curcumin in yeast cell carriers and YCWPs to that in Pickering emulsions, and confirmed that yeast cells and YCWPs provided higher oxidative and thermal stability respectively, to encapsulated curcumin (Young and Nitin, 2019). The author attributed protection of the encapsulated constituent from degradation to the cell structures, which include the cell wall and intracellular components with endogenous antioxidant capacity. As discussed in Section 1.2.3, bacteria share key structural features with yeast cells, and research has indicated the antioxidant properties of intracellular content of bacteria (Aguilar-Toalá *et al.*, 2019). These observations suggest the potential of bacterial carriers in protecting encapsulated bioactive. Different types of microcarriers and the protection they can provide against heat, oxidation and other adverse conditions could be further evaluated in the future.

### **1.3.3 Binding and targeted delivery**

Encapsulation carriers' ability to bind and interact with target tissue or cells is key to maximize target delivery of encapsulated bioactives. Pre-formed microcarriers, such as yeast, bacteria, or mammalian cells, naturally acquire unique mechanisms to bind with target tissue/cells, and this has led to a variety of bio-inspired and biomimetic carriers (Yoo *et al.*, 2011). For instance, the enhanced delivery of a chlorine-based sanitizer and inactivation of pathogenic biofilms was partially attributed to the high binding affinity of YCWPs with bacterial and fungal pathogens (Huang *et al.*, 2019). In this study, the efficiency of diverse microbes in binding YCWPs and

different components of YCWPs including  $\beta$ -1,3-d-glucan, chitin and mannan was tested. The results demonstrated that the binding affinity with YCWPs and YCWPs coated with the individual biochemical components varied among Gram positive bacteria, Gram negative bacteria, and fungal cells. In the antimicrobial treatment, the binding affinity between the sanitizers, microcarriers, and the target pathogenic cells, was shown to be favorable to improving the inactivation of pathogens in the biofilm. Future studies could be carried out to improve the binding efficiency of cell carriers for target delivery sites.

Other structures like bacterial ghosts (bacterial structure without cytoplasmic content), virus-based particles (reconstituted or self-assembled viral particles), eukaryotic cells and the mimetics have been widely applied for the delivery of drug, vaccine, DNA, and cancer-targeted therapy (Lubitz et al., 2009; Muzykantov, 2010; Roger et al., 2010; Waelti et al., 2002; Wu et al., 2009). Key attributes and challenges of the applications have been summarized by Yoo *et al* (2011). The summary reviewed applications that utilized the unique features of the natural carriers i.e. cell entry mechanism, antigenic components and physiochemical properties – that are yet to be fully understood or recognized (Yoo et al., 2011, p. 2). As a step ahead, more delivery systems could be developed to modify existing synthetic carriers (e.g. polymer-based capsules) and incorporate and leverage the natural binding and targeting mechanisms in a more controlled and appropriately designed system.

#### **1.3.4 Controlled release and bioavailability**

The ability to release encapsulated compounds at a controlled rate is another advantage that microencapsulation systems have to offer. This property becomes appealing when it is desirable to control the release rate of the retained compounds to match the needs of the application. The versatility and variety of microencapsulation carriers have enabled numerous applications. For example, slow, sustained release of pharmaceutical agents is usually optimal to eliminate potential

health hazards due to insufficient or excessive exposure of the delivered compounds (Birnbaum et al., 2000). Controlled release formulations using microcarriers are also applied in the food industry to retain aroma or flavor compounds for an extended period of time (Madene et al., 2006; Tari and Singhal, 2002). With polymer-based carriers, controlled release of the encapsulated content usually occurs through both diffusion and erosion as the polymer hydrolyzes (Göpferich, 1997; Langer and Peppas, 1983). The rate of release could therefore be controlled via the rate of degradation of the selected polymer matrix with appropriate physical characteristics (Birnbaum et al., 2000; Langer and Peppas, 1983). The release mechanism might be different for cell-based carriers. The natural carriers possess more complex structures with the presence of cell membrane, cell wall and subcellular components, as discussed above. The structural and chemical complexity of the carrier play an important role in controlling the release of the encapsulated content. By comparing the release profile of yeast cells and YCWPs, Young *et al.* observed that YCWPs with less intracellular content release the encapsulated content at a faster rate during simulated gastrointestinal digestion as compared to yeast cells (Young et al., 2020). It is also worth noting that the cell barrier remained intact with limited structural changes after the simulated digestion (Young et al., 2020), which might suggest that the encapsulated compounds were delivered mostly through diffusion.

Bioavailability is another key aspect for evaluating the effective delivery of microencapsulation processes. Bioavailability has been defined as the rate and extent to which the therapeutic moiety becomes available at the site of drug action for absorption, metabolism, tissue distribution, and bioactivity (Fernández-García et al., 2012). Bioaccessibility, which is often used interchangeably with bioavailability, is defined as the fraction of a compound that is released from its matrix in the gastrointestinal tract and thus becomes available for intestinal absorption (Benito and Miller, 1998). How microencapsulation technology could enhance bioavailability and/or

bioaccessibility of bioactives for a diversity of nutritional and therapeutic purposes has been extensively reviewed in the literature (Annunziata et al., 2020; Gómez-Mascaraque et al., 2017; Hartlieb et al., 2017; Soukoulis and Bohn, 2018). For instance, polyphenols' low water solubility and degradation that easily occurs in the gastrointestinal tract after ingestion limited the amount of compounds that could cross the intestinal barrier and release into the bloodstream (Ozkan et al., 2019). Microencapsulation, as one of the emerging solutions, has been found to be essential in stabilizing the compounds in various physiochemical conditions, protect the bioactives from rapid degradation and increase the water solubility, thus significantly improving the cellular uptake and absorption rate of polyphenols (Annunziata et al., 2020). Yeast-based carriers and the role of intracellular composition and cell barriers in moderating the bioaccessibility of phytochemicals in the process of gastrointestinal delivery have also been evaluated (Young et al., 2020). Further optimization of the absorption and consequent blood and tissue distribution of the target bioactives requires physio-chemical understanding of the delivery mechanism by which compounds are released and interact with the host cell, tissue, enzymes and/or microbiome through future studies.

### **1.3.5 Metabolism and biotransformation**

Another potential application of cell-based encapsulation that is yet to be explored in the literature is to leverage the innate metabolizing activities of the microbial carriers. In biomedical research, scientists have developed drug delivery strategies using recombinant bacteria, which are bacteria that are genetically modified to generate antigens and biologically active proteins *in situ* (Hanniffy et al., 2007; Yuvaraj et al., 2007). The difference with active encapsulation carriers is that functional compounds were produced as the metabolites of encapsulated compounds. A range of bioactive compounds, e.g. most phenolics, require a hydrolyzation and transformation process by intestinal enzymes and microbes to become bioavailable to the human host (D'Archivio et al., 2010; Kawabata et al., 2019). However, this transformation process is largely limited by the

complexity of the digestive process and the chances that the compound is released from the food matrix and becomes available to interact with the target tissue or symbiotic bacteria. Studies could be carried out to investigate encapsulation using live cell carriers so that the bioactives are physically combined with the capable bacteria or other cells. Further research could evaluate the potential of this approach to transform and deliver the active form of the target compounds *in situ*, besides protect the core compounds with the complex cell barriers and delivering them to the target sites with natural or modified binding properties.

#### **1.4 Current gaps in the knowledge for cell-based carriers**

As one of the most widely utilized natural microcarriers, yeast cells have been applied for microencapsulation across industries (Fang and Bhandari, 2010; Kavetsou et al., 2019; Nguyen et al., 2018; Normand et al., 2005). The low cost, robust cellular structure and versatility of the final products have made yeast cells very attractive for encapsulation of both hydrophobic and hydrophilic molecules (Dadkhodazade et al., 2021; Paramera et al., 2014). In addition, the pre-formed microcapsules dramatically simplified industrial production by eliminating the needs for additional material and procedures (Paramera et al., 2014). While extensive studies have shown that yeast cells are good carriers for a range of liable bioactive nutraceuticals, gaps in the knowledge of advanced cell-based encapsulation systems still exist.

Firstly, there is limited understanding of the delivery of core compounds in diverse biological environments. While current literature has demonstrated that yeast and its derivative microcarriers sustained release of core compounds (Dardelle et al., 2007) and protected the core against extreme environmental factors such as heat and radiation in simulated conditions (e.g. immersed in oil, water or solutions) (Dardelle et al., 2007; Shi et al., 2008; Young and Nitin, 2019), limited studies have focused on the release and delivery of target compounds with biological samples without excess liquid. The understanding of the delivery that is naturally

constrained by real-life conditions upon application is essential to further the development of cell-based carriers and optimize for target deliveries.

In addition, there is a lack of research on cell carriers besides eukaryotic structures. For instance, current literature has mostly focused on yeast cells, plasmolyzed yeast cells and/or YCWPs as the model carrier (Bishop et al., 1998; Coradello and Tirelli, 2021; Dadkhodazade et al., 2021; Nelson et al., 2006; Pham-Hoang et al., 2013), whereas bacteria cells that also possess complex cellular structure and functionalities have not been thoroughly investigated as microencapsulation carriers. In addition, purified chemicals are often used as the core compounds (Salari et al., 2015; Shi et al., 2008, 2007), which has limited application due to the high cost of the compound source. Encapsulation and characterization of complex profiles of phenolics from crude sources with natural and diverse carriers would massively facilitate industrial applications of the microencapsulation technology.

Besides the current lack of diversity in cell carriers and compound sources, the intrinsic functionalities of microbial carriers for encapsulation, target delivery and potential biotransformation of the core compounds have not been explored. Current applications have mostly focused on the loading and release efficiencies of the cell carrier (Dardelle et al., 2007; Nguyen et al., 2018; Paramera et al., 2011). Research has also theorized that the protection of core compounds is attributed to the barrier properties of natural cell structures (Coradello and Tirelli, 2021; Nakhaee Moghadam et al., 2019). Exploration of the other intrinsic characteristics of the microbial carriers and how these characteristics would potentially benefit the encapsulation and delivery processes is not currently available. For instance, further studies on the microcapsules' binding affinity with different delivery sites will enable target release and improve the delivery efficiency without requiring extensive and sophisticated modifications. Potential biotransformation of the core compounds will shed light on a generation of novel,



active cell carriers. Equipped with natural homing tendency to a target site (Yoo et al., 2011) and/or metabolic activities modulated by gene expression that could be selectively modified with modern bioengineering techniques, active cell carriers have the potential to achieve targeted delivery of bioactive substances with optimized efficacy.

## **1.5 Overview of dissertation study**

With the natural complexity and functional characteristics described in previous sections, cell carriers lend themselves to a broad range of applications as versatile encapsulation and delivery materials. The rest of the study focuses on the following applications: 1) delivery of antimicrobial agents in food or medical environments; 2) topical delivery of bioactive compounds into and across human skin; 3) encapsulation and protection of mixed plant phenolics from crude plant sources; and 4) encapsulation and biotransformation of target bioactives using live cell carriers. These applications aim to leverage cell carriers' intrinsic functionalities such as binding with target sites, controlled release and potential modification of carried compounds. In addition, these model systems enable research of cell carrier interactions with and their release profile in biological tissues, with minimal interferences from the environment. The listed applications lay the foundation for future studies that focus on more complex applications with the presence of additional biochemical or physical processes. Vacuum-assisted infusion was applied throughout this study. This encapsulation approach was selected based on the enhanced encapsulation efficiency with cell-based carriers and the low-energy, rapid process. Prior study that compared the performance of vacuum infusion with conventional passive diffusion has shown that the vacuum technique, which takes 5 min and is followed by a 10-min incubation, increased encapsulation efficiency by 100%-200% when compared to the 24-hr passive diffusion. Encapsulation parameters were chosen based on the

same study, which optimized the encapsulation conditions for encapsulation efficiency of phenolic compounds.

The overall hypothesis of the study is that cell-based encapsulation carriers will encapsulate and protect complex profiles of phytochemicals, bind to the target cells and control the release of encapsulated compounds. In addition, live cell carriers will also transform the encapsulated compounds and release their metabolites. The following objectives were designated to test the hypotheses.

- **Objective 1:** Characterize encapsulation of a model bioactive in yeast cells and yeast derived cell-based carriers and evaluate *ex-vivo* binding properties of these cell-based carriers with model biological targets. In this aim, microbial biofilms and skin tissue will be used as model systems;
- **Objective 2:** Determine the bacterial cell carrier's capacity for encapsulating complex profile of polyphenols from crude plant sources and the efficacy in protecting the encapsulated bioactive compounds against thermal treatments;
- **Objective 3:** Evaluate *in-vitro* modification and release of encapsulated polyphenolic compounds by live bacterial cell carriers.

In summary, this dissertation evaluated functional properties of cell-based encapsulation carriers in a diversity of applications. Chapter 2 and Chapter 3 evaluated the encapsulation and binding properties of yeast cell carriers as they apply to biofilm inactivation and transdermal bioactive delivery. Chapter 4 examined bacterial carriers' potential of encapsulating a complex profile of phytochemicals from crude plant sources and improving the stability of bioactives during thermal treatments. Chapter 5 characterized the live cell carrier's encapsulation and

transformation of the target compounds. Chapter 6 provided a brief summary of conclusions and recommendations for future research.

## Reference

- Aguilar-Toalá, J.E., Estrada-Montoya, M.C., Liceaga, A.M., Garcia, H.S., González-Aguilar, G.A., Vallejo-Cordoba, B., González-Córdova, A.F., Hernández-Mendoza, A., 2019. An insight on antioxidant properties of the intracellular content of *Lactobacillus casei* CRL-431. *LWT* 102, 58–63. <https://doi.org/10.1016/j.lwt.2018.12.015>
- Aksu, Z., 2005. Application of biosorption for the removal of organic pollutants: a review. *Process Biochemistry* 40, 997–1026. <https://doi.org/10.1016/j.procbio.2004.04.008>
- Annunziata, G., Jiménez-García, M., Capó, X., Moranta, D., Arnone, A., Tenore, G.C., Sureda, A., Tejada, S., 2020. Microencapsulation as a tool to counteract the typical low bioavailability of polyphenols in the management of diabetes. *Food and Chemical Toxicology* 139, 111248. <https://doi.org/10.1016/j.fct.2020.111248>
- Benito, P., Miller, D., 1998. Iron absorption and bioavailability: An updated review. *Nutrition Research* 18, 581–603. [https://doi.org/10.1016/S0271-5317\(98\)00044-X](https://doi.org/10.1016/S0271-5317(98)00044-X)
- Bernard F. Gibbs, C.N.M., Selim Kermasha, Inteaz Alli, 1999. Encapsulation in the food industry: a review. *International Journal of Food Sciences and Nutrition* 50, 213–224. <https://doi.org/10.1080/096374899101256>
- Birnbaum, D.T., Kosmala, J.D., Henthorn, D.B., Brannon-Peppas, L., 2000. Controlled release of  $\beta$ -estradiol from PLAGA microparticles:: The effect of organic phase solvent on encapsulation and release. *Journal of Controlled Release* 65, 375–387. [https://doi.org/10.1016/S0168-3659\(99\)00219-9](https://doi.org/10.1016/S0168-3659(99)00219-9)

- Bishop, J.R.P., Nelson, G., Lamb, J., 1998. Microencapsulation in yeast cells. *Journal of Microencapsulation* 15, 761–773. <https://doi.org/10.3109/02652049809008259>
- Brown, L., Wolf, J.M., Prados-Rosales, R., Casadevall, A., 2015. Through the wall: extracellular vesicles in Gram-positive bacteria, mycobacteria and fungi. *Nat Rev Microbiol* 13, 620–630. <https://doi.org/10.1038/nrmicro3480>
- Ciamponi, F., Duckham, C., Tirelli, N., 2012. Yeast cells as microcapsules. Analytical tools and process variables in the encapsulation of hydrophobes in *S. cerevisiae*. *Applied Microbiology and Biotechnology* 95, 1445–1456. <https://doi.org/10.1007/s00253-012-4127-8>
- Coradello, G., Tirelli, N., 2021. Yeast Cells in Microencapsulation. General Features and Controlling Factors of the Encapsulation Process. *Molecules* 26, 3123. <https://doi.org/10.3390/molecules26113123>
- Czerniak, A., Kubiak, P., Białas, W., Jankowski, T., 2015. Improvement of oxidative stability of menhaden fish oil by microencapsulation within biocapsules formed of yeast cells. *Journal of Food Engineering, Food Science and Technology for a Sustainable Bioeconomy \_ ISEKI\_Food* 2014 167, 2–11. <https://doi.org/10.1016/j.jfoodeng.2015.01.002>
- Dadkhodazade, E., Khanniri, E., Khorshidian, N., Hosseini, S.M., Mortazavian, A.M., Kia, E.M., 2021. Yeast cells for encapsulation of bioactive compounds in food products: A review. *Biotechnology Progress* 37, e3138. <https://doi.org/10.1002/btpr.3138>
- Dadkhodazade, E., Mohammadi, A., Shojaee-Aliabadi, S., Mortazavian, A.M., Mirmoghtadaie, L., Hosseini, S.M., 2018. Yeast Cell Microcapsules as a Novel Carrier for Cholecalciferol Encapsulation: Development, Characterization and Release Properties. *Food Biophysics* 13, 404–411. <https://doi.org/10.1007/s11483-018-9546-3>

- D'Archivio, M., Filesi, C., Vari, R., Scazzocchio, B., Masella, R., 2010. Bioavailability of the Polyphenols: Status and Controversies. *International Journal of Molecular Sciences* 11, 1321–1342. <https://doi.org/10.3390/ijms11041321>
- Dardelle, G., Normand, V., Steenhoudt, M., Bouquerand, P.-E., Chevalier, M., Baumgartner, P., 2007. Flavour-encapsulation and flavour-release performances of a commercial yeast-based delivery system. *Food Hydrocolloids, Food Colloids* 2006 21, 953–960. <https://doi.org/10.1016/j.foodhyd.2006.12.013>
- Desai, K.G.H., Park, H.J., 2005. Recent Developments in Microencapsulation of Food Ingredients. *Drying Technology* 23, 1361–1394. <https://doi.org/10.1081/DRT-200063478>
- Dimopoulos, G., Katsimichas, A., Tsimogiannis, D., Oreopoulou, V., Taoukis, P., 2021. Cell permeabilization processes for improved encapsulation of oregano essential oil in yeast cells. *Journal of Food Engineering* 294, 110408. <https://doi.org/10.1016/j.jfoodeng.2020.110408>
- Doshi, N., Zahr, A.S., Bhaskar, S., Lahann, J., Mitragotri, S., 2009. Red blood cell-mimicking synthetic biomaterial particles. *PNAS* 106, 21495–21499. <https://doi.org/10.1073/pnas.0907127106>
- Dou, F., Huang, K., Nitin, N., 2021. Targeted Photodynamic Treatment of Bacterial Biofilms Using Curcumin Encapsulated in Cells and Cell Wall Particles. *ACS Appl. Bio Mater.* 4, 514–522. <https://doi.org/10.1021/acsabm.0c01051>
- Errenst, C., Petermann, M., Kilzer, A., 2021. Encapsulation of limonene in yeast cells using the concentrated powder form technology. *The Journal of Supercritical Fluids* 168, 105076. <https://doi.org/10.1016/j.supflu.2020.105076>

- Fakruddin, Md., Hossain, Md.N., Ahmed, M.M., 2017. Antimicrobial and antioxidant activities of *Saccharomyces cerevisiae* IFST062013, a potential probiotic. *BMC Complementary and Alternative Medicine* 17, 64. <https://doi.org/10.1186/s12906-017-1591-9>
- Fang, Z., Bhandari, B., 2010. Encapsulation of polyphenols – a review. *Trends in Food Science & Technology* 21, 510–523. <https://doi.org/10.1016/j.tifs.2010.08.003>
- Fernández-García, E., Carvajal-Lérida, I., Jarén-Galán, M., Garrido-Fernández, J., Pérez-Gálvez, A., Hornero-Méndez, D., 2012. Carotenoids bioavailability from foods: From plant pigments to efficient biological activities. *Food Research International, Functional Foods and Nutraceuticals* 46, 438–450. <https://doi.org/10.1016/j.foodres.2011.06.007>
- Forestier, C., De Champs, C., Vatoux, C., Joly, B., 2001. Probiotic activities of *Lactobacillus casei rhamnosus*: in vitro adherence to intestinal cells and antimicrobial properties. *Research in Microbiology* 152, 167–173. [https://doi.org/10.1016/S0923-2508\(01\)01188-3](https://doi.org/10.1016/S0923-2508(01)01188-3)
- Galdeano, C.M., Perdigón, G., 2006. The Probiotic Bacterium *Lactobacillus casei* Induces Activation of the Gut Mucosal Immune System through Innate Immunity. *Clinical and Vaccine Immunology* 13, 219–226. <https://doi.org/10.1128/CVI.13.2.219-226.2006>
- Gómez-Mascaraque, L.G., Casagrande Sipoli, C., de La Torre, L.G., López-Rubio, A., 2017. Microencapsulation structures based on protein-coated liposomes obtained through electrospraying for the stabilization and improved bioaccessibility of curcumin. *Food Chemistry* 233, 343–350. <https://doi.org/10.1016/j.foodchem.2017.04.133>
- Göpferich, A., 1997. Polymer Bulk Erosion. *Macromolecules* 30, 2598–2604. <https://doi.org/10.1021/ma961627y>
- Grillitsch, K., Connerth, M., Köfeler, H., Arrey, T.N., Rietschel, B., Wagner, B., Karas, M., Daum, G., 2011. Lipid particles/droplets of the yeast *Saccharomyces cerevisiae* revisited:

- Lipidome meets Proteome. *Biochimica et Biophysica Acta (BBA) - Molecular and Cell Biology of Lipids* 1811, 1165–1176. <https://doi.org/10.1016/j.bbalip.2011.07.015>
- Hanniffy, S.B., Carter, A.T., Hitchin, E., Wells, J.M., 2007. Mucosal Delivery of a Pneumococcal Vaccine Using *Lactococcus lactis* Affords Protection against Respiratory Infection. *The Journal of Infectious Diseases* 195, 185–193. <https://doi.org/10.1086/509807>
- Hartlieb, K.J., Ferris, D.P., Holcroft, J.M., Kandela, I., Stern, C.L., Nassar, M.S., Botros, Y.Y., Stoddart, J.F., 2017. Encapsulation of Ibuprofen in CD-MOF and Related Bioavailability Studies. *Mol. Pharmaceutics* 14, 1831–1839. <https://doi.org/10.1021/acs.molpharmaceut.7b00168>
- Huang, K., Dou, F., Nitin, N., 2019. Biobased Sanitizer Delivery System for Improved Sanitation of Bacterial and Fungal Biofilms. *ACS Appl. Mater. Interfaces*. <https://doi.org/10.1021/acsami.9b02428>
- Jakubowski, W., 2000. 2,7-DICHLOROFLUORESCIN OXIDATION AND REACTIVE OXYGEN SPECIES: WHAT DOES IT MEASURE? *Cell Biology International* 24, 757–760. <https://doi.org/10.1006/cbir.2000.0556>
- Jyothi, N.V.N., Prasanna, P.M., Sakarkar, S.N., Prabha, K.S., Ramaiah, P.S., Srawan, G.Y., 2010. Microencapsulation techniques, factors influencing encapsulation efficiency. *Journal of Microencapsulation* 27, 187–197. <https://doi.org/10.3109/02652040903131301>
- Kavetsou, E., Koutsoukos, S., Daferera, D., Polissiou, M.G., Karagiannis, D., Perdakis, D.Ch., Detsi, A., 2019. Encapsulation of *Mentha pulegium* Essential Oil in Yeast Cell Microcarriers: An Approach to Environmentally Friendly Pesticides. *J. Agric. Food Chem.* 67, 4746–4753. <https://doi.org/10.1021/acs.jafc.8b05149>

- Kawabata, K., Yoshioka, Y., Terao, J., 2019. Role of Intestinal Microbiota in the Bioavailability and Physiological Functions of Dietary Polyphenols. *Molecules* 24, 370.  
<https://doi.org/10.3390/molecules24020370>
- Kleinig, A.R., Middelberg, A.P.J., 1998. On the mechanism of microbial cell disruption in high-pressure homogenisation. *Chemical Engineering Science* 53, 891–898.  
[https://doi.org/10.1016/S0009-2509\(97\)00414-4](https://doi.org/10.1016/S0009-2509(97)00414-4)
- Lanao, J.M., Gutiérrez-Millán, C., Colino, C.I., 2020. Cell-Based Drug Delivery Platforms. *Pharmaceutics* 13, 2. <https://doi.org/10.3390/pharmaceutics13010002>
- Langer, R., Peppas, N., 1983. Chemical and Physical Structure of Polymers as Carriers for Controlled Release of Bioactive Agents: A Review. *Journal of Macromolecular Science, Part C* 23, 61–126. <https://doi.org/10.1080/07366578308079439>
- Lee, E.S., Kim, D., Youn, Y.S., Oh, K.T., Bae, Y.H., 2008. A virus-mimetic nanogel vehicle. *Angew Chem Int Ed Engl* 47, 2418–2421. <https://doi.org/10.1002/anie.200704121>
- Legras, J.-L., Merdinoglu, D., Cornuet, J.-M., Karst, F., 2007. Bread, beer and wine: *Saccharomyces cerevisiae* diversity reflects human history. *Molecular Ecology* 16, 2091–2102. <https://doi.org/10.1111/j.1365-294X.2007.03266.x>
- Li, T., Dong, H., Zhang, C., Mo, R., 2018. Cell-based drug delivery systems for biomedical applications. *Nano Res.* 11, 5240–5257. <https://doi.org/10.1007/s12274-018-2179-5>
- Li, W., Wang, H., Xu, X.G., Yu, Y., 2020. Simultaneous Nanoscale Imaging of Chemical and Architectural Heterogeneity on Yeast Cell Wall Particles. *Langmuir* 36, 6169–6177.  
<https://doi.org/10.1021/acs.langmuir.0c00627>
- Lipke, P.N., Ovalle, R., 1998. Cell Wall Architecture in Yeast: New Structure and New Challenges. *Journal of Bacteriology* 180, 3735–3740.  
<https://doi.org/10.1128/JB.180.15.3735-3740.1998>



- Lopez, M., Li, N., Kataria, J., Russell, M., Neu, J., 2008. Live and Ultraviolet-Inactivated Lactobacillus Rhamnosus GG Decrease Flagellin-Induced Interleukin-8 Production in Caco-2 Cells. *The Journal of Nutrition* 138, 2264–2268.  
<https://doi.org/10.3945/jn.108.093658>
- Lubitz, P., Mayr, U.B., Lubitz, W., 2009. Applications of Bacterial Ghosts in Biomedicine, in: MD, C.A.G., FAHA, G.Z.F.M., MSc (Eds.), *Pharmaceutical Biotechnology, Advances in Experimental Medicine and Biology*. Springer New York, pp. 159–170.  
[https://doi.org/10.1007/978-1-4419-1132-2\\_12](https://doi.org/10.1007/978-1-4419-1132-2_12)
- Madene, A., Jacquot, M., Scher, J., Desobry, S., 2006. Flavour encapsulation and controlled release – a review. *International Journal of Food Science & Technology* 41, 1–21.  
<https://doi.org/10.1111/j.1365-2621.2005.00980.x>
- Muzykantov, V.R., 2010. Drug delivery by red blood cells: vascular carriers designed by Mother Nature. *Expert Opin Drug Deliv* 7, 403–427.  
<https://doi.org/10.1517/17425241003610633>
- Nakhaee Moghadam, M., Khameneh, B., Fazly Bazzaz, B.S., 2019. Saccharomyces cerevisiae as an Efficient Carrier for Delivery of Bioactives: a Review. *Food Biophysics* 14, 346–353.  
<https://doi.org/10.1007/s11483-019-09584-0>
- Naoi, M., Wu, Y., Shamoto-Nagai, M., Maruyama, W., 2019. Mitochondria in Neuroprotection by Phytochemicals: Bioactive Polyphenols Modulate Mitochondrial Apoptosis System, Function and Structure. *Int J Mol Sci* 20. <https://doi.org/10.3390/ijms20102451>
- Nelson, G., Duckham, S.C., Crothers, M.E.D., 2006. Microencapsulation in Yeast Cells and Applications in Drug Delivery, in: Svenson, S. (Ed.), *Polymeric Drug Delivery I*. American Chemical Society, Washington, DC, pp. 268–281. <https://doi.org/10.1021/bk-2006-0923.ch019>

- Nguyen, T.-T., Phan-Thi, H., Pham-Hoang, B.-N., Ho, P.-T., Tran, T.T.T., Waché, Y., 2018. Encapsulation of Hibiscus sabdariffa L. anthocyanins as natural colours in yeast. *Food Research International* 107, 275–280. <https://doi.org/10.1016/j.foodres.2018.02.044>
- Nobel, J.G.D., Klis, F.M., Priem, J., Munnik, T., Ende, H.V.D., 1990. The glucanase-soluble mannoproteins limit cell wall porosity in *Saccharomyces cerevisiae*. *Yeast* 6, 491–499. <https://doi.org/10.1002/yea.320060606>
- Normand, V., Dardelle, G., Bouquerand, P.-E., Nicolas, L., Johnston, D.J., 2005. Flavor Encapsulation in Yeasts: Limonene Used as a Model System for Characterization of the Release Mechanism. *J. Agric. Food Chem.* 53, 7532–7543. <https://doi.org/10.1021/jf0507893>
- Orlean, P., 1997. Biogenesis of Yeast Wall and Surface Components. *Cold Spring Harbor Monograph Archive* 21, 229–362. <https://doi.org/10.1101/0.229-362>
- Osumi, M., 1998. The ultrastructure of yeast: Cell wall structure and formation. *Micron* 29, 207–233. [https://doi.org/10.1016/S0968-4328\(97\)00072-3](https://doi.org/10.1016/S0968-4328(97)00072-3)
- Ozkan, G., Franco, P., De Marco, I., Xiao, J., Capanoglu, E., 2019. A review of microencapsulation methods for food antioxidants: Principles, advantages, drawbacks and applications. *Food Chemistry* 272, 494–506. <https://doi.org/10.1016/j.foodchem.2018.07.205>
- Paramera, E.I., Karathanos, V.T., Konteles, S.J., 2014. Chapter 23 - Yeast Cells and Yeast-Based Materials for Microencapsulation, in: Gaonkar, A.G., Vasisht, N., Khare, A.R., Sobel, R. (Eds.), *Microencapsulation in the Food Industry*. Academic Press, San Diego, pp. 267–281. <https://doi.org/10.1016/B978-0-12-404568-2.00023-6>

- Paramera, E.I., Konteles, S.J., Karathanos, V.T., 2011. Microencapsulation of curcumin in cells of *Saccharomyces cerevisiae*. *Food Chemistry* 125, 892–902.  
<https://doi.org/10.1016/j.foodchem.2010.09.063>
- Pham-Hoang, B.N., Romero-Guido, C., Phan-Thi, H., Waché, Y., 2013. Encapsulation in a natural, preformed, multi-component and complex capsule: yeast cells. *Appl Microbiol Biotechnol* 97, 6635–6645. <https://doi.org/10.1007/s00253-013-5044-1>
- Pradhan, A.A., Rhee, K.S., Hernández, P., 2000. Stability of catalase and its potential role in lipid oxidation in meat. *Meat Science* 54, 385–390. [https://doi.org/10.1016/S0309-1740\(99\)00114-X](https://doi.org/10.1016/S0309-1740(99)00114-X)
- Roger, M., Clavreul, A., Venier-Julienne, M.-C., Passirani, C., Sindji, L., Schiller, P., Montero-Menei, C., Menei, P., 2010. Mesenchymal stem cells as cellular vehicles for delivery of nanoparticles to brain tumors. *Biomaterials* 31, 8393–8401.  
<https://doi.org/10.1016/j.biomaterials.2010.07.048>
- Salari, R., Rajabi, O., Khashyarmanesh, Z., Fathi Najafi, M., Fazly Bazzaz, B.S., 2015. Characterization of Encapsulated Berberine in Yeast Cells of *Saccharomyces cerevisiae*. *Iran J Pharm Res* 14, 1247–1256.
- Salton, M.R.J., Kim, K.-S., 1996. Structure, in: Baron, S. (Ed.), *Medical Microbiology*. University of Texas Medical Branch at Galveston, Galveston (TX).
- Scherrer, R., Loudon, L., Gerhardt, P., 1974. Porosity of the Yeast Cell Wall and Membrane. *J Bacteriol* 118, 534–540.
- Shahidi, F., Han, X.-Q., 1993. Encapsulation of food ingredients. *Critical Reviews in Food Science and Nutrition* 33, 501–547. <https://doi.org/10.1080/10408399309527645>

- Shi, G., Rao, L., Yu, H., Xiang, H., Pen, G., Long, S., Yang, C., 2007. Yeast-cell-based microencapsulation of chlorogenic acid as a water-soluble antioxidant. *Journal of Food Engineering* 80, 1060–1067. <https://doi.org/10.1016/j.jfoodeng.2006.06.038>
- Shi, G., Rao, L., Yu, H., Xiang, H., Yang, H., Ji, R., 2008. Stabilization and encapsulation of photosensitive resveratrol within yeast cell. *International Journal of Pharmaceutics* 349, 83–93. <https://doi.org/10.1016/j.ijpharm.2007.07.044>
- Soto, E.R., Ostroff, G.R., 2008. Characterization of Multilayered Nanoparticles Encapsulated in Yeast Cell Wall Particles for DNA Delivery. *Bioconjugate Chem.* 19, 840–848. <https://doi.org/10.1021/bc700329p>
- Soukoulis, C., Bohn, T., 2018. A comprehensive overview on the micro- and nano-technological encapsulation advances for enhancing the chemical stability and bioavailability of carotenoids. *Critical Reviews in Food Science and Nutrition* 58, 1–36. <https://doi.org/10.1080/10408398.2014.971353>
- Stewart, G.G., 2017. The Structure and Function of the Yeast Cell Wall, Plasma Membrane and Periplasm, in: Stewart, G.G. (Ed.), *Brewing and Distilling Yeasts*, *The Yeast Handbook*. Springer International Publishing, Cham, pp. 55–75. [https://doi.org/10.1007/978-3-319-69126-8\\_5](https://doi.org/10.1007/978-3-319-69126-8_5)
- Stirke, A., Celiesiute-Germaniene, R., Zimkus, A., Zurauskiene, N., Simonis, P., Dervinis, A., Ramanavicius, A., Balevicius, S., 2019. The link between yeast cell wall porosity and plasma membrane permeability after PEF treatment. *Sci Rep* 9, 14731. <https://doi.org/10.1038/s41598-019-51184-y>
- Sun, Y., Lee, C.-C., Hung, W.-C., Chen, F.-Y., Lee, M.-T., Huang, H.W., 2008. The Bound States of Amphipathic Drugs in Lipid Bilayers: Study of Curcumin. *Biophysical Journal* 95, 2318–2324. <https://doi.org/10.1529/biophysj.108.133736>

- Sun, Y., Su, J., Liu, G., Chen, J., Zhang, X., Zhang, R., Jiang, M., Qiu, M., 2017. Advances of blood cell-based drug delivery systems. *European Journal of Pharmaceutical Sciences* 96, 115–128. <https://doi.org/10.1016/j.ejps.2016.07.021>
- Svenson, S. (Ed.), 2006. *Polymeric Drug Delivery I: Particulate Drug Carriers*, ACS Symposium Series. American Chemical Society, Washington, DC. <https://doi.org/10.1021/bk-2006-0923>
- Tari, T.A., Singhal, R.S., 2002. Starch based spherical aggregates: reconfirmation of the role of amylose on the stability of a model flavouring compound, vanillin. *Carbohydrate Polymers* 50, 279–282. [https://doi.org/10.1016/S0144-8617\(02\)00033-4](https://doi.org/10.1016/S0144-8617(02)00033-4)
- Tiptiri-Kourpeti, A., Spyridopoulou, K., Santarmaki, V., Aindelis, G., Tompoulidou, E., Lamprianidou, E.E., Saxami, G., Ypsilantis, P., Lampri, E.S., Simopoulos, C., Kotsianidis, I., Galanis, A., Kourkoutas, Y., Dimitrellou, D., Chlichlia, K., 2016. *Lactobacillus casei* Exerts Anti-Proliferative Effects Accompanied by Apoptotic Cell Death and Up-Regulation of TRAIL in Colon Carcinoma Cells. *PLOS ONE* 11, e0147960. <https://doi.org/10.1371/journal.pone.0147960>
- Tofalo, R., Suzzi, G., 2016. Yeasts, in: Caballero, B., Finglas, P.M., Toldrá, F. (Eds.), *Encyclopedia of Food and Health*. Academic Press, Oxford, pp. 593–599. <https://doi.org/10.1016/B978-0-12-384947-2.00762-5>
- Waelti, E., Wegmann, N., Schwaninger, R., Wetterwald, A., Wingenfeld, C., Rothen-Rutishauser, B., Gimmi, C.D., 2002. Targeting HER-2/neu with Antirat Neu Virosomes for Cancer Therapy. *Cancer Res* 62, 437–444.
- Weber, C., Pohl, S., Poertner, R., Pino-Grace, P., Freimark, D., Wallrapp, C., Geigle, P., Czermak, P., 2010. Production Process for Stem Cell Based Therapeutic Implants: Expansion of the Production Cell Line and Cultivation of Encapsulated Cells, in: Kasper,

- C., van Griensven, M., Pörtner, R. (Eds.), *Bioreactor Systems for Tissue Engineering II: Strategies for the Expansion and Directed Differentiation of Stem Cells*, *Advances in Biochemical Engineering / Biotechnology*. Springer, Berlin, Heidelberg, pp. 143–162.  
[https://doi.org/10.1007/10\\_2009\\_25](https://doi.org/10.1007/10_2009_25)
- Wu, W., Hsiao, S.C., Carrico, Z.M., Francis, M.B., 2009. Genome-Free Viral Capsids as Multivalent Carriers for Taxol Delivery. *Angewandte Chemie International Edition* 48, 9493–9497. <https://doi.org/10.1002/anie.200902426>
- Yoo, J.-W., Irvine, D.J., Discher, D.E., Mitragotri, S., 2011. Bio-inspired, bioengineered and biomimetic drug delivery carriers. *Nat Rev Drug Discov* 10, 521–535.  
<https://doi.org/10.1038/nrd3499>
- Young, S., Dea, S., Nitin, N., 2017. Vacuum facilitated infusion of bioactives into yeast microcarriers: Evaluation of a novel encapsulation approach. *Food Research International* 100, 100–112. <https://doi.org/10.1016/j.foodres.2017.07.067>
- Young, S., Nitin, N., 2019. Thermal and oxidative stability of curcumin encapsulated in yeast microcarriers. *Food Chemistry* 275, 1–7. <https://doi.org/10.1016/j.foodchem.2018.08.121>
- Young, S., Rai, R., Nitin, N., 2020. Bioaccessibility of curcumin encapsulated in yeast cells and yeast cell wall particles. *Food Chemistry* 309, 125700.  
<https://doi.org/10.1016/j.foodchem.2019.125700>
- Yuvaraj, S., Peppelenbosch, M.P., Bos, N.A., 2007. Transgenic probiotica as drug delivery systems: the golden bullet? *Expert Opinion on Drug Delivery* 4, 1–3.  
<https://doi.org/10.1517/17425247.4.1.1>

## Chapter 2

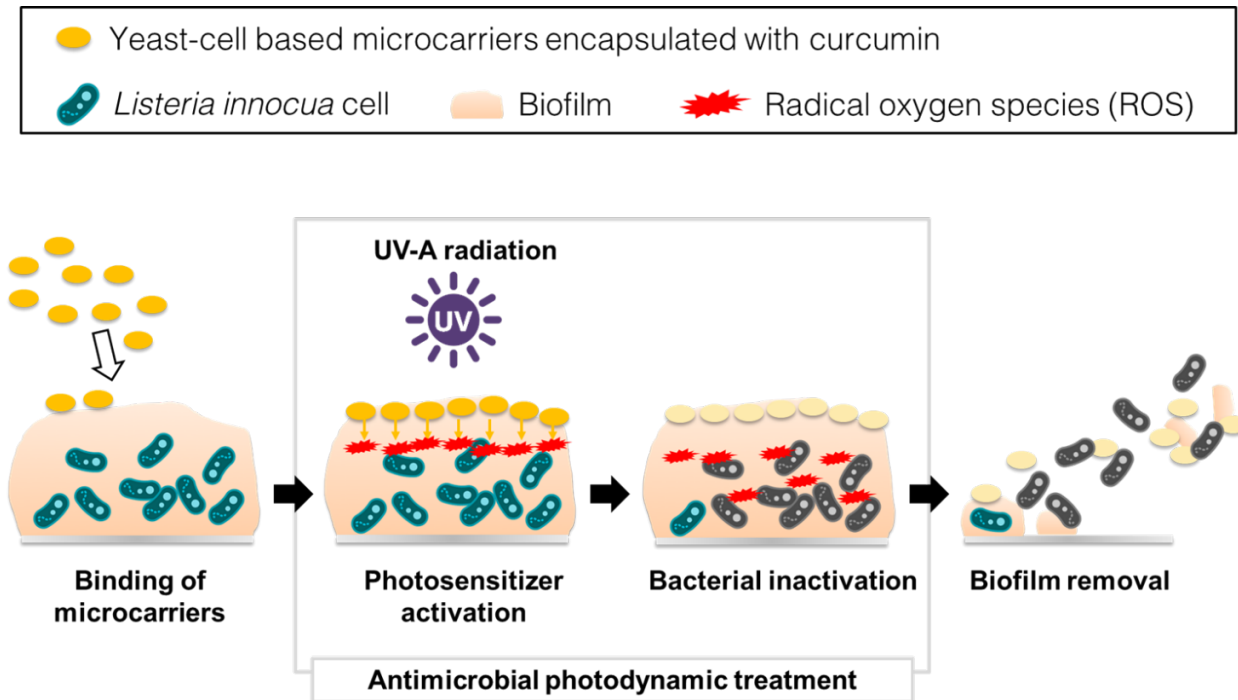
# Targeted Photodynamic Treatment of Bacterial Biofilms using Curcumin Encapsulated in Cells and Cell Wall Particles

### Abstract

Efficient inactivation and removal of pathogenic biofilms in food and biomedical environments remain a significant challenge for the food safety applications and medical facilities. This research aims to develop food-grade microcarriers for the targeted delivery of the photosensitizer, curcumin and photodynamic inactivation of a model pathogenic bacterial biofilm. The microcarriers evaluated in this study include alive yeast cell carriers (aYC), deactivated yeast cell carriers (dYC), and yeast cell wall particles (YCWP). The microcarriers were evaluated based on encapsulation yield of a model photosensitizer (curcumin), binding of the microcarriers to biofilms and inactivation of the bacteria in the biofilms. The results illustrate that the combination of binding affinity, encapsulation yield and the intracellular composition of the microcarriers influenced the overall inactivation of bacteria in the biofilms. All the selected compositions achieved more than 93% inactivation of the bacteria in the biofilm using the photodynamic treatment and the yeast cell wall particles with curcumin achieved over 99% inactivation of the bacteria in the biofilm matrix. In addition, all the selected compositions demonstrated significant potential to remove biofilm from the plastic surface suggesting the role of binding affinity of the microcarriers in removal of

the biofilm from surfaces. Overall, this study advances the development of biomaterial formulations for targeted photodynamic inactivation and potential removal of biofilms.

### Graphical Abstract





## 2.1. Introduction

Biofilms are a major problem in the food industry and medical facilities (Paz-Méndez et al., 2017; Vogeleer et al., 2016). It is well recognized that bacterial biofilms exhibit higher resistance to antimicrobial treatments than planktonic cells (Lemos et al., 2011; Simões et al., 2006). This resistance results due to both biological and physico-chemical factors. The biological factors include prevalence and spread of antimicrobial resistance in biofilms. The physico-chemical factors include restrictive transport of antimicrobials in the exopolysaccharide matrix and the presence of organic and abiotic compounds in the food-contact environment. Together these biological and physico-chemical factors can decrease efficacy of antimicrobials and thus contribute to enhanced antimicrobial resistance of biofilms. Therefore, inactivation and elimination of pathogenic biofilms in food-contact and biomedical environments remains a key issue for the food industry and medical facilities.

In order to deactivate pathogenic biofilms, various anti-biofilm strategies have been evaluated. Current approaches include: 1) chemical disinfectants (e.g. chlorine-based compounds(Taylor et al., 2000), ozone(Bialoszewski et al., 2011; Taylor et al., 2000), hydrogen peroxide(Lin et al., 2011), chelating agents and surfactants(Chen and Stewart, 2000)); 2) physical removal of biofilms (e.g. plasma(Lee et al., 2009), high hydrostatic pressure(Smith and Oliver, 1991), shear stress(Gião and Keevil, 2013), and ultrasound(Baumann et al., 2009)); and 3) biological treatments (e.g. bacteriocins(Mathur et al., 2018), bacteriophages(Soothill, 2013) and enzymes(Johansen et al., 1997)). Although some of these approaches are used in the food industry and medical facilities to inactivate and remove biofilms from contact surfaces, there is an unmet need to address some of the key limitations in these processes. Major limitations include: 1) rapid quenching kinetics(Daly et al., 1998), lack of effectiveness in the presence of organic compounds(Vandekinderen et al.,

2009), and health-adverse effects of chemical disinfectants(Winder, 2001); 2) deterred diffusion of chemical and biological agents, such as chlorine, phage and the produced enzymes, due to the extracellular polymeric substance (EPS) barrier(Behnke et al., 2011; González et al., 2018); 3) inefficiency of the physical destruction methods, especially for the inactivation of endospores and cell residues(Faille et al., 2014).

Synergistic antimicrobial approaches are being developed with superior disinfection efficiency compared to these conventional approaches while preventing antimicrobial resistance(Cheesman et al., 2017). Among these approaches, antimicrobial photodynamic therapy (aPDT), also known as photodynamic inactivation or photodynamic antimicrobial chemotherapy, has shown potential to efficiently inactivate antibiotic-resistant bacteria and biofilms(Lee et al., 2017). The principle mechanism for the aPDT is based on synergy between a photosensitizer and light energy at appropriate wavelength. The synergistic reaction produces reactive oxygen species (ROS) in the presence of molecular oxygen, increases the intracellular oxidative stress in microorganisms and results in eventual microbial cell death(Biel et al., 2011). aPDT offers many advantages including rapid reaction, broad-spectrum activities, and potential avoidance of antibiotic-resistance development(Biel et al., 2011; Jori et al., 2006). However, the application of this approach is still limited due to regulated use of common photosensitizers such as methylene blue with potential cancer-causing properties. Furthermore, many of the common photosensitizers, such as toluidine blue O, methylene blue and hypericin, are hydrophobic and require additional formulations for their dispersal in aqueous environments(Sibani et al., 2008). Encapsulation systems such as nanostructures are commonly used for dispersing PDT agents in aqueous environments and increasing photochemical efficiency by preventing aggregation of PDT agents(Schwartz et al., 2009). Nonetheless, most of the PDT agents and the nanoparticles are not approved for use in a

food environment. The high cost and sophisticated preparation procedures of these nano-scale formulations also limit the mass production and industrial penetration of such technologies for surface sanitation.

In this study we evaluated the efficacy of the PDT treatment for inactivation of a model biofilm using curcumin encapsulated yeast cell based microcarriers. Curcumin is a polyphenol found on Turmeric (*Curcuma longa*) rhizomes that has been widely used in the food industry as a natural colorant. Prior research has demonstrated effectiveness of curcumin as a photosensitizer for the inactivation of planktonic bacteria and surface attached bacteria (Hegge et al., 2012; Lee et al., 2017). Despite promising results, there are significant limitations and challenges. These challenges result due to limited solubility of curcumin in aqueous environment, lack of affinity of curcumin and conventional encapsulation systems for curcumin to bind biofilms, and limited hydrolytic stability of curcumin. To address these challenges, this study evaluates the use of cell-based carriers as an encapsulation and delivery system for curcumin aPDT of biofilms. The cell-based carriers selected in this study include yeast cells (YC), including alive yeast cell carrier (aYC) and deactivated yeast cell carrier (dYC), and yeast cell wall particles (YCWP.) Yeast microcarrier and its derivatives are widely-accepted encapsulation matrix for food applications based on their “generally recognizes as safe” (GRAS) status (Pham-Hoang et al., 2018; Salari et al., 2015; Shi et al., 2008). YC and YCWP possess high encapsulation yield for polyphenolic compounds such as curcumin and significantly enhance physico-chemical stability as demonstrated in the literature and our recent studies (Soto et al., 2010; Young et al., 2017). Moreover, fungal-bacterial binding interactions are found ubiquitously in the environment and particularly in biofilms (Adam et al., 2002; Millsap et al., 1998; Shirtliff et al., 2009). Therefore, based on this background knowledge, this study evaluated the role of these diverse cell carrier compositions derived from yeast cells for

the encapsulation of curcumin, binding of cell carrier compositions to biofilms, their efficacy in inactivation of bacteria in the selected biofilm model and influence on the structure of the biofilm after treatment with the selected compositions. *Listeria innocua* (ATCC 33090) was selected as a non-pathogenic surrogate for the foodborne pathogen *Listeria monocytogenes*, which is a serious concern for the food industry based on its ubiquitous presence in the environment and biofilm-forming ability (Colagiorgi et al., 2017). In summary, the results of this study will illustrate the potential of cell-based GRAS encapsulation compositions for aPDT treatment of biofilms, including binding of cell carrier compositions to biofilms as well as their potential to deliver a model photosensitizer compound to biofilms.

## **2.2. Material and Method**

### **2.2.1 Preparation of YCWP and YC**

Three different yeast-based microcarriers were used in this study. Yeast cells were prepared by suspending 0.5g of commercial baker's yeast (Fleischmann's Active Dry Yeast) in 3.25 ml of phosphate buffered saline (PBS, Fisher BioReagents). Deactivated yeast cells were prepared by heat inactivation of yeast cells at 97°C for 30 min. Following the inactivation, a viability reduction of 2.3 log cfu/ml was confirmed by plate counting. Yeast cell wall particles were prepared according to a previously reported hydrolysis protocol. (Soto and Ostroff, 2008) Briefly, baker's yeast was suspended and heated in 1 M NaOH at 80°C for 1 hr and then in acidic solution with pH 4 - 5 at 55°C for 1 hr. Then the insoluble residue was washed with water (1 time), isopropanol (4 times) and acetone (2 times). The resulting slurry was dried under vacuum at room temperature overnight to obtain the YCWP powder. The obtained YCWP consists mainly of yeast cell wall glucan and a minor fraction of cell wall mannans (Soto and Ostroff, 2008). Prior to each

experiment, YCWP and active YC powder were washed twice with Milli-Q water and the pellet was collected by centrifuge at 4,400 rpm for 5 min.

### **2.2.2 Encapsulation of curcumin in YCWP and YC and their characterization**

To encapsulate curcumin in cell-based carriers, 0.5 g of the wet pellet was suspended in a 5 ml solution that consists of 65% PBS and 35% ethanolic solution of curcumin (2.5 mg/ml). Control samples were prepared by using 35% ethanol instead. Encapsulation was carried out by using a patented pressure-facilitated infusion approach (Young et al., 2017). After the encapsulation, the cell pellet was washed using Milli-Q water for three times or until no curcumin was detected from the supernatant.

Curcumin in the encapsulated YCWP and YC was extracted using methanol with bead beating at 6.0 m/s, 40 s for 3 cycles (FastPrep-24™ 5G Instrument, MP Biomedicals). The curcumin content was quantified using the UV-Vis spectrometry (Genesys™ 10 UV-Vis Spectrophotometer, Thermo Scientific) at 425nm. Encapsulation efficiency was calculated based on the curcumin content encapsulated in cell carriers measured using the spectroscopy and curcumin's initial concentration. The equation is shown below:

$$\text{Encapsulation efficiency} = \frac{\text{Curcumin content in the cell carriers}}{\text{Initial curcumin content used for encapsulation}} \times 100\%$$

The intracellular localization of curcumin in cell carriers were also visualized using confocal laser scanning microscopy (CLSM). Images were acquired in triplicates using with a Leica TCS SP8 STED 3X confocal microscope. The auto-fluorescence of curcumin was captured using an excitation laser at 488/15 nm, an emission detection from 498-591 nm using a band pass filter and a 100x oil immersion objective. Images were captured using the software Leica Application Suite X Version 13. Scale bars were added to the images by using the software ImageJ64.

### **2.2.3 Bacteria strain and biofilm formation**

To evaluate efficacy of the curcumin encapsulation system for the inactivation of *Listeria* biofilm, a rifampin-resistant *Listeria innocua* (ATCC 33090; ATCC, Manassas, VA, USA) provided by Trevor Suslow's laboratory (University of California, Davis) was selected as a surrogate for a human pathogen, *Listeria monocytogenes*. A single colony was picked from an agar plate, cultured in a 10 ml tryptic soy broth (TSB), and the suspension was incubated with a constant shaking rate (150 rpm) at 37°C overnight. (Cossu et al., 2017) Bacteria culture was used for the following experiments after it reached an absorbance of 1.5 AU at 600 nm, which corresponds approximately to  $1 \times 10^9$  CFU/ml.

Biofilms were grown in a sterile 24-well surface-treated polystyrene plate (Corning, Corning, NY, USA). Volumes of 0.1 mL of the *L. innocua* overnight culture and 0.9 mL of the 1X M9 medium with minimal salts (Sigma-Aldrich, St. Louis, MO, USA), supplemented with 0.4% glucose (Fisher Scientific, Hampton, NH, USA) and 0.4% tryptone (Sigma-Aldrich, St. Louis, MO, USA), were added to each well. The plate was then incubated at room temperature for 72 hr. Before performing the biofilm inactivation assay, the medium in each well was discarded, and the wells were gently washed with 1 ml sterile phosphate-buffered saline (PBS) (United States Biological Co. Ltd., Cleveland, OH, USA) three times in order to remove planktonic cells.

#### **2.2.4 Quantification of cell carrier binding on biofilm**

YCWP and YC were stained with Calcofluor white dye (Sigma-Aldrich, St. Louis, MO, USA) using a constant shaking rate of 100 rpm at room temperature for 1 hr. The cells were washed with sterile PBS twice after staining, and then suspended in PBS at a concentration of 0.1 g/ml. One milliliter of stained cell carrier suspension was added to each well. After incubation with biofilm for 1 hour, the unbound cell carriers were removed with pipette and the wells were gently washed twice with PBS. The fluorescence intensity of the carriers adhered on the biofilm was determined

using a fluorescence plate reader (SpectraMax® M5 Microplate Reader System, Molecular Devices Corporation) with an excitation/emission at 350/440 nm. The fluorescence data was normalized to the total fluorescent signal for the stained cell carriers used for the initial incubation with the biofilm.

### **2.2.5 Biofilm inactivation assay with curcumin encapsulation systems and UV-A treatment**

The ability of encapsulated cell carriers to inactivate biofilm bacteria was assessed by inactivation of *Listeria* cells in a biofilm model. Encapsulated cell carriers were suspended in sterile PBS at a concentration of 0.1g/ml and incubated with biofilm samples in a 24 well plastic plate for 1 hr. The biofilms incubated with PBS for 1 hour were used as a control group. After incubation, the biofilm samples were gently washed with PBS to remove excess cell carriers. To demonstrate efficacy of using a combination of UV-A and curcumin-encapsulated microcarriers for the inactivation of biofilm bacteria, 200 µl PBS was added to each well in order to prevent biofilms from drying. Then the biofilms after incubation with cell carriers or PBS were exposed to UV-A for 30 min. The average light intensity of the UV-A lamp was  $4.8 \pm 0.1$  mW/cm<sup>2</sup>. As a comparison group, biofilms after the same treatments were kept in the dark for 30 min. After treatment, the residual PBS was removed from each well.

After treatments, the viability of the biofilm was evaluated using the standard plate counting method. Bacterial cells from the biofilm samples were recovered from the plastic plate by adding 1 ml of sterile maximum recovery buffer supplemented with 0.1% v/v Tween-20. The plate was vortexed vigorously for 30 sec and then treated using a bath sonication device (Branson 2510 Ultrasonic Cleaner, Branson Ultrasonics Corp., Danbury, CT, USA) for 2 min. The plates were sealed with sterile parafilm to prevent leaking of the recovery buffer. Quantification of viable bacteria recovered from biofilm was performed by serial dilution, spread plating on TSA agar

plates and incubating at 37°C for 24 hr. Control groups for this experiment include 1) biofilms incubated in PBS with/without UV-A treatment; 2) biofilms incubated with cell carriers without curcumin, with or without UV-A; and 3) biofilms incubated with curcumin-encapsulated cell carriers and without UV-A. The enzymatic activity of the cells after treatment were evaluated by the resazurin metabolism assay. After UV-A treatment, 1 ml of resazurin solution (50  $\mu$ M in M9 medium) was added to each well and the curves of resazurin reduction were monitored using a microplate reader (TECAN SpectraFluor Plus Microplate Reader, Tecan Group Ltd., Switzerland) for 14 hr with an excitation/emission at 530/580 nm. In this assay, the fluorescence signal is produced by the reduction of resazurin to resorufin based on the enzymatic activity of microbes (Mariscal et al., 2009; Van den Driessche et al., 2014). The time required to reach the peak fluorescence signal indicates the population of viable and metabolically active cells. Control groups for this experiment include biofilms incubated with only PBS buffer without antibacterial treatment (used to indicate normal growth of the biofilm sample, data not shown in the following figures) and biofilms incubated with PBS and treated with UV-A light (PBS).

### **2.2.6 SEM imaging**

The binding of cell carriers to biofilms and the changes in morphology of biofilms after treatment was visualized using scanning electron microscopy (SEM). For SEM imaging, the biofilms were fixed using a 4% glutaraldehyde solution in PBS (pH 7.4  $\pm$  0.1) at 4°C for 3-4 hours and washed once using milliQ water. The biofilm samples were then mounted onto aluminum stubs with a carbon conductive adhesive tape, and sputter coated with 10 nm of gold deposits. Electron microscopy was performed using a Philips XL-30 electron microscope at 5 kV accelerating voltage.

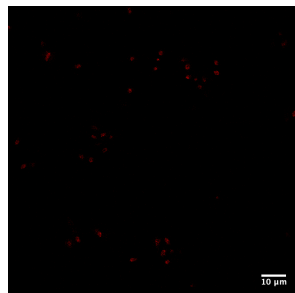
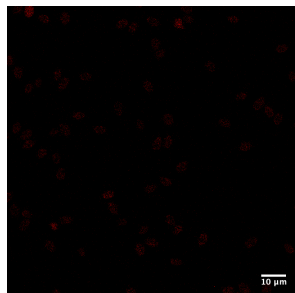
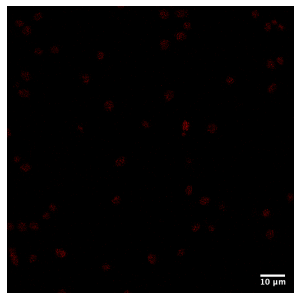
### **2.2.7 Statistical analysis**



Statistical analysis was performed using the GraphPad Prism software V.7.0a (Graphpad Software, Inc., La Jolla, CA). All experiments were performed in triplicate. The significant differences between treatments for each type of cell carriers were determined based on one-way ANOVA with the significance level at  $p < 0.05$ . Pairwise comparison was conducted through Tukey's Test with the significance level at  $p < 0.01$ .

## 2.3. Result and Discussion

### 2.3.1 Encapsulation yields of curcumin in yeast cell and YCWP carriers

Encapsulation content and efficiency			
Curcumin	YCWP	aYC	dYC
mg curcumin/ml suspension (0.1g yeast cell carriers on wet basis/ml Milli-Q water)	$0.41 \pm 0.010$	$0.70 \pm 0.010$	$0.83 \pm 0.04$
Encapsulation efficiency	18%	31%	37%
Representative confocal images			
Control groups: cell carriers <u>without</u> encapsulated curcumin			

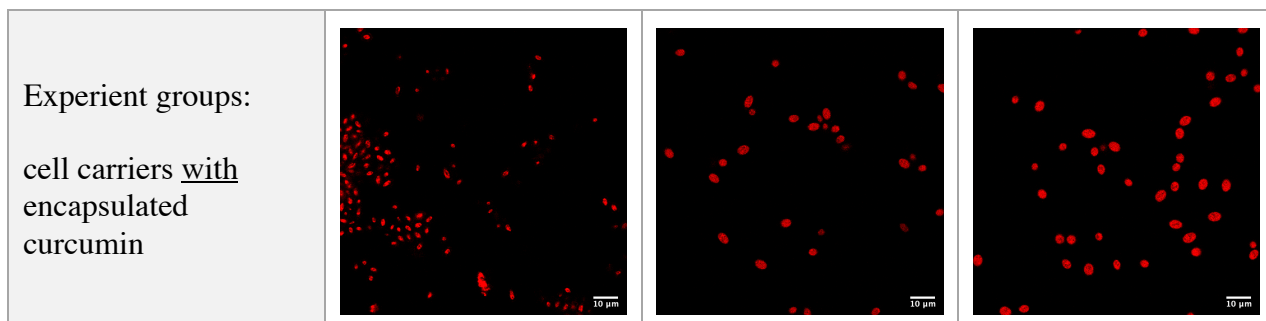


**Table 2.1.** Encapsulation yield, encapsulation efficiency and representative confocal images of curcumin in YCWP, alive yeast cells (aYC) and deactivated yeast cells (dYC). Confocal images were acquired with an excitation laser at 488 nm, and an emission detection range from 498-591 nm. The scale bars below the images represent the length of 10  $\mu\text{m}$ .

The quantification of curcumin in the encapsulated cell carriers showed that encapsulation efficiencies for aYC, dYC and YCWP were 31%, 37% and 18%, respectively (Table 1). The encapsulation yield of curcumin in YCWP was 4.1 mg curcumin encapsulated per gram of particles (wet basis). In comparison, the encapsulation yields of curcumin in alive yeast cells (aYC) and heat deactivated yeast cells (dYC) were 7.0 mg and 8.3 mg respectively per gram of yeast particles (wet basis).

The intracellular distribution of curcumin in these cell carriers were evaluated by CLSM based on the endogenous fluorescence properties of curcumin. Images were taken and analyzed in triplicates to ensure consistency of the observation. The images in Table. 1 show intact cells with relatively uniform distribution of curcumin across the intracellular compartment. There is observable signal from cells in the control groups, which might be attributed to the auto-fluorescence of the microbial cell and is lower than the cells with encapsulated curcumin. The imaging results also indicate that the concentration of residual curcumin outside the cells dissolved

or dispersed in the solution is too low to be detected, which may result from precipitation of curcumin during the encapsulation process.

The encapsulation yields of curcumin in YCWP and YC are consistent with the results of a prior study (Young et al., 2017). The pressure-facilitated encapsulation technique adopted in this study expedited the encapsulation process and avoided the use of high temperature incubation conditions for the encapsulation of curcumin (Young et al., 2017). Differences in the encapsulation yields of curcumin in YCs and YCWP can be attributed to structural and compositional variations between YCWP and YC. Curcumin with an octanol-water log-P value of approximately 3.0 (Priyadarsini, 2014) favors hydrophobic interactions and hydrogen bonding with yeast cellular components such as phospholipid membrane, glucan and proteins located in the cell membrane and cell organelles (Paramera et al., 2011). In contrast, YCWP are relatively hollow and porous microspheres that are composed primarily of  $\beta$ -1,3-D-glucan and chitin and devoid of cellular content (Soto and Ostroff, 2008). The loss of significant fraction of cytoplasmic components such as lipids and proteins may result in reduced partitioning of curcumin and hence reduce the encapsulation yield of curcumin in YCWP compared to YC.

### 2.3.2 Binding affinity of the cell carriers with *L. innocua* biofilm

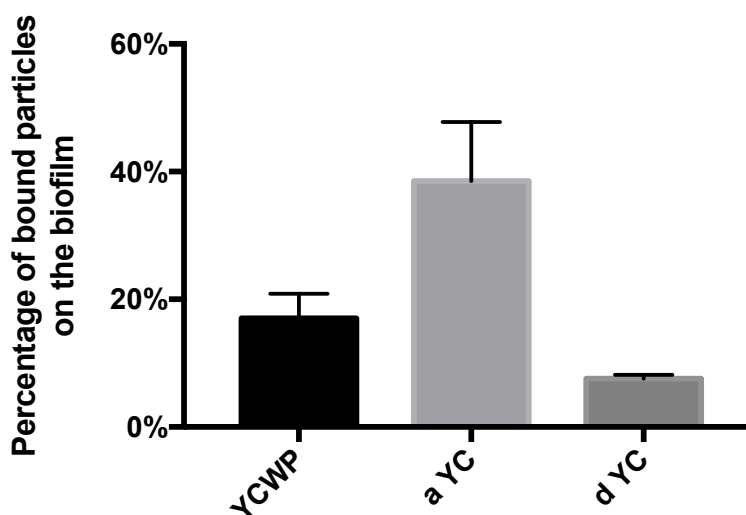


**Figure 2.1.** Efficiency of alive/deactivated *S. cerevisiae* and YCWPs to bind *L. innocua* biofilms. Different letters (a-c) in the graphs indicate statistically significant differences ( $p < 0.05$ ).

Binding of cell carriers to biofilms can aid in increasing localized concentration of PDT agents within the biofilm matrix. The results in Figure 1 show that aYC had the highest percentage of cells bound to the biofilm with approximately 38% of the incubated cells bound to the biofilm, while the heat deactivated yeast cells had a significant reduction in binding with only 7.6% of the incubated cells bound to the biofilm. The YCWP had a moderate level of binding to the biofilm, with approximately 17 % of the incubated yeast cell wall particles bound to the biofilm.

The result of fluorescence measurements using a plate reader were further validated using SEM analysis. The SEM results illustrated the morphological aspects of interactions between cell carriers and biofilm and provides a qualitative assessment of binding interactions (Figure S2.2). The images demonstrate binding of the yeast and yeast cell wall carriers to the bacterial biofilm. Note that the flattened morphology of YCWP in the SEM images (Figure S2.2(b)) might be caused by fixation or vacuum sputtering process during sample preparation (Tang et al., 2014). Furthermore, multiple rinse steps in preparing biofilm samples for SEM analysis can influence the ultra-structure of the biofilm. In addition, binding of cell carriers can further impact the biofilm structure during these preparation steps as illustrated in the results of Fig. S2.2. The bacterial cell density on biofilm samples incubated with cell carriers was qualitatively lower, compared to the control (Fig. S2.2). The attachment of multiple bacteria around individual yeast cells highlighted the polyvalent interactions between the YC and YCWP with bacteria.

The fungal-biofilm attachment as shown in Figure S2.2 has also been observed in previous studies (Hogan et al., 2007; Hwang et al., 2017; Millsap et al., 1998, p. 1998; Wargo and Hogan, 2006), including binding of alive and inactivated yeast cells to pathogenic bacteria (Tiago et al.,

2012). In general, ability of fungi to bind bacteria can be attributed to passive physical interactions followed by specific ligand-receptor interactions between yeast cell wall glycoproteins (known as adhesins) and bacterial cell wall polysaccharides (Holmes et al., 1996). As an example, *S. cerevisiae* is known to produce lectin-like adhesins which bind to sugar residues on the surface of other fungi, bacterial or mammalian cells (Verstrepen and Klis, 2006). Damages inflicted on the cell wall structure and physical properties upon thermal treatment may explain the reduction in attachment of the dYC to bacterial biofilm when compared to aYC (Guyot et al., 2015; McEldowney and Fletcher, 1988). The results in Figure 1 indicated that the YCWP have a moderate level of attachment with *L. innocua* biofilm compared to native yeast cells. Adhesion between YCWP and bacteria and or the EPS of the biofilm might be mostly attributed to the beta-glucan on the surface of YCWP, since the preparation of the YCWP in this study led to a composition of particles enriched in beta-glucan (Upadhyay et al., 2017). The simultaneous binding of multiple bacterial cells to individual YCs or YCWPs may be due to polyvalent interactions between oligosaccharide-binding sites on the yeast cell wall and the surface composition of bacterial cells. These multiple binding events lead to increased avidity of the fungal-bacterial adhesion (Mulvey et al., 2001).

To the best of our knowledge, no prior study has reported binding facilitated delivery of PDT molecules to biofilms. This limitation in prior reports might be the results of a lack of affinity of the carriers for the biofilms. Most of the prior formulations for PDT had focused on improving dispersibility of lipophilic PDT agents. In this study, both the yeast cells and yeast cell wall particles have significant ability to bind bacterial biofilm based on endogenous molecules on the cell surface. This provides a unique advantage for the use of natural carriers such as yeast in contrast to synthetic assemblies such as nanoparticles. In addition, affinity for biofilms and the

ability to bind to them can also be helpful for the targeted delivery of PDT agents to biofilms under dynamic conditions. These conditions may include sanitation of food contact surfaces, sanitation of food materials under dynamic washing conditions as well as treatment of infections in the oral cavity.

### 2.3.3 Inactivation of biofilm bacteria assisted with UV-A light

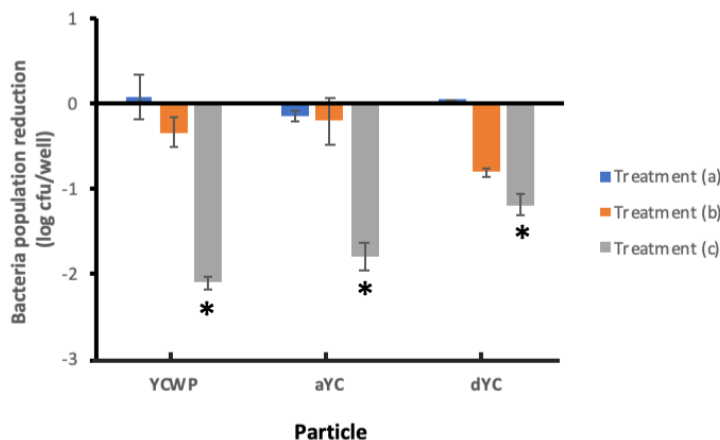


**Figure 2.2.** Inactivation of *L. innocua* in a model 4-day old biofilm using a combination of encapsulated curcumin in cell based microcarriers and UV-A light for 30 min: Treatment (a) cell carriers without curcumin; (b) cell carrier with encapsulated curcumin; (c) cell carriers with encapsulated curcumin and UV-A treatment. Reduction was calculated in comparison to biofilms without treatments. The symbol \* indicates statistically significant differences ( $p < 0.05$ ).

To investigate the synergistic antimicrobial activity of encapsulated curcumin in cell based microcarriers with UV-A, biofilm inactivation and metabolic activity was characterized using the standard plate counting and the resazurin metabolic assay, respectively. The plate counting method assesses the absolute reduction in the number of colony forming units (CFU) of bacteria in the biofilm, while metabolic activity validates the reduction of total viable cell population including viable but growth inhibited cells (Mariscal et al., 2009). The controls for plate counting

quantification included yeast carriers without UV-A treatment and UV-A treatment alone. Results in Figure 2 showed that curcumin-encapsulated YCWPs in combination with UV-A achieved a 2.1 log<sub>10</sub> (CFU/cm<sup>2</sup>), 99.2% reduction in the *L. innocua* population in a 4-day old biofilm. In comparison, a combination of curcumin encapsulated in aYC and UV-A achieved a reduction of 1.8 log CFU/ cm<sup>2</sup> of bacterial cells under the same set of experiments (98.4% reduction), while the similar combination of curcumin in dYC and UV-A achieved reduction of 1.18 log CFU/cm<sup>2</sup> (93.3% reduction). Overall, all the three carriers exhibited significant inactivation (over 93%) of *L. innocua* cells in a biofilm matrix using a combination of encapsulated curcumin in cell-based carriers and UV-A light. In contrast, samples treated with encapsulation carriers but without light exposure, and samples treated with UV-A light solely, showed no significant reduction in the bacterial plate count of biofilm samples (one-way ANOVA test with significance level of 0.05, data not shown here). In addition, biofilms in the control group that were not exposed to UV-A treatment or cell carriers showed a reduction of 0.31 log CFU/well on average, and were used as the baseline to calculate the reduced log counts shown in Figure 2.

These results demonstrated that the synergistic interaction of microencapsulated curcumin with UV-A light is comparable or more effective when compared to other emerging biofilm treatments in food and biomedical applications. For example, Sharma et al. (2005) has shown that bacteriophage KH1 was reduced by 1.2 log CFU after 4-day treatment at 4 °C from a lower initial population of 2.6 log CFU/coupon(Sharma et al., 2005). When compared to other aPDT applications of curcumin as a natural photosensitizer, a similar efficacy of ≤ 3 log reduction was achieved with equal or greater concentrations in solution of DMSO or ethanol (0.75-5 mg/ml) (Dahl et al., 1989; Najafi et al., 2016). Although conventional chlorine-based treatments usually report higher log reductions (Bremer et al., 2002), the various limitations associated with

chlorination as discussed in the previous section still remain and signify the need to develop safe and efficient alternatives in order to control hazardous biofilms in food and health related environments.

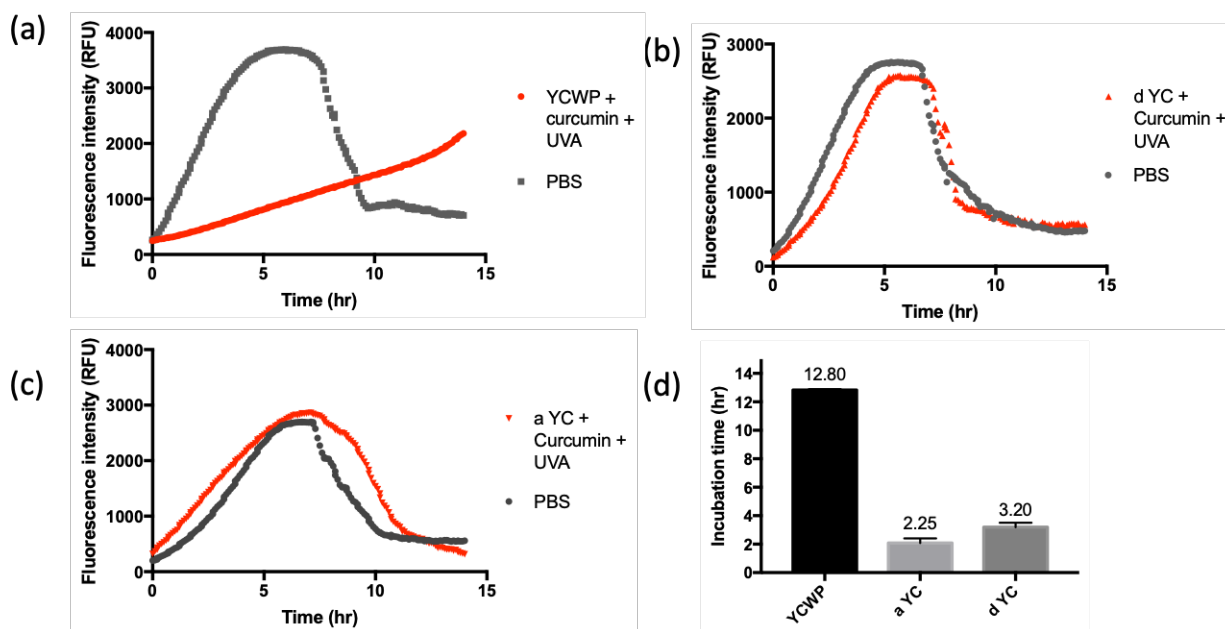


**Figure 2.3.** Metabolic activity of *L. innocua* biofilm after 30 min UV-A treatment in the presence of curcumin encapsulated in (a) YCWP, (b) dYC, and (c) aYC. (d) Additional incubation time required to reach 50% of the peak fluorescence intensity compared to the control sample.

Metabolic activities of the biofilms after treatments were quantified using the resazurin assay. Results in Figure 3(a – c) show that YCWP with curcumin has the most inactivation efficacy with UVA treatment with a time lag of 12.8 hr for the bioconversion of resazurin, whereas aYC and dYC carriers with curcumin and UV-A light had a time lag of 2.25 and 3.20 hours respectively for the bioconversion of resazurin. The observed antibiofilm efficiency of YCWP is consistent with the plate count results in the Figure 2. The biofilm inactivation by aYC and dYC is lower than YCWP. Note that biofilm treated with aYC showed higher metabolic activity when compared to



dYC by comparing Figure 3b and 3c, which is the contrary to the plate counting results in the Fig.2. This is due to the fact that besides the bacterial biofilm, aYC also contributed to the amplification of fluorescence signal by metabolizing resazurin. This is demonstrated by the control groups' spectrum shown in Figure S1.

The inactivation and metabolic activity results highlight that YCWP is the most effective antimicrobial carrier among the three tested carriers. It is worth noting that dYC has the greatest encapsulation efficiency among the three carriers and the least binding efficiency, while aYC has relatively high encapsulation efficiency and the most binding capability. These results indicate that the observed anti-biofilm activity of the PDT treatments depends on multiple factors, including the binding rate of the microcarriers, the encapsulation yield, interactions of the encapsulated PDT agent with the biofilm and with the activating UV-A light. The dependence on multiple factors highlight potential differences among yeast derived micro-carriers. These differences include the binding rate of micro-carriers that may influence the localized concentration of curcumin at the surface of a biofilm. In addition to binding rate, differences in intracellular compositions in these micro-carriers may also contribute to the observed differences in the overall antimicrobial activity. For example, in our earlier study we demonstrated that yeast cells and YCWPs are significantly different in their overall antioxidant potential (Young and Nitin, 2019). Since PDT treatment is based on generating ROS species upon photo-activation of curcumin, these differences in antioxidant potential of the micro-carriers can influence the overall activity of ROS species. Furthermore in our prior study we also observed differences in the release properties of encapsulated bioactive compounds from the yeast cell and YCWPs (Young et al., 2020), and these differences may also influence the PDT efficiency. In addition to these factors, we have also observed non-linear responses from curcumin based on its concentration levels (de Oliveira et al.,

2018). At high concentration, curcumin exhibits significantly reduced light-induced antimicrobial activity compared to its activity at low concentration levels. This could be attributed to a combination of factors, including the balance between pro-oxidant and anti-oxidant behavior of diverse polyphenolics, and the potential attenuation of light transmission at relatively high concentration levels of curcumin.

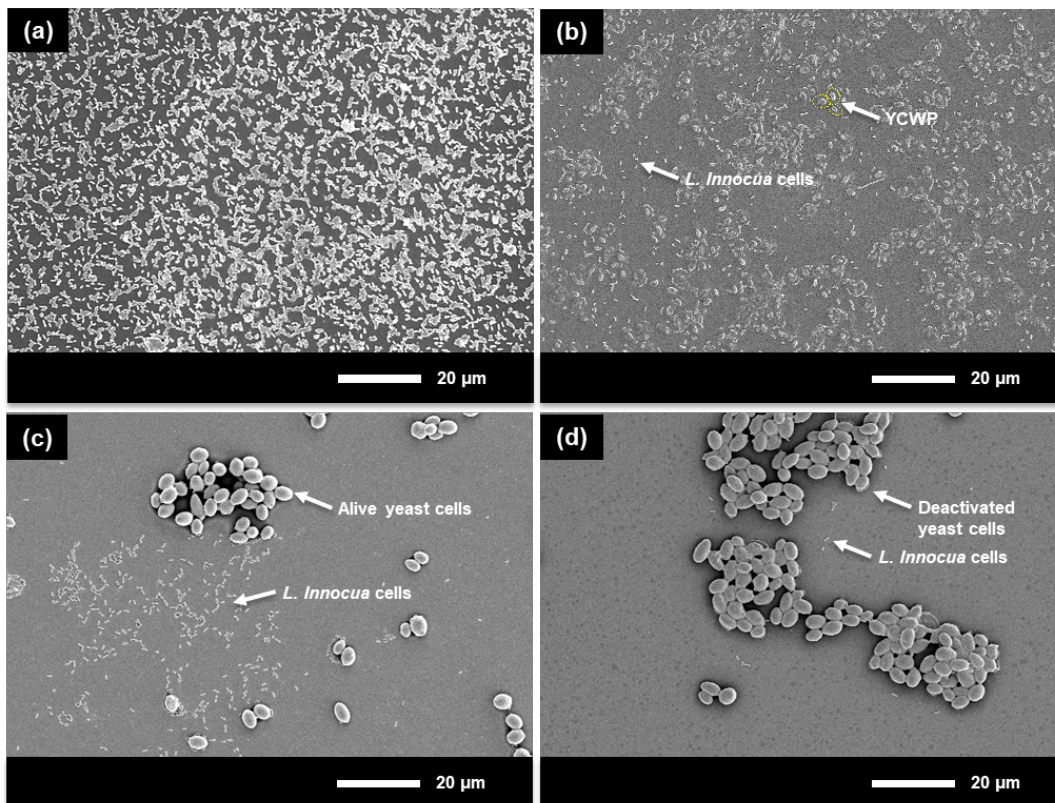


**Figure 2.4.** Characterization of *L. innocua* biofilm after UV-A treatment with different cell carriers. Representative SEM image of (a) control group: *L. innocua* biofilm before treatment; (b) *L. innocua* biofilm treated with YCWP (representative YCWP shown in yellow dash circles); (c) *L. innocua* biofilm treated with aYC; (d) *L. innocua* biofilm treated with dYC. The scale bars below the images represent the length of 20  $\mu\text{m}$ .

In order to characterize the binding of cell carriers to biofilms and the morphological changes of biofilms after treatment, SEM analysis was conducted on biofilm samples after treatment with curcumin-encapsulated cell carriers under UV-A radiation. From the images in Figure 4, we observed removal of the biofilm matrix from the surface after YC and YCWP treatment combined with UV-A light. This removal of the biofilm could be due to the combined effect of biocidal and bacterial/EPS binding properties of the carriers. Studies have demonstrated that biofilm inactivation and removal are distinct phenomena (Chen and Stewart, 2000; Rabinovitch and Stewart, 2006). Removing bacteria and EPS residue in addition to inactivation is desirable since it prevents the microbial substances from conditioning the surface and precludes the formation of new biofilms.

## **Conclusion**

In summary, this research demonstrated targeted inactivation of a model biofilm based on specific delivery of a photosensitization agent, curcumin, to the surface of a model biofilm using cell-based carriers. This combination of curcumin encapsulated in cell-based carriers and UV-A light resulted in significant inactivation of bacterial cells in a biofilm matrix compared to the controls. For these selected carriers, the level of bacterial inactivation in a model biofilm ranged from 93.3% - 99.2%. The unique advantages of high encapsulation efficiency of curcumin in yeast cell carriers, tendency of the carriers to bind biofilms, and photoactivation of curcumin with UV-A light, resulted in synergistic inactivation of a biofilm. The results indicate the role of intracellular composition of cell carriers in influencing the photodynamic activity of curcumin. The results illustrate the potential of this approach to also facilitate removal of the inactivated biomass from the surface, further illustrating the affinity of the cell-based carriers to the biofilm matrix. In summary, the significant photodynamic antimicrobial activity of these treatment highlighted the potential of these biomaterial compositions for application in food and biomedical industries.

## Supporting information

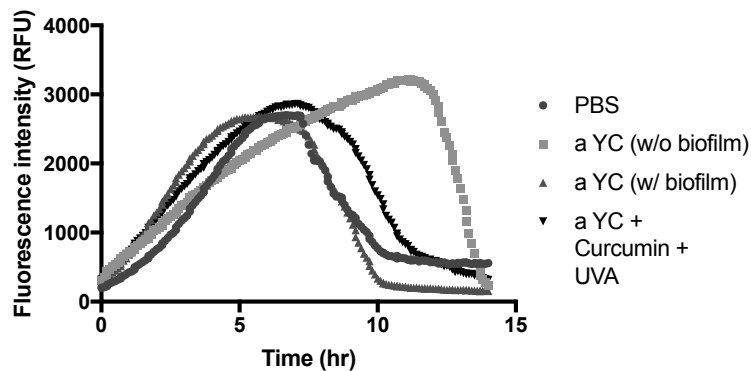


**Figure S2.1** Metabolic activity of *L. innocua* biofilm after 1 hr UV treatment with aYC encapsulated with curcumin and control groups.

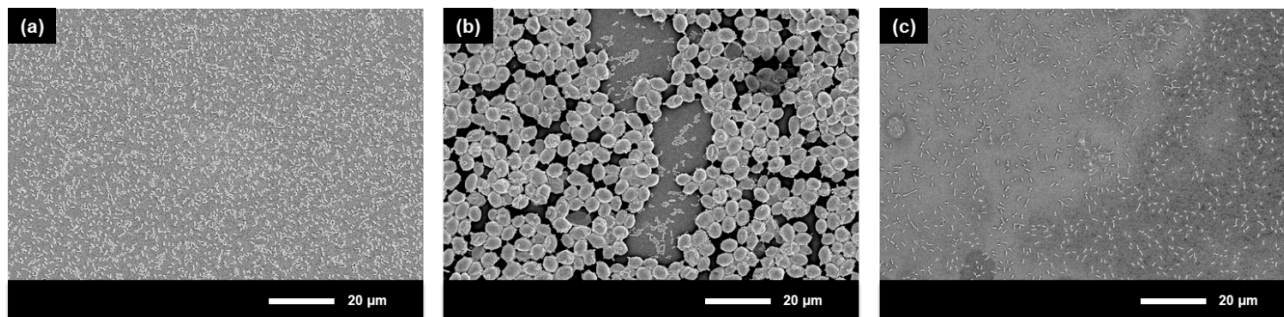


**Figure S2.2** Representative SEM image of control groups of biofilms: (a) *L. innocua* biofilm with UV-A irradiation only; (b) *L. innocua* biofilm treated with aYC without UV-A irradiation; (c) *L. innocua* biofilm treated with YCWP without UV-A irradiation. The scale bars below the images represent the length of 20 μm.

## References

- Adam, B., Baillie, G.S., Douglas, L.J., 2002. Mixed species biofilms of *Candida albicans* and *Staphylococcus epidermidis*. *Journal of Medical Microbiology* 51, 344–349. <https://doi.org/10.1099/0022-1317-51-4-344>
- Baumann, A.R., Martin, S.E., Feng, H., 2009. Removal of *Listeria monocytogenes* Biofilms from Stainless Steel by Use of Ultrasound and Ozone. *Journal of Food Protection* 72, 1306–1309. <https://doi.org/10.4315/0362-028X-72.6.1306>
- Behnke, S., Parker, A.E., Woodall, D., Camper, A.K., 2011. Comparing the Chlorine Disinfection of Detached Biofilm Clusters with Those of Sessile Biofilms and Planktonic Cells in Single- and Dual-Species Cultures. *Appl Environ Microbiol* 77, 7176–7184. <https://doi.org/10.1128/AEM.05514-11>
- Bialoszewski, D., Pietruczuk-Padzik, A., Kalicinska, A., Bocian, E., Czajkowska, M., Bukowska, B., Tyski, S., 2011. Activity of ozonated water and ozone against *Staphylococcus aureus* and *Pseudomonas aeruginosa* biofilms. *Med Sci Monit* 17, BR339–BR344. <https://doi.org/10.12659/MSM.882044>
- Biel, M.A., Sievert, C., Usacheva, M., Teichert, M., Balcom, J., 2011. Antimicrobial photodynamic therapy treatment of chronic recurrent sinusitis biofilms. *International Forum of Allergy & Rhinology* 1, 329–334. <https://doi.org/10.1002/alr.20089>
- Bremer, P.J., Monk, I., Butler, R., 2002. Inactivation of *Listeria monocytogenes*/*Flavobacterium* spp. biofilms using chlorine: impact of substrate, pH, time and concentration. *Letters in Applied Microbiology* 35, 321–325. <https://doi.org/10.1046/j.1472-765X.2002.01198.x>
- Cheesman, M.J., Ilanko, A., Blonk, B., Cock, I.E., 2017. Developing New Antimicrobial Therapies: Are Synergistic Combinations of Plant Extracts/Compounds with Conventional

- Antibiotics the Solution? *Pharmacogn Rev* 11, 57–72.  
[https://doi.org/10.4103/phrev.phrev\\_21\\_17](https://doi.org/10.4103/phrev.phrev_21_17)
- Chen, X., Stewart, P.S., 2000. Biofilm removal caused by chemical treatments. *Water Research* 34, 4229–4233. [https://doi.org/10.1016/S0043-1354\(00\)00187-1](https://doi.org/10.1016/S0043-1354(00)00187-1)
- Colagiorgi, A., Bruini, I., Di Ciccio, P.A., Zanardi, E., Ghidini, S., Ianieri, A., 2017. *Listeria monocytogenes* Biofilms in the Wonderland of Food Industry. *Pathogens* 6. <https://doi.org/10.3390/pathogens6030041>
- Cossu, A., Si, Y., Sun, G., Nitin, N., 2017. Antibiofilm Effect of Poly (Vinyl Alcohol-co-Ethylene) Halamine Film against *Listeria innocua* and *Escherichia coli* O157: H7. *Applied and environmental microbiology* 83, e00975-17.
- Dahl, T.A., McGowan, W.M., Shand, M.A., Srinivasan, V.S., 1989. Photokilling of bacteria by the natural dye curcumin. *Arch. Microbiol.* 151, 183–185. <https://doi.org/10.1007/BF00414437>
- Daly, B., Betts, W.B., Brown, A.P., O’Neill, J.G., 1998. Bacterial loss from biofilms exposed to free chlorine. *Microbios* 96, 7–21.
- de Oliveira, E.F., Tosati, J.V., Tikekar, R.V., Monteiro, A.R., Nitin, N., 2018. Antimicrobial activity of curcumin in combination with light against *Escherichia coli* O157:H7 and *Listeria innocua*: Applications for fresh produce sanitation. *Postharvest Biology and Technology* 137, 86–94. <https://doi.org/10.1016/j.postharvbio.2017.11.014>
- Faille, C., Bénézech, T., Midelet-Bourdin, G., Lequette, Y., Clarisse, M., Ronse, G., Ronse, A., Slomianny, C., 2014. Sporulation of *Bacillus* spp. within biofilms: A potential source of contamination in food processing environments. *Food Microbiology* 40, 64–74. <https://doi.org/10.1016/j.fm.2013.12.004>

- Gião, M.S., Keevil, C.W., 2013. Hydrodynamic shear stress to remove *Listeria monocytogenes* biofilms from stainless steel and polytetrafluoroethylene surfaces. *J. Appl. Microbiol.* 114, 256–265. <https://doi.org/10.1111/jam.12032>
- González, S., Fernández, L., Gutiérrez, D., Campelo, A.B., Rodríguez, A., García, P., 2018. Analysis of Different Parameters Affecting Diffusion, Propagation and Survival of Staphylophages in Bacterial Biofilms. *Frontiers in Microbiology* 9, 2348. <https://doi.org/10.3389/fmicb.2018.02348>
- Guyot, S., Gervais, P., Young, M., Winckler, P., Dumont, J., Davey, H.M., 2015. Surviving the heat: heterogeneity of response in *Saccharomyces cerevisiae* provides insight into thermal damage to the membrane. *Environ Microbiol* 17, 2982–2992. <https://doi.org/10.1111/1462-2920.12866>
- Hegge, A.B., Bruzell, E., Kristensen, S., Tønnesen, H.H., 2012. Photoinactivation of *Staphylococcus epidermidis* biofilms and suspensions by the hydrophobic photosensitizer curcumin – Effect of selected nanocarrier: Studies on curcumin and curcuminoides XLVII. *European Journal of Pharmaceutical Sciences* 47, 65–74. <https://doi.org/10.1016/j.ejps.2012.05.002>
- Hogan, D.A., Wargo, M.J., Beck, N., 2007. Bacterial biofilms on fungal surfaces. *Biofilm mode of life: mechanisms and adaptations* 13, 235–245.
- Holmes, A.R., McNab, R., Jenkinson, H.F., 1996. *Candida albicans* binding to the oral bacterium *Streptococcus gordonii* involves multiple adhesin-receptor interactions. *Infection and Immunity* 64, 4680.
- Hwang, G., Liu, Y., Kim, D., Li, Y., Krysan, D.J., Koo, H., 2017. *Candida albicans* mannans mediate *Streptococcus mutans* exoenzyme GtfB binding to modulate cross-kingdom



- biofilm development in vivo. *PLOS Pathogens* 13, e1006407.  
<https://doi.org/10.1371/journal.ppat.1006407>
- Johansen, C., Falholt, P., Gram, L., 1997. Enzymatic Removal and Disinfection of Bacterial Biofilms. *APPL. ENVIRON. MICROBIOL.* 63, 5.
- Jori, G., Fabris, C., Soncin, M., Ferro, S., Coppelotti, O., Dei, D., Fantetti, L., Chiti, G., Roncucci, G., 2006. Photodynamic therapy in the treatment of microbial infections: Basic principles and perspective applications. *Lasers in Surgery and Medicine* 38, 468–481.  
<https://doi.org/10.1002/lsm.20361>
- Lee, H.-J., Kang, S.-M., Jeong, S.-H., Chung, K.-H., Kim, B.-I., 2017. Antibacterial photodynamic therapy with curcumin and *Curcuma xanthorrhiza* extract against *Streptococcus mutans*. *Photodiagnosis and Photodynamic Therapy* 20, 116–119.  
<https://doi.org/10.1016/j.pdpdt.2017.09.003>
- Lee, M.H., Park, B.J., Jin, S.C., Kim, D., Han, I., Kim, J., Hyun, S.O., Chung, K.-H., Park, J.-C., 2009. Removal and sterilization of biofilms and planktonic bacteria by microwave-induced argon plasma at atmospheric pressure. *New J. Phys.* 11, 115022.  
<https://doi.org/10.1088/1367-2630/11/11/115022>
- Lemos, M., Pereira, A.M., Abreu, A.C., Saavedra, M.J., 2011. Persister cells in a biofilm treated with a biocide.
- Lin, S.-M., Svoboda, K.K.H., Giletto, A., Seibert, J., Puttaiah, R., 2011. Effects of Hydrogen Peroxide on Dental Unit Biofilms and Treatment Water Contamination. *Eur J Dent* 5, 47–59.
- Mariscal, A., Lopez-Gigosos, R.M., Carnero-Varo, M., Fernandez-Crehuet, J., 2009. Fluorescent assay based on resazurin for detection of activity of disinfectants against bacterial biofilm. *Appl. Microbiol. Biotechnol.* 82, 773–783. <https://doi.org/10.1007/s00253-009-1879-x>

- Mathur, H., Field, D., Rea, M.C., Cotter, P.D., Hill, C., Ross, R.P., 2018. Fighting biofilms with lantibiotics and other groups of bacteriocins. *npj Biofilms and Microbiomes* 4, 9. <https://doi.org/10.1038/s41522-018-0053-6>
- McEldowney, S., Fletcher, M., 1988. Effect of pH, temperature, and growth conditions on the adhesion of a gliding bacterium and three nongliding bacteria to polystyrene. *Microb Ecol* 16, 183–195. <https://doi.org/10.1007/BF02018913>
- Millsap, K.W., Mei, V.D., C, H., Bos, R., Busscher, H.J., 1998. Adhesive interactions between medically important yeasts and bacteria. *FEMS Microbiol Rev* 21, 321–336. <https://doi.org/10.1111/j.1574-6976.1998.tb00356.x>
- Mulvey, G., Kitov, P.I., Marcato, P., Bundle, D.R., Armstrong, G.D., 2001. Glycan mimicry as a basis for novel anti-infective drugs. *Biochimie* 83, 841–847.
- Najafi, S., Khayamzadeh, M., Paknejad, M., Poursepanj, G., Kharazi Fard, M.J., Bahador, A., 2016. An In Vitro Comparison of Antimicrobial Effects of Curcumin-Based Photodynamic Therapy and Chlorhexidine, on *Aggregatibacter actinomycetemcomitans*. *J Lasers Med Sci* 7, 21–25. <https://doi.org/10.15171/jlms.2016.05>
- Paramera, E.I., Konteles, S.J., Karathanos, V.T., 2011. Microencapsulation of curcumin in cells of *Saccharomyces cerevisiae*. *Food Chemistry* 125, 892–902. <https://doi.org/10.1016/j.foodchem.2010.09.063>
- Paz-Méndez, A.M., Lamas, A., Vázquez, B., Miranda, J.M., Cepeda, A., Franco, C.M., 2017. Effect of Food Residues in Biofilm Formation on Stainless Steel and Polystyrene Surfaces by *Salmonella enterica* Strains Isolated from Poultry Houses. *Foods* 6. <https://doi.org/10.3390/foods6120106>

- Pham-Hoang, B.-N., Winckler, P., Waché, Y., 2018. Fluorescence Lifetime and UV-Vis Spectroscopy to Evaluate the Interactions Between Quercetin and Its Yeast Microcapsule. *Biotechnology Journal* 13, 1700389. <https://doi.org/10.1002/biot.201700389>
- Priyadarsini, K., 2014. The Chemistry of Curcumin: From Extraction to Therapeutic Agent. *Molecules* 19, 20091–20112. <https://doi.org/10.3390/molecules191220091>
- Rabinovitch, C., Stewart, P.S., 2006. Removal and Inactivation of *Staphylococcus epidermidis* Biofilms by Electrolysis. *Appl. Environ. Microbiol.* 72, 6364–6366. <https://doi.org/10.1128/AEM.00442-06>
- Salari, R., Rajabi, O., Khashyarmanesh, Z., Fathi Najafi, M., Fazly Bazzaz, B.S., 2015. Characterization of Encapsulated Berberine in Yeast Cells of *Saccharomyces cerevisiae*. *Iran J Pharm Res* 14, 1247–1256.
- Schwartz, J., Wiehe, A., Gräfe, S., Gitter, B., Epple, M., 2009. Calcium phosphate nanoparticles as efficient carriers for photodynamic therapy against cells and bacteria. *Biomaterials* 30, 3324–3331. <https://doi.org/10.1016/j.biomaterials.2009.02.029>
- Sharma, M., Ryu, J.-H., Beuchat, L.R., 2005. Inactivation of *Escherichia coli* O157:H7 in biofilm on stainless steel by treatment with an alkaline cleaner and a bacteriophage. *Journal of Applied Microbiology* 99, 449–459. <https://doi.org/10.1111/j.1365-2672.2005.02659.x>
- Shi, G., Rao, L., Yu, H., Xiang, H., Yang, H., Ji, R., 2008. Stabilization and encapsulation of photosensitive resveratrol within yeast cell. *International Journal of Pharmaceutics* 349, 83–93. <https://doi.org/10.1016/j.ijpharm.2007.07.044>
- Shirtliff, M.E., Peters, B.M., Jabra-Rizk, M.A., 2009. Cross-kingdom interactions: *Candida albicans* and bacteria. *FEMS Microbiol Lett* 299, 1–8. <https://doi.org/10.1111/j.1574-6968.2009.01668.x>

- Sibani, S.A., McCarron, P.A., Woolfson, A.D., Donnelly, R.F., 2008. Photosensitiser delivery for photodynamic therapy. Part 2: systemic carrier platforms. *Expert Opinion on Drug Delivery* 5, 1241–1254. <https://doi.org/10.1517/17425240802444673>
- Simões, M., Simões, L.C., Machado, I., Pereira, M.O., Vieira, M.J., 2006. Control of Flow-Generated Biofilms with Surfactants: Evidence of Resistance and Recovery. *Food and Bioproducts Processing, Fouling, Cleaning and Disinfection in Food Processing* 84, 338–345. <https://doi.org/10.1205/fbp06022>
- Smith, J.E., Oliver, J.D., 1991. The effects of hydrostatic pressure on bacterial attachment. *Biofouling* 3, 305–310. <https://doi.org/10.1080/08927019109378184>
- Soothill, J., 2013. Use of bacteriophages in the treatment of *Pseudomonas aeruginosa* infections. *Expert Review of Anti-infective Therapy* 11, 909–915. <https://doi.org/10.1586/14787210.2013.826990>
- Soto, E., Kim, Y.S., Lee, J., Kornfeld, H., Ostroff, G., 2010. Glucan Particle Encapsulated Rifampicin for Targeted Delivery to Macrophages. *Polymers* 2, 681–689. <https://doi.org/10.3390/polym2040681>
- Soto, E.R., Ostroff, G.R., 2008. Characterization of Multilayered Nanoparticles Encapsulated in Yeast Cell Wall Particles for DNA Delivery. *Bioconjugate Chem.* 19, 840–848. <https://doi.org/10.1021/bc700329p>
- Tang, S.-Y., Zhang, W., Soffe, R., Nahavandi, S., Shukla, R., Khoshmanesh, K., 2014. High Resolution Scanning Electron Microscopy of Cells Using Dielectrophoresis. *PLOS ONE* 9, e104109. <https://doi.org/10.1371/journal.pone.0104109>
- Taylor, R.H., Falkinham, J.O., Norton, C.D., LeChevallier, M.W., 2000. Chlorine, Chloramine, Chlorine Dioxide, and Ozone Susceptibility of *Mycobacterium avium*. *Appl. Environ. Microbiol.* 66, 1702–1705. <https://doi.org/10.1128/AEM.66.4.1702-1705.2000>

- Tiago, F.C.P., Martins, F.S., Souza, E.L.S., Pimenta, P.F.P., Araujo, H.R.C., Castro, I.M., Brandao, R.L., Nicoli, J.R., 2012. Adhesion to the yeast cell surface as a mechanism for trapping pathogenic bacteria by *Saccharomyces* probiotics. *Journal of Medical Microbiology* 61, 1194–1207. <https://doi.org/10.1099/jmm.0.042283-0>
- Upadhyay, T.K., Fatima, N., Sharma, D., Saravanakumar, V., Sharma, R., 2017. Preparation and characterization of beta-glucan particles containing a payload of nanoembedded rifabutin for enhanced targeted delivery to macrophages. *EXCLI J* 16, 210–228. <https://doi.org/10.17179/excli2016-804>
- Van den Driessche, F., Rigole, P., Brackman, G., Coenye, T., 2014. Optimization of resazurin-based viability staining for quantification of microbial biofilms. *Journal of Microbiological Methods* 98, 31–34. <https://doi.org/10.1016/j.mimet.2013.12.011>
- Vandekinderen, I., Devlieghere, F., Van Camp, J., Kerkaert, B., Cucu, T., Ragaert, P., De Bruyne, J., De Meulenaer, B., 2009. Effects of food composition on the inactivation of foodborne microorganisms by chlorine dioxide. *International Journal of Food Microbiology* 131, 138–144. <https://doi.org/10.1016/j.ijfoodmicro.2009.02.004>
- Verstrepen, K.J., Klis, F.M., 2006. Flocculation, adhesion and biofilm formation in yeasts. *Molecular Microbiology* 60, 5–15. <https://doi.org/10.1111/j.1365-2958.2006.05072.x>
- Vogeleer, P., Tremblay, Y.D.N., Jubelin, G., Jacques, M., Harel, J., 2016. Biofilm-Forming Abilities of Shiga Toxin-Producing *Escherichia coli* Isolates Associated with Human Infections. *Appl. Environ. Microbiol.* 82, 1448–1458. <https://doi.org/10.1128/AEM.02983-15>
- Wargo, M.J., Hogan, D.A., 2006. Fungal—bacterial interactions: a mixed bag of mingling microbes. *Current Opinion in Microbiology* 9, 359–364. <https://doi.org/10.1016/j.mib.2006.06.001>

- Winder, C., 2001. The Toxicology of Chlorine. *Environmental Research* 85, 105–114.  
<https://doi.org/10.1006/enrs.2000.4110>
- Young, S., Dea, S., Nitin, N., 2017. Vacuum facilitated infusion of bioactives into yeast microcarriers: Evaluation of a novel encapsulation approach. *Food Research International* 100, 100–112. <https://doi.org/10.1016/j.foodres.2017.07.067>
- Young, S., Nitin, N., 2019. Thermal and oxidative stability of curcumin encapsulated in yeast microcarriers. *Food Chemistry* 275, 1–7. <https://doi.org/10.1016/j.foodchem.2018.08.121>
- Young, S., Rai, R., Nitin, N., 2020. Bioaccessibility of curcumin encapsulated in yeast cells and yeast cell wall particles. *Food Chemistry* 309, 125700.  
<https://doi.org/10.1016/j.foodchem.2019.125700>

## Chapter 3

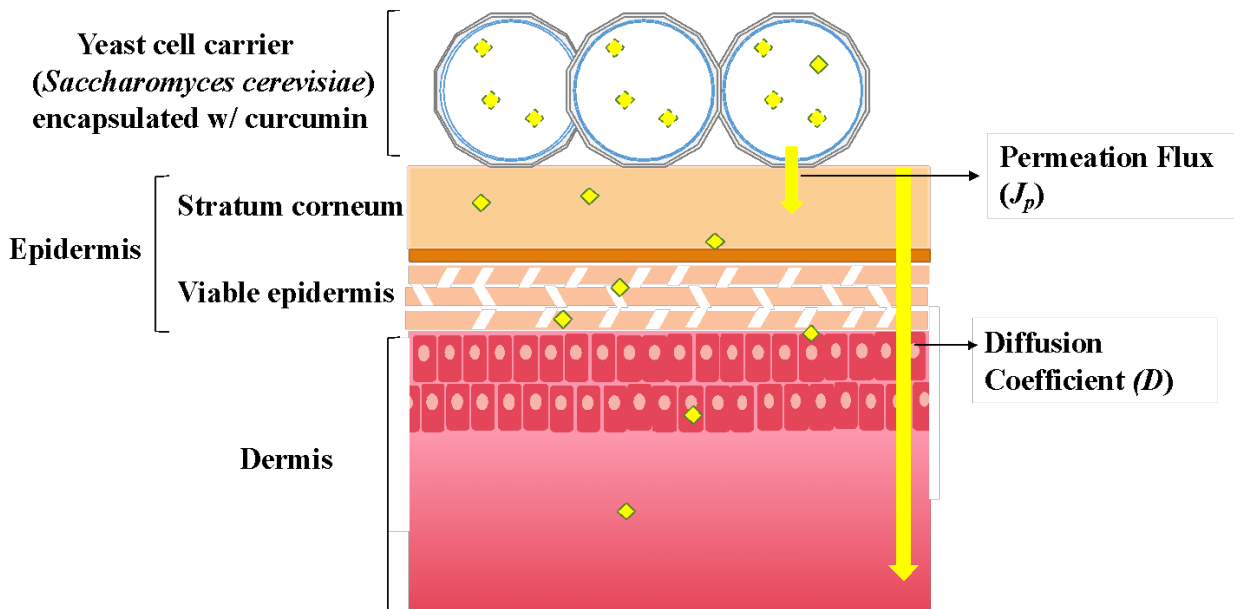
# Yeast cell microcarriers for delivery of a model bioactive compound in skin

### Abstract

This study was aimed at developing a cell-based encapsulation carrier for topical delivery of bioactives to the skin. The overall objectives were to evaluate the ability of the yeast-cell based carrier to bind to the skin surface following topical application, and to quantify controlled release of curcumin as a model bioactive in *ex-vivo* skin models, using a combination of imaging, modeling and analytical measurements. Both porcine skin tissue and clinically obtained human skin biopsies were studied. The results demonstrated that upon incubation with the *ex-vivo* skin tissues, the cell carriers rapidly bound to the skin surface following topical delivery and provided sustained release of encapsulated curcumin. The microcarrier binding and penetration of curcumin in the dermal compartment was also shown to increase with incubation time. The average flux  $J_p$  of curcumin in human skin biopsies was  $0.89 \pm 0.02$  ug/cm<sup>2</sup>/h. These results illustrated the potential of a novel cell-based carrier for high-affinity binding to skin surfaces, efficient encapsulation of a model bioactive and controlled release from the cell carrier to the skin, with enhanced permeation to the dermis section. Overall, this study demonstrated a new class of cost-

effective carriers for improving delivery of bioactives to the skin and potentially other epithelial tissues.

### Graphical Abstract





### 3.1. Introduction

Dermal and transdermal delivery systems aim to deliver therapeutic and cosmetic actives to skin sub-layers and across the skin tissue (Karande and Mitragotri, 2009). The dermal route offers certain advantages over oral delivery and hypodermal injections as it circumvents the first-pass metabolism and reduces discomfort and safety issues of the injectables (Brown et al., 2006; Karande and Mitragotri, 2009). Cutaneous delivery systems therefore present a noninvasive approach to address dermal and systemic pathologies, cosmetic needs, and delivery of vaccines (Thomas and Finnin, 2004). Diverse delivery systems such as micro- or nano-scale emulsions (Liu et al., 2011; Su et al., 2017; Teichmann et al., 2007; Zillich et al., 2013), liposomes (Margalit et al., 1992), and nanostructured carriers (Contri et al., 2014b, 2014a; Rachmawati et al., 2013; Ramezanli et al., 2017; Silva et al., 2016) has been evaluated for these applications. However, various factors including retention of bioactives on the skin surface and constrained permeation into the tissue are some of the key challenges limiting topical delivery of bioactives (Couto et al., 2014; Elias, 1983; Teichmann et al., 2007). Therefore, diverse encapsulation systems for enhanced retention, improved permeation and controlled release of the encapsulated bioactives are being evaluated for the topical delivery of bioactives to the skin.

Most of these current encapsulation systems do not have endogenous mechanisms to bind to the skin surface with high avidity. It is widely recognized that ability of the encapsulation carriers to bind the tissue surface and provide controlled release of encapsulated actives are some of the key desirable features for effective delivery of the bioactives (Contri et al., 2014b, 2014a; Shalaby and El-Refaie, 2018). In the case of topical skin applications, binding of the carriers to the skin surfaces can reduce removal of the carrier and encapsulated compounds due to normal perspiration and physical activities during an extended period. Furthermore, these carriers may provide

controlled release of bioactives into the skin tissue for an extended period and thus achieve higher permeation into the skin tissue and optimal biological activity for the delivered actives. To achieve these objectives, encapsulation carriers incorporated with synthetic ligands have been proposed for the active binding of the nano-micro carriers to various target cells or tissues (Allen, 2002; Kim et al., 2005; Margalit et al., 1992). However, technical complexity in modifying carriers with targeting ligands and cost barriers limit applications of this approach for the topical delivery to skin (Srinivasarao and Low, 2017). Thus, there is an unmet need for cost effective encapsulation carriers with high encapsulation yield and binding avidity.

Cell based encapsulation approaches such as yeast cells and cell wall particles have emerged as an effective encapsulation carrier for diverse bioactives based on encapsulation yields and efficiencies (Nelson et al., 2006; Paramera et al., 2011; Salari et al., 2015; Soto and Ostroff, 2008; Young et al., 2017). The encapsulation of compounds in cell-based carriers is significantly influenced by partitioning properties of the encapsulants in cells, and the rate of encapsulation or infusion of compounds in cell-based carriers can be influenced by various factors, including composition of cell-based carriers and exogenous factors such as pressure and temperature (Bishop et al., 1998; Ciamponi et al., 2012; Shi et al., 2008; “US5288632A - Encapsulation of material in microbial cells - Google Patents,” n.d.; Young et al., 2017). Cell-based carriers, based on their unique composition and structure, can be a host to diversity of hydrophilic and hydrophobic compounds and also simultaneously encapsulate diversity of compounds (Young et al., 2017). The micro-scale size of the carriers eliminate the need to fabricate microparticles and the diversity of compositions can be achieved by selecting cell-based carriers from diverse sources including microbial cells. In addition, the microcarriers offer enhanced protection against oxidative and thermal stability of bioactives compared to colloidal carriers such as emulsions (Young and Nitin,

2019). With our expanding understanding of the skin microbiome and its functions, it is well established that a diversity of microbes, including yeast, are present on the skin surface (Belkaid and Tamoutounour, 2016; Findley et al., 2013). These microbes have developed specific mechanisms to bind to the skin surface and persist on the skin surface upon exposure to perspiration and other physical stresses (Dranginis et al., 2007; Grice and Segre, 2011; Romero-Steiner et al., 1990). Many microbes such as probiotic bacteria such as *Bifidobacteria longum* and *Bifidobacteria bifidum* (De et al., 2017), *Lactobacillus rhamnosus* and *Lactobacillus reuteri* (O'Neill and McBain, 2013) and yeast *Saccharomyces cerevisiae* substances (Gaspar et al., 2017) have also been proposed or patented as beneficial ingredients for skin products. Thus, these microbial compositions provide an opportunity to develop solutions for topical dermal delivery of bioactives for both therapeutic and cosmetic applications.

The overall motivation of this study was to evaluate the functionality of yeast cell carriers for the topical delivery of beneficial bioactives using ex-vivo skin tissue models. To the best of our knowledge, this is the first study reporting development and application of cell based microcarriers for transdermal topical delivery of bioactives. The overall hypothesis of this study is that cell-based carriers with relatively high encapsulation yield of compounds, and endogenous properties enabling them to bind to the skin surface, can be an effective transdermal topical delivery system for the skin. As a part of the human skin microflora, *Saccharomyces* has a thick cell wall which is composed of highly crosslinked glucan associated with a mannoprotein layer and a small amount of chitin (Findley et al., 2013; Kollár et al., 1997). Based on the cell wall composition, yeast cells have a potential to bind biological tissues without additional modifications such as attaching ligands or antibodies to the surface. In this study, curcumin was selected as a model bioactive compound. Curcumin is one of the widely studied bioactive compound with antioxidant and anti-

carcinogenic properties for both oral and topical applications (Chun et al., 2003; Griesser et al., 2011; Vaughn et al., 2016). Curcumin has been proposed for the treatment of various inflammatory diseases of the skin (Vollono et al., 2019); for example, topical alcoholic gels of curcumin have been evaluated for the treatment of Psoriasis (Heng et al., 2000). The proposed mechanism is based on reduction in expression of TNF-alpha by macrophages treated with curcumin. Similarly, topical application of curcumin has been considered for the reduction of erythema and itching in patients affected by eczema (Rawal et al., 2009). Despite beneficial properties of curcumin, its hydrophobicity and limited stability are some of the key limitations for its applications in product formulations (Tønnesen et al., 2002). Therefore, microencapsulation of curcumin in yeast cells could potentially improve curcumin's applicability in hydrophilic topical delivery formulations and enhance delivery to the skin tissue, overcoming the poor water solubility and stability of the compound (Paramera et al., 2011).

In summary, this study evaluates binding of yeast cell-based encapsulation carriers to skin tissue and the delivery of encapsulated curcumin. The novel aspects of this study include: (1) the topical delivery and attachment of the yeast encapsulation carrier for enhancing delivery of curcumin to the skin and (2) the evaluation of percutaneous diffusion of bioactive compounds from yeast cell carriers. This research overall aims to develop a new delivery system for topical applications of bioactive compounds for cosmetic and pharmaceutical industries.

## **3.2. Materials and Methods**

### **3.2.1 Materials**

Both porcine and human skin samples were collected to evaluate the cell-based delivery system in this study. Specifically, porcine tissue was used for the topical attachment experiment and curcumin permeation test. Human biopsies were then collected to validate and quantify the

transdermal permeation of curcumin. Porcine skin samples were obtained from the Meat Science Laboratory, Department of Animal Science (University of California, Davis). Skin tissue of 6-month-old pigs was collected within 3 hours of slaughtering. Collected tissue was snap frozen in a liquid nitrogen and stored at -80°C. Prior to the experiments, frozen skin pieces were thawed at room temperature. Skin integrity was examined visually and also subsequently with microscopic imaging. Healthy human facial skin biopsies were collected from patients who were undergoing Mohs surgery according to the IRB guidelines (Department of Dermatology, University of California, Davis). After surgical removal, the skin was cleaned with saline and analyzed within 6 hours after surgery to ensure vitality and intactness of the tissue. A total of 13 biopsies from 7 patients were collected and analyzed. Curcumin, isopentane, Dispase I (protease), HPLC grade acetone, methanol and ammonium acetate were purchased from Sigma-Aldrich (St. Louis, MO, USA). Corning 12mm Transwell with 0.4 µm pore polyester membrane inserts were purchased from Sigma-Aldrich (St. Louis, MO, USA).

### **3.2.2 Preparation of curcumin-encapsulated yeast cells**

Yeast cells were encapsulated with curcumin via a negative pressure-facilitated process as described in our previous study (Young et al., 2017). Briefly, 0.5 g of the yeast wet pellet was suspended in a 5 ml solution that consists of 65% PBS and 35% ethanolic solution of curcumin (2.5 mg/ml). Control samples without curcumin were prepared using 35% ethanol instead. After encapsulation, the cell pellet was washed five times using Milli-Q water until no curcumin was detectable in the supernatant based on the UV-Vis analysis (curcumin absorption peak at 425 nm).

### **3.2.3 Quantification of encapsulation efficiency**

Encapsulated curcumin in yeast cells was extracted using methanol. After suspension of cells in methanol, the yeast cells were disrupted by bead beating at a speed 6.0 m/s with 3 cycles of 40

sec (FastPrep-24™ 5G Instrument, MP Biomedicals) and followed by sonication for 10 min (Branson 2510 Ultrasonic Cleaner, Branson Ultrasonics Corp., Danbury, CT, USA). After centrifugation at 16,100 rcf for 20 min, the curcumin content in methanol extract was measured based on the peak absorbance of curcumin at 425 nm by using a UV-Vis spectrophotometer and quantified using a standard curve of serially diluted curcumin solutions in methanol (Genesys™ 10 UV-Vis Spectrophotometer, Thermo Scientific).

### **3.2.4 In-vitro release of curcumin in solution from yeast cell microcarriers**

The release of curcumin from the yeast cells was measured using a transwell diffusion chamber. In this approach, yeast carriers are separated from the release solution by a membrane, thus limiting the direct contact of the cell carriers with the solution. Release of curcumin from yeast carriers was characterized as a function of DMSO concentration. DMSO was selected as it is a water miscible, non-volatile solvent that is commonly used to disperse hydrophobic molecules in aqueous phases (Modrzyński et al., 2019). In addition, studies have evaluated the role of DMSO in generating hydrophobic hydration to enhance the solubility of hydrophobic solutes in aqueous phases (Panuszko et al., 2019). A binary mixture of water-DMSO was selected to illustrate the role of the hydrophobic environment of the skin surface in promoting the release of curcumin from yeast microcarriers (De Luca and Valacchi, 2010). Thus, by increasing the % of DMSO in aqueous solution, we can evaluate the role of lipid-rich regions of the skin surface in influencing the release of curcumin from yeast cell carriers.

### **3.2.5 Ex-vivo skin penetration experiments**

Skin samples were incubated with the encapsulation formulations in a Transwell chamber. 1 ml of the tissue culture medium (Iscove's Modified Dulbecco's Medium supplemented with 10% Fetal Bovine Serum, 2.5 mg/ml Amphotericin B, and 100 unit/ml Penicillin-Streptomycin, Gibco by Life Technology) was added into each bottom well. The skin biopsy sample was carefully

placed in the insert, with the epidermis on the top. 1-2 ml of yeast cell slurry with encapsulated curcumin was then added topically to the biopsy material and incubated at 32°C with 5% CO<sub>2</sub> in the dark. The volume of topically applied yeast cell slurry was adjusted to cover the top surface of the skin sample. After a series of incubation time intervals, the skin surface was rinsed with PBS to remove unattached yeast cells.

### **3.2.6 Analysis of yeast cell carrier's attachment to the skin surface**

The overall goal of this measurement was to characterize binding of yeast cells to the skin surface. For this measurement, yeast cells were stained with a DNA staining dye (Propidium Iodide (PI)) at a final concentration of 50 mM for 20 min. Excess dye was removed by dispersing the cell pellet in MilliQ water and centrifuging at 4400 rpm for 5 min. DNA staining dye was selected based on its enhanced binding of nucleic acids in the pre-stained yeast cells and lack of release of the dye upon extended incubation in solution and other biological mediums (data not shown). After incubation of tissue samples with the stained yeast cells as described in the previous section, macroscale fluorescence images of the intact skin biopsies were acquired using the Maestro™ *in-vivo* fluorescence imaging system 2.0 (Cambridge Research & Instrumentation, Inc., Woburn, MA, USA). Images of the skin samples were acquired with an excitation wavelength of 535 nm and emission was detected from 600 to 630 nm. Average fluorescence intensity was calculated using the Maestro version 2.10.0 software. For this measurement, regions of interest (ROI) was drawn on the images of each skin biopsy surface to quantify the average fluorescence signal of the PI dye on the skin surface, which corresponds to the number of yeast carriers attached on the skin surface. 10-20 ROI per image was chosen at random to represent the overall signal.

### **3.2.7 Visualization of encapsulated curcumin penetration profile in skin tissue**

After incubation with curcumin-loaded yeast cell carriers, skin tissue samples were snap frozen in a liquid nitrogen with isopentane as a freezing medium, and then cryo-sectioned into 20  $\mu\text{m}$  cross-sectional slice using a research cryostat microtome (Leica CM1950). Fluorescence images of the tissue slices were then obtained using a confocal laser scanning microscope with a 63x objective lens (Leica TCS SP8 STED). To measure relative distribution of curcumin in a tissue section, the tissue samples were excited using a UV laser with an excitation wavelength of 405 nm and the fluorescence signal corresponding to curcumin fluorescence was detected using a band pass emission filter 495 nm - 561 nm. To identify contributions from the endogenous fluorescence of skin tissue samples, confocal images were also obtained for the control tissue samples not incubated with curcumin. The brightfield images were captured using the transmission channel simultaneously. Triplicate images were then analyzed and annotated using the ImageJ software to assess the mean fluorescence intensity corresponding to delivery of curcumin in the tissue.

### **3.2.8 Quantification of penetrated curcumin in skin layers**

#### **3.2.8.1 Tissue preparation and extraction**

After incubation with curcumin-encapsulated cell carriers, stratum corneum, remaining epidermis and the dermis layer were separated from the treated skin tissue and extracted separately from the tissue samples for a HPLC analysis of curcumin. The corneum layer was firstly removed by tape stripping based on well-established protocols (Breternitz et al., 2007; Nagelreiter et al., 2015). Briefly, regular adhesive tape (3M Deutschland GmbH, Neuss, Germany) was pressed onto the skin top surface using a roller and pressed gently across the tape. The tape was then removed with forceps in one swift movement. The first tape was discarded. Tape stripping was then repeated for 30 times on each site or stopped earlier when small glistening spots indicated that the glistening



layer was reached (Breternitz et al., 2007). The remaining tissue was then soaked in dispase solution (100 units/ml) overnight at 4°C. The epidermis layer was then carefully peeled off from the dermis layer (Kitano and Okada, 1983). Excess enzyme was then washed off using PBS. In order to extract curcumin from the skin tissues, the tapes, epidermis layer and dermis layer were submerged separately in methanol (4 ml) and sonicated for 15 min, followed by gentle shaking for 2 hr in the dark. The obtained methanolic extract solution was then passed through 0.2 µm PTFE filters (Titan 3, Thermo Scientific, Madison, WI, USA) prior to chromatography analysis.

#### 3.2.8.2 HPLC analysis to quantify delivery of curcumin from cell-based carriers

Curcumin extracted from tissue samples was analyzed using a HPLC equipped with a refractive index and a diode array detector (Prominence Liquid Chromatograph, Shimadzu Corp., Kyoto, Japan). Curcumin was separated from the mobile phase using a reverse phase C<sub>18</sub> column (ZORBAX SB-C18, 4.6 · 250 mm, particle size 5-µm, Agilent), and quantified using a binary mobile phase adopted from the previously reported protocol (Heukelem et al., 1992). Briefly, during the first phase of LC separation, solvent A (methanol: 0.5M ammonium acetate, 80:20, acidified to a final pH of 5 using 3 M hydrochloride acid) was maintained for 10 min at a flow rate of 1 ml/min. After the initial 10 min, a linear gradient was programmed to reach 100% of solvent B (methanol: acetone, 70:30) at 20 min. Solvent B was continued for 5 min before returning to the initial conditions. Curcumin was detected using a diode array detector based on the characteristic absorbance peak wavelength of curcumin at 425 nm. The curcumin peak was evident at an elution time around 4.05 min. Extracted curcumin concentration was quantified based on a standard curve generated using a serial dilution of curcumin solution in methanol.

#### **3.2.9 Estimation of the Effective Diffusion Coefficient**

To estimate the effective diffusivity of curcumin from yeast cell carriers to the skin tissue, the fluorescence imaging data was quantified using the Image J software (64-bit, version 1.48). The mean fluorescence signal intensity per unit area (pixel/cm<sup>2</sup>) in porcine tissue cross-section images was quantified as a function of incubation time. Three representative fluorescence images were acquired at each of the four time points (0 hr, 3 hr, 6 hr and 12 hr). This normalized mean fluorescence intensity per unit area was calculated to represent the cumulative concentration of curcumin in a tissue sample as a function of time. Penetration of curcumin in a tissue was modeled based on the Fickian diffusion model for a semi-infinite 1-D slab (the geometries are shown in Fig. 1).

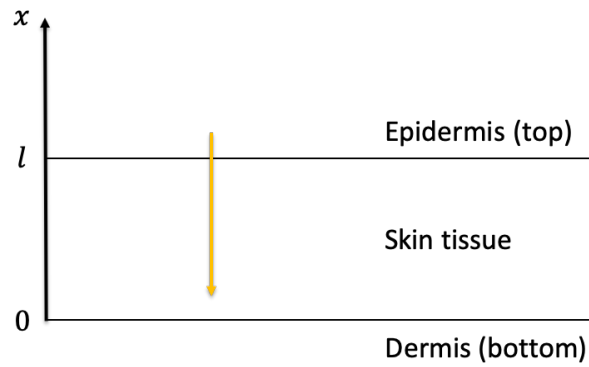


**Figure 3.1.** The 1-D semi-infinite slab diffusion model used to model the diffusion of encapsulated curcumin from microcarriers into skin samples

Fick's Second Law of Diffusion is expressed as  $\frac{\partial C}{\partial t} = D_{eff} \frac{\partial^2 C}{\partial x^2}$ , where  $C$  is the penetrant concentration at depth  $x$  and incubation time  $t$ . The equation was then solved using the following initial and boundary conditions:  $C = C_{cur}$ ,  $x = l$ ,  $t \geq 0$ ;  $C = 0$ ,  $x = 0$ ,  $t \geq 0$ ;  $C = 0$ ,  $0 < x < l$ ,  $t = 0$ . Here the curcumin concentration in the applied yeast matrix was assumed to be constant ( $C_{cur}$ ) on the skin surface ( $x = l$ ), the concentration at the dermis end layer was zero based on the assumed perfect sink condition (Hansen et al., 2013; Todo et al., 2013), and the initial curcumin

concentration within the tissue ( $0 < x < l$ ) was also assumed to be zero as no exogenous curcumin was added to the tissue prior to its incubation with curcumin encapsulated in yeast cells.

The effective diffusion coefficient ( $D_{eff}$ ) was then calculated using the equation 1 based on the total amount  $M_t$  of curcumin in the skin tissue as a function of time  $t$

$$\frac{M_t}{M_\infty} = 1 - \sum_{n=0}^{\infty} \frac{8}{(2n+1)^2\pi^2} \exp\left[-\frac{D_{eff}(2n+1)^2\pi^2 t}{l^2}\right] \quad (\text{Equation 1})$$

$M_\infty$  denotes the uptake quantity after infinite time (the data obtained at 24 hr), and  $l$  (m) denotes the thickness of skin tissue, which was the average value obtained from bright field images. A similar approach has been used to describe the mass transport in skin tissue from microencapsulation carriers (Carreras et al., 2015; Sigurdsson et al., 2013). The effective diffusion coefficient  $D_{eff}$  was then obtained by using a non-linear least square method using the Curve Fitting Function of the MATLAB software. The model was validated with goodness-of-fit parameters RMSE and adjusted  $R^2$ .

### 3.2.10 Statistical analyses

Results are presented as mean  $\pm$  standard deviation. Statistical analyses were conducted using MS Excel. One-way ANOVA and Tukey test were carried out to determine significance variation among groups at level 0.001.

## 3.3. Results and Discussion

### 3.3.1 *S. cerevisiae* cells as encapsulation carriers for hydrophobic compounds

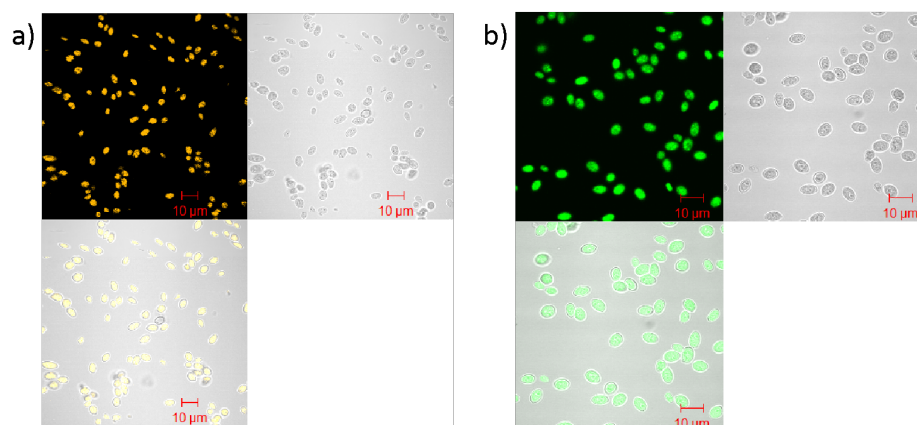


**Figure 3.2.** Fluorescence microscopy images of a) Nile red and b) curcumin encapsulated in yeast cells. The images were acquired using an Olympus IX-7I inverted fluorescence microscope with a 100x objective.

Encapsulation of curcumin and Nile red (as a fluorescence marker) in yeast cells was carried out using the negative pressure-facilitated infusion techniques as described in the materials and methods section. With this encapsulation process, the encapsulation yield was 7.00 mg curcumin/g ( $\pm 0.33$  mg/g) of yeast cell (wet weight). The encapsulation yield is comparable to that found in prior studies that reporting encapsulation yields for curcumin in nanoparticles and other micro- and nano-scale structures (Krausz et al., 2015; Mazzarino et al., 2012; Mukerjee and Vishwanatha, 2009). Using the pressure-assisted encapsulation technology, our group has previously demonstrated significant improvement in encapsulation yield (3 times more curcumin into yeast cell carriers) and process kinetics (more than 200 times faster) compared to passive-diffusion based encapsulation methods (Young et al., 2017).

Fluorescence imaging was used to characterize the intracellular localization of curcumin and Nile red encapsulated in yeast cells respectively. The images in Figure 2(a) and (b) illustrate that encapsulated compounds had a uniform distribution within the cell and the yeast cells maintained structural integrity during the encapsulation process. This result is consistent with the observations

reported in our previous study (Young et al., 2017). A prior study by Paramera et al. (2011) also demonstrated the interactions of curcumin with yeast intracellular components using differential scanning calorimetry (DSC) thermograms. The size and surface charge of the cell-based carriers and chemical properties of the carriers before and after encapsulation was also characterized in our study and the results are presented in the supplementary Table S3.1, given in the Supplementary Information section at the end of the chapter.

### 3.3.2 Attachment of microcarriers to skin surface

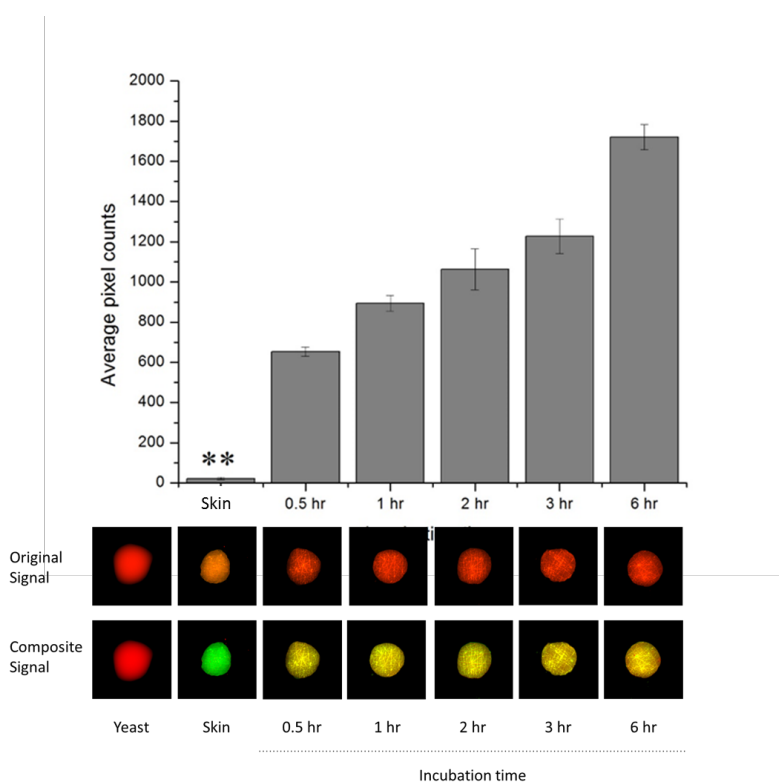


**Figure 3.3.** Maestro *in vitro* fluorescence macro-images of yeast attachment on porcine skin biopsies. The images were acquired using x excitation and y emission channels corresponding to the PI fluorescence properties. The control images of skin biopsies without labeled cells were acquired for spectral unmixing. Original signal represented the raw image, and the composite signal represented the processed signals that represented the source of the fluorescence, e.g. yeast

signal was labelled as red and skin sample signal was labelled as green. The yellow color of incubated skin samples indicated the composite signal of both skin and yeast cells.

We evaluated the affinity of yeast cell carriers to bind the skin surface using quantitative macro-scale imaging. For this imaging, the Maestro™ *in-vivo* fluorescence imaging system was used as described in the materials and methods section. Yeast cells were labeled with a DNA binding PI dye to enable fluorescence measurements. Fluorescence signals of bound yeast cells on the skin tissue samples were acquired as described in the materials and methods section. To distinguish the emission signals of the labeled yeast cells from the endogenous autofluorescence of the tissue, obtained images were processed using the spectral unmixing function, which help differentiate signals with different spectrum and label them with distinct colors. Representative images of the skin tissue upon incubation with yeast cell carriers for different incubation times are shown in Figure 3a. Figure 3b characterizes changes in the mean fluorescence signal intensity corresponding to the binding of yeast cell carriers with the skin tissue as a function of incubation time, e.g. the color changed to yellow after 30min incubation and became increasingly red that resembles yeast signal with longer incubation time. Statistical analysis of the image quantification data showed that significant initial binding took place within the first 30 min of incubation. The amount of bound yeast also increased with an increase in incubation time of yeast cells with the skin tissue. In summary, these results indicate yeast cell carrier has intrinsic bioadhesion properties and is able to bind onto skin surface efficiently with a relatively uniform coverage of the skin tissue.

Although topical binding of *S. cerevisiae* to the skin surface for drug delivery has not been extensively reported before, our observations are consistent with preceding studies regarding *ex vivo* adherence of other fungi species (Duek et al., 2004; Law et al., 1997). The adherence to

epithelial surface is recognized as a first step of microbial colonization and proliferation. Generally, the microbial attachment is initiated by non-specific associations between biomolecules such as hydrophobic interactions between epithelial and fungal lipids. These early, non-specific interactions may facilitate interactions among mannan proteins from yeast cell wall with the glycoproteins or glycolipids on the skin surface, resulting in extended attachment to target sites (Coad et al., 2014; Law et al., 1997). This enhanced binding of encapsulation carriers to target tissues can provide significant advantage for the delivery of bioactive compounds. Bioadhesive liposomes (Margalit et al., 1992), hydrogel (Parente et al., 2015) and nanoparticles (Contri et al., 2014b; Suh et al., 2019) have been proposed to improve topical retention time of the particles, and therefore reduce administration frequency and improve delivery compared to non-adherent particles (Deng et al., 2015). Both non-specific and specific modifications of non-adherent carriers have been proposed to increase their bioadhesion. The examples of non-specific modifications include particle size (Verma et al., 2003), surface charge of the particles, and optimized viscosity of the formulation (Hua et al., 2004). Specific modifications to improve bioadhesion include anchoring specific ligands covalently to the particle surface, which enables high affinity binding to the target membrane receptors or the extracellular matrix (Allen, 2002; Kim et al., 2005; Margalit et al., 1992). In comparison, yeast cell carriers provide intrinsic bioadhesion properties and do not require external modifications to achieve the desired binding of the delivery carriers to the skin surface.

### **3.3.3 Curcumin permeation in porcine skin tissue**

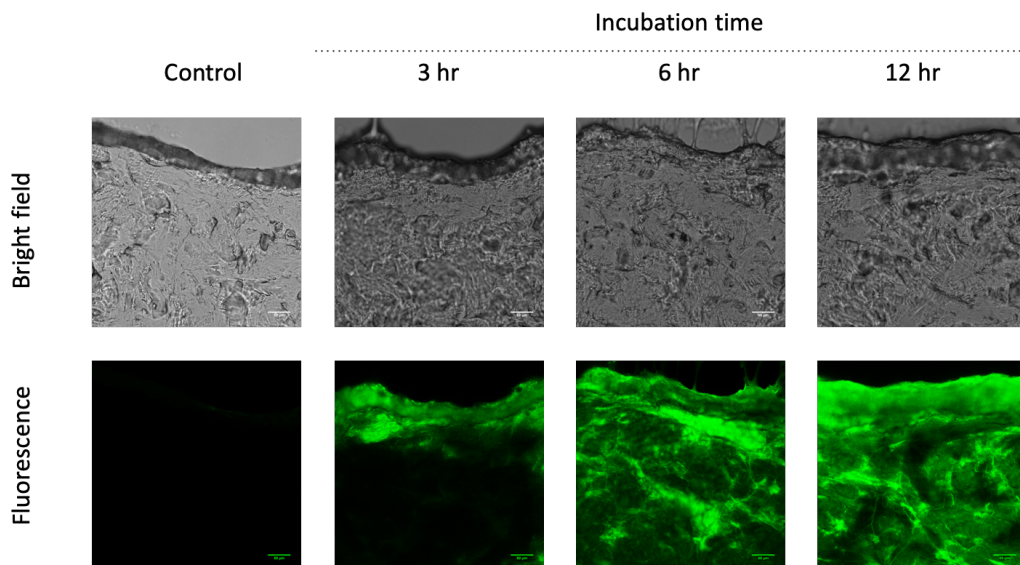


**Figure 3.4.** Curcumin penetration from yeast encapsulation carrier in porcine skin. Bright field and fluorescence microscopy images were acquired using a Leica confocal laser scanning platform TCS SP8 with a 63x objective.

In-vitro release of curcumin in solution from yeast cell carriers was characterized as described in the methods section. The results are presented in the supplementary information section. The results (Fig. S1) illustrate an increase in release of curcumin from yeast cell carriers with an increase in the % DMSO in aqueous solution. After evaluation of release in solution, the release of curcumin from yeast cell carriers was evaluated using skin tissues. Yeast cell carriers with and without curcumin were incubated with porcine skin tissues samples using the vertical Franz *in vitro* diffusion cell. The transdermal distribution of curcumin in a porcine skin was visualized as a function of incubation time using confocal microscopy. The fluorescence imaging data is based on curcumin's intrinsic fluorescence properties and the images illustrate the distribution of curcumin in cross-sectional tissue slices as a function of incubation time. Imaging data was quantified as described in the materials and methods sections. Confocal laser scanning microscopy (CLSM) has been extensively used for visualizing penetration of compounds in the skin (Alvarez-Román et al.,



2004). As shown in Figure 4, curcumin penetrated through stratum corneum within 3 hours of incubation. After incubation for 6 hours, curcumin reached the dermis compartment with a relatively uniform distribution in the dermis. This is consistent with the results of previous studies where curcumin's delivery to the dermis compartment was observed using CLSM after 12-24 hours of *ex vivo* incubation (Lei et al., 2015; Naz and Ahmad, 2015). Furthermore, curcumin release from cells and its penetration into skin tissue was modeled as the Fickian diffusion process through a continuous non-polar pathway based on the moderate hydrophobicity and molecule size of curcumin (Draeos, 2016; Rachmawati et al., 2013; Zhao et al., 2013).

To assess the overall release and diffusion rate of encapsulated compound from yeast cell carrier into skin tissue, the fluorescence imaging data representing the diffusion of curcumin in tissue was quantified to represent the relative concentration levels of curcumin in the tissue. Based on this quantification, the release profile of curcumin as a function of incubation time in the human skin tissue was assessed. This data set (Figure S3.2) represents the normalized average increase in fluorescence intensity of curcumin in the skin tissue. Based on the analytical solution for the 1-D Fickian diffusion in a slab, the effective diffusion coefficient for the transport of curcumin was obtained. The curve fit in supplementary Fig. S2 represents solution of the 1-D diffusion equation as described in the materials and methods section. Equation 1 was solved iteratively to calculate the effective diffusion coefficient for curcumin release into the skin tissue from yeast cell carriers. The key assumption in this calculation is that the transport of curcumin is based on passive diffusion. This assumption is valid as yeast cells remain intact on the surface of skin with extended incubation (data not shown), suggesting that cell lysis has limited role in the transport of curcumin from the carrier to the skin tissue. Thus, the release of curcumin from yeast cell carriers is mediated by passive release from yeast cell carriers followed by diffusion into the skin. Based on these

assumptions the effective diffusion coefficient was calculated to be  $D_{eff} = 2.00 \times 10^{-7}$  cm<sup>2</sup>/hr.

The model fit the observations well with RMSE of 0.0780 and adjusted R<sup>2</sup> of 0.96.

Assessment of an effective diffusion coefficient can provide a quantitative measure to compare the results across different studies (Couto et al., 2014). The effective diffusion coefficient calculated from the imaging measurements is of the same order of magnitude reported for curcumin with other bio-adherent nanoparticle carriers in human buccal tissue (Mazzarino et al., 2012). In some studies, effective diffusion coefficients of higher magnitudes have also been reported for curcumin released from different carriers such as microemulsions (Liu et al., 2011), nanoemulsion (Naz and Ahmad, 2015) and topical gels (Patel et al., 2009) in skin tissue. In many cases, these formulations were combined with chemical diffusion enhancers such as surfactants and organic solvents that may enhance the rate of permeation of curcumin. Many of these surfactants and solvents are potential irritants and thus cannot be used in most product formulations (Al-Rohaimi, 2015). Some of the micro- and nano-scale carriers may also penetrate into the skin through various pathways, which would increase the effective diffusion coefficient of the encapsulated curcumin. This penetration, however, has also raised concerns regarding potential risks for human health (Larese Filon et al., 2015). Furthermore, the slower diffusion rate observed for the yeast cell carriers may indicate the role of yeast cell components such as cell walls and intracellular components in retarding the release of encapsulated curcumin. Higher viscosity of cell-based formulations compared to emulsions may also contribute to the slower release of curcumin from cell-based carriers (Hua et al., 2004). Thus, yeast cell carriers may provide an extended release of curcumin. Retention of encapsulated compounds might be desirable to sustain the release for a longer period of time and reduce administration frequency, especially for compounds with adverse side effects when administered in acute dosages.

Based on our understanding, the release of encapsulated compounds is based on partitioning of the compounds between the yeast cell and its surroundings, based on the chemical potential of the compound in the yeast cell and surrounding compartment. During this partitioning process, the compound can diffuse across a semi-permeable cell wall of yeast microcarriers. In the case of skin tissue, this partitioning is largely influenced by the relative partitioning of compounds between yeast microcarriers and the keratin and lipid rich domain of stratum corneum (Das and Olmsted, 2016). Thus, the rate limiting steps for the topical delivery of curcumin from the cell carriers are adsorption into the stratum corneum from the cell carrier surface, and penetration across this outermost hydrophobic layer on the skin surface, as reported in previous studies (Mitragotri, 2003; Trommer and Neubert, 2006). The partitioning properties of yeast microcarriers can be modified by pre-treatment processes, such as those causing changes in the intracellular composition of yeast cells, and can influence the release properties. This was validated in a simulated gastric and intestinal digestion studies in our prior research. This study also validated the cellular structure of yeast cells including cell wall and intracellular content was maintained despite after extensive treatment with proteases, acids, and surfactants (Young et al., 2020). Thus, the release mechanisms are not induced by degradation of the microcarriers, but rather based on the concentration difference and partitioning properties. Future studies can be designed to evaluate the role of factors such as cell wall integrity and intracellular composition in controlling the release of encapsulated compounds.

In this study, average fluorescence intensities of curcumin and depth of diffusion at different incubation time periods were quantified from confocal images and used for calculating the effective diffusion coefficient. Technically, the flux and the effective diffusion coefficients calculated from imaging measurements might not be directly comparable with those from chemical quantifications due to the limitation of natural fluorophores. The fluorescence quenching of the

fluorophores and the background signal of biological tissues might also limit the sensitivity of fluorescence measurements. Despite these constraints, imaging data provides relative quantitative information of the spatial diffusion profile across different layers in a skin tissue and this information is helpful as localization of the delivered compound in different skin compartments is fundamentally associated with its biological functionalities (Brown et al., 2006; Yamashita and Hashida, 2003). Such quantitative information is usually not easily attainable using conventional analytical approaches, which often require extraction of compounds from tissue samples.

### 3.3.4 Visualization and quantification of curcumin retention in human skin tissue

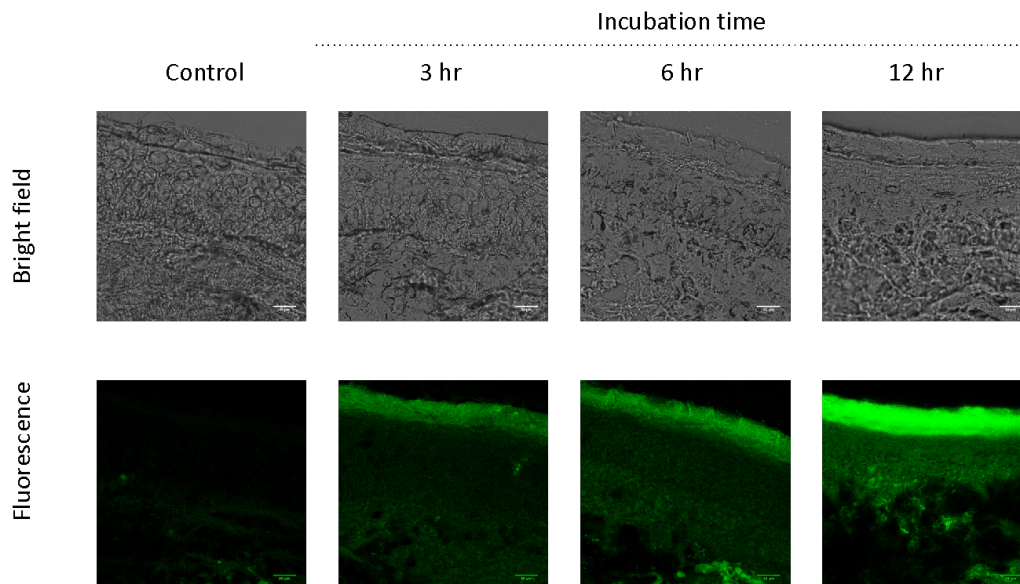


**Figure 3.5.** Curcumin penetration from yeast encapsulation carrier in human skin. Bright field and fluorescence microscopy images were taken in triplicates using a Leica confocal laser scanning platform TCS SP8 with a 63x objective.

In order to validate the observations made using a porcine tissue model, delivery of curcumin in a human skin biopsy model system was further evaluated. 13 pieces of healthy human facial skin biopsies were collected from 7 Mohs surgery patients and analyzed using a combination of

fluorescence imaging and HPLC quantification. Consistent with the results in Figure 4, Figure 5 shows that curcumin penetrated the stratum corneum within 3 hours of topical application on the ex-vivo biopsy skin of the yeast cell carriers with encapsulated curcumin. After incubation for 12 hours, curcumin was distributed relatively uniformly in both the stratum corneum and dermis compartments of the human skin biopsies. Overall, these results suggest efficient release of curcumin from cell carriers on the skin surface followed by permeation across the stratum corneum to the epidermis and dermis compartments of the tissue (Alkilani et al., 2015; Mitragotri, 2003).

The observed transdermal delivery of curcumin in human skin tissue (Fig. 4) is consistent with the pattern shown by the porcine ex-vivo skin model in the previous section (Fig. 3). Pig skin tissue has been widely used as a model for human skin in transdermal studies since pig skin tissue shares similar anatomic and physiological characteristics with human tissue (Barbero and Frasch, 2009; Godin and Touitou, 2007). Based on the imaging observations of human biopsies, the overall fluorescence intensity was lower in the case of human tissue when compared to pig tissue. Higher permeability of hydrophobic substances in porcine skin has been observed in previous studies (Godin and Touitou, 2007). In this study, the difference in the quantities of delivered curcumin between porcine and human tissue might also be attributed to the structural intactness of biopsied human skin. Before harvesting, the porcine skin underwent mechanical and chemical treatments, such as scalding and hair removal agents, which could reduce the barrier property of the stratum corneum and increase the tissue permeability.

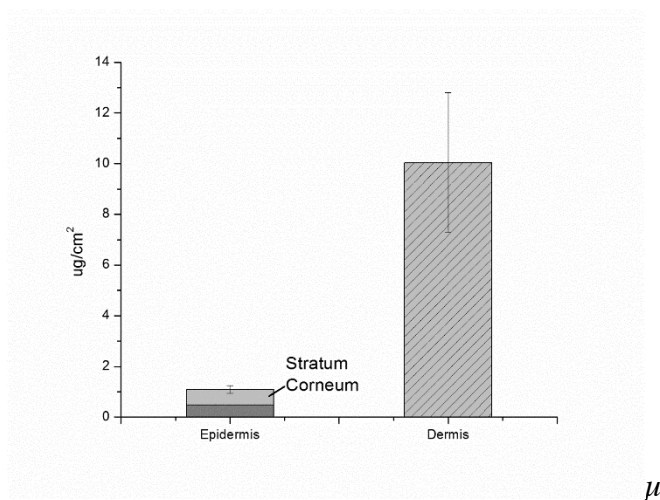


**Figure 3.6.** HPLC quantification of cumulated curcumin in human facial skin tissue by a) tape-stripping and dispase separation of dermis and epidermis. Measurement was carried out after 12 hr incubation of skin topically with curcumin-yeast encapsulation system.

To quantitatively understand cutaneous delivery of curcumin from yeast encapsulation carriers, curcumin deposition in different layers of human skin tissue after 12 hours of incubation was analyzed using HPLC (Figure 6). The amount of curcumin retained in the stratum corneum, the epidermis and the dermis layer were  $0.64 \pm 0.07 \mu\text{g}/\text{cm}^2$ ,  $0.40 \pm 0.19 \mu\text{g}/\text{cm}^2$  and  $9.85 \pm 1.38 \mu\text{g}/\text{cm}^2$ , respectively (Figure 6). Based on this cumulative measurement of curcumin, the average flux of curcumin in the skin tissue  $J_p$  equals  $0.89 \pm 0.02 \mu\text{g}/\text{cm}^2/\text{h}$ . The total amount of delivered curcumin is within the range of results reported by previous studies on curcumin and other related phenolic compounds in skin tissue (Chen et al., 2012; Friedrich et al., 2015; Liu et al., 2011).

In Figure 5 is also observed a significantly higher brightness in the outermost corneum layer of the tissue cross-sections. This is consistent with the HPLC analysis results, which suggested that the stratum corneum, with 10% of the total thickness of the epidermis layer, contained 57% of the total amount of curcumin that had been delivered into the epidermis of the skin samples.

This phenomenon was previously referred to as the reservoir function of the stratum corneum (Jacobi et al., 2005) and can be observed in the confocal imaging data as well. This localization could result from the moderate hydrophobicity of the curcumin, which facilitates the hydrophobic interactions with the lipophilic composition of the stratum corneum.

Furthermore, Figure 6 showed that a significant amount of curcumin accumulated in the dermis layer after 12 hours for incubation. This trend is in agreement with a prior study using a topical delivery of curcumin in a skin tissue (Friedrich et al., 2015). The accumulation of curcumin in the dermis could be attributed to the fact that dermis occupies a majority of the tissue mass per surface area (van der Maaden et al., 2012) and curcumin continuously diffused from the epidermis layer through non-polar pathways into the dermis region (Goates and Knutson, 1994). Both the imaging results and analytical quantification using HPLC demonstrate efficient permeation of curcumin in the human skin tissue using the yeast cell carriers.

## **Conclusion**

In summary, this study demonstrates the efficacy of a novel topical delivery carrier for the controlled release of bioactive compounds to the skin tissue. The results illustrate rapid binding of the cell-based encapsulation carrier (yeast cells) to the skin tissue upon topical incubation. The binding of the cell based microcarrier increased with incubation time on the skin tissue. The cell-based microcarriers encapsulated a model bioactive with relatively high efficiency compared to conventional encapsulation approaches. The microcarriers provided controlled release of the encapsulated bioactive into the skin tissue and enhanced both the released amount and the permeation of the bioactive to the dermal section of the *ex-vivo* skin tissue. Overall, the results of this study illustrate a novel, cost-effective encapsulation and controlled release system for topical delivery of bioactives to the skin tissue. Further studies, including clinical studies, will develop clinical applications of this delivery system to promote health and clinical needs.



## Supporting information

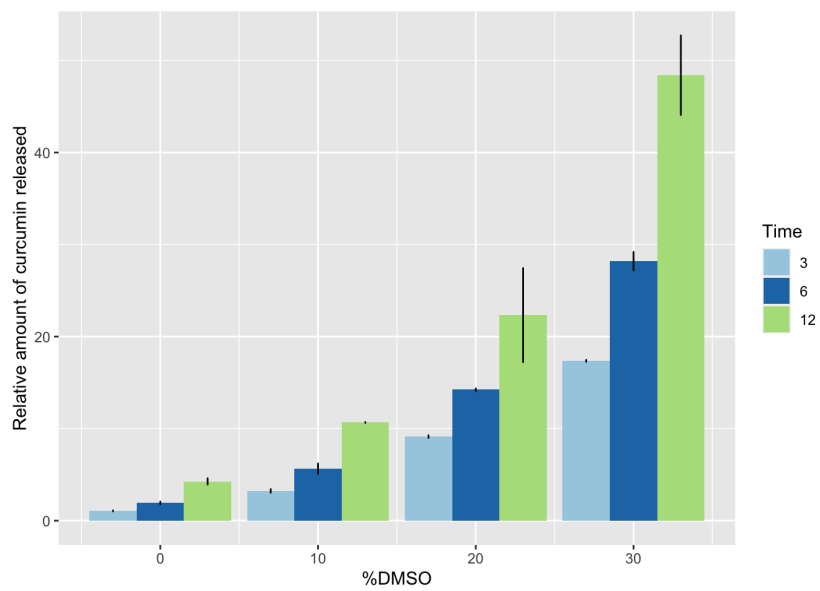


**Figure S3.1** The release of curcumin from yeast cell carriers as function of incubation time and percentage of DMSO in aqueous solution using a Transwell chamber.

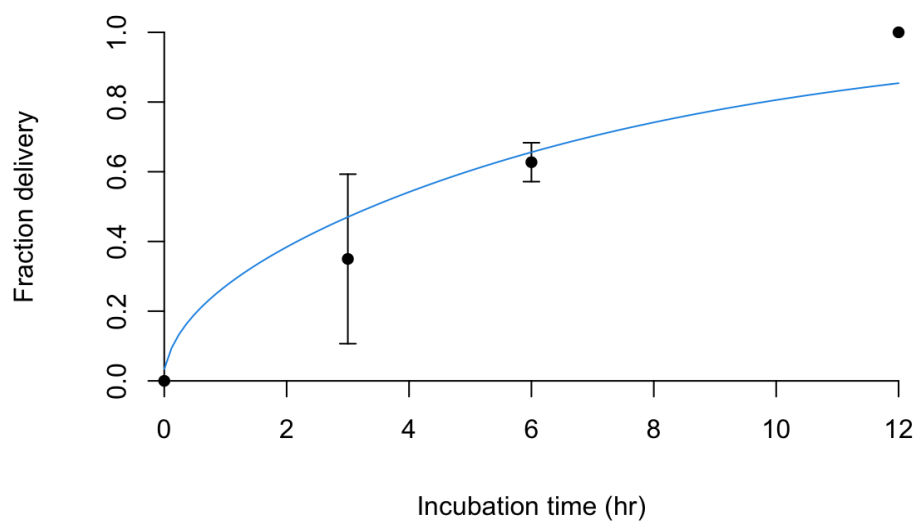


**Fig S3.2** Release of curcumin from yeast cell carriers into human skin tissue measured based on the quantification of average fluorescence intensity in the skin tissue as a function of topical incubation time of yeast cell carriers with curcumin on the isolated skin tissue.

**Table S3.1** Particle size and zeta potential of native yeast carriers and yeast carriers after infusion of curcumin

	Particle size (um) (mean±sd)	PDI	Zeta potential (mV) (mean±sd)
Native yeast carrier	6.10±0.427	0.09±0.024	-22.51±0.414
Curcumin infused yeast carrier	6.86±0.036	0.17±0.003	-21.60±0.844

## References

- Alkilani, A.Z., McCrudden, M.T.C., Donnelly, R.F., 2015. Transdermal Drug Delivery: Innovative Pharmaceutical Developments Based on Disruption of the Barrier Properties of the stratum corneum. *Pharmaceutics* 7, 438–470. doi:10.3390/pharmaceutics7040438
- Allen, T.M., 2002. Ligand-targeted therapeutics in anticancer therapy. *Nat. Rev. Cancer* 2, 750–763. doi:10.1038/nrc903
- Al-Rohaimi, A.H., 2015. Comparative anti-inflammatory potential of crystalline and amorphous nano curcumin in topical drug delivery. *J. Oleo Sci.* 64, 27–40. doi:10.5650/jos.ess14175
- Alvarez-Román, R., Naik, A., Kalia, Y.N., Fessi, H., Guy, R.H., 2004. Visualization of skin penetration using confocal laser scanning microscopy. *Eur J Pharm Biopharm* 58, 301–316. doi:10.1016/j.ejpb.2004.03.027
- Barbero, A.M., Frasc, H.F., 2009. Pig and guinea pig skin as surrogates for human in vitro penetration studies: a quantitative review. *Toxicol. In Vitro* 23, 1–13. doi:10.1016/j.tiv.2008.10.008
- Belkaid, Y., Tamoutounour, S., 2016. The influence of skin microorganisms on cutaneous immunity. *Nat. Rev. Immunol.* 16, 353–366. doi:10.1038/nri.2016.48
- Bishop, J.R., Nelson, G., Lamb, J., 1998. Microencapsulation in yeast cells. *J Microencapsul* 15, 761–773. doi:10.3109/02652049809008259
- Breternitz, M., Flach, M., Prässler, J., Elsner, P., Fluhr, J.W., 2007. Acute barrier disruption by adhesive tapes is influenced by pressure, time and anatomical location: integrity and cohesion assessed by sequential tape stripping. A randomized, controlled study. *Br. J. Dermatol.* 156, 231–240. doi:10.1111/j.1365-2133.2006.07632.x
- Brown, M.B., Martin, G.P., Jones, S.A., Akomeah, F.K., 2006. Dermal and transdermal drug delivery systems: current and future prospects. *Drug Deliv* 13, 175–187.

doi:10.1080/10717540500455975

Carreras, N., Alonso, C., Martí, M., Lis, M.J., 2015. Mass transport model through the skin by microencapsulation system. *J Microencapsul* 32, 358–363.

doi:10.3109/02652048.2015.1028495

Chen, Y., Wu, Q., Zhang, Z., Yuan, L., Liu, X., Zhou, L., 2012. Preparation of curcumin-loaded liposomes and evaluation of their skin permeation and pharmacodynamics. *Molecules* 17, 5972–5987. doi:10.3390/molecules17055972

Chun, K.-S., Keum, Y.-S., Han, S.S., Song, Y.-S., Kim, S.-H., Surh, Y.-J., 2003. Curcumin inhibits phorbol ester-induced expression of cyclooxygenase-2 in mouse skin through suppression of extracellular signal-regulated kinase activity and NF-kappaB activation. *Carcinogenesis* 24, 1515–1524. doi:10.1093/carcin/bgg107

Ciamponi, F., Duckham, C., Tirelli, N., 2012. Yeast cells as microcapsules. Analytical tools and process variables in the encapsulation of hydrophobes in *S. cerevisiae*. *Appl. Microbiol. Biotechnol.* 95, 1445–1456. doi:10.1007/s00253-012-4127-8

Coad, B.R., Kidd, S.E., Ellis, D.H., Griesser, H.J., 2014. Biomaterials surfaces capable of resisting fungal attachment and biofilm formation. *Biotechnol. Adv.* 32, 296–307. doi:10.1016/j.biotechadv.2013.10.015

Contri, R.V., Frank, L.A., Kaiser, M., Pohlmann, A.R., Guterres, S.S., 2014a. The use of nanoencapsulation to decrease human skin irritation caused by capsaicinoids. *Int. J. Nanomedicine* 9, 951–962. doi:10.2147/IJN.S56579

Contri, R.V., Katzer, T., Ourique, A.F., da Silva, A.L.M., Beck, R.C.R., Pohlmann, A.R., Guterres, S.S., 2014b. Combined effect of polymeric nanocapsules and chitosan hydrogel on the increase of capsaicinoids adhesion to the skin surface. *J Biomed Nanotechnol* 10, 820–830. doi:10.1166/jbn.2014.1752

- Couto, A., Fernandes, R., Cordeiro, M.N.S., Reis, S.S., Ribeiro, R.T., Pessoa, A.M., 2014. Dermic diffusion and stratum corneum: a state of the art review of mathematical models. *J. Control. Release* 177, 74–83. doi:10.1016/j.jconrel.2013.12.005
- Das, C., Olmsted, P.D., 2016. The physics of stratum corneum lipid membranes. *Philos. Trans. A, Math. Phys. Eng. Sci.* 374. doi:10.1098/rsta.2015.0126
- De Luca, C., Valacchi, G., 2010. Surface lipids as multifunctional mediators of skin responses to environmental stimuli. *Mediators Inflamm.* 2010, 321494. doi:10.1155/2010/321494
- De, M.C.V.P.L., DOMENES, P.R.D., NICOLI, J.R., DOS, S.M.F., SOARES, S.A.K., DA, S.S.H., 2017. Cosmetic composition having probiotic bacteria. WO2017063066 A1.
- Deng, Y., Ediriwickrema, A., Yang, F., Lewis, J., Girardi, M., Saltzman, W.M., 2015. A sunblock based on bioadhesive nanoparticles. *Nat. Mater.* 14, 1278–1285. doi:10.1038/nmat4422
- Draelos, Z.K. (Ed.), 2016. *Cosmetic dermatology: products and procedures*, Second edition. ed. John Wiley & Sons, Ltd, Chichester, West Sussex, UK ; Hoboken, NJ, USA.
- Dranginis, A.M., Rauceo, J.M., Coronado, J.E., Lipke, P.N., 2007. A biochemical guide to yeast adhesins: glycoproteins for social and antisocial occasions. *Microbiol. Mol. Biol. Rev.* 71, 282–294. doi:10.1128/MMBR.00037-06
- Duek, L., Kaufman, G., Ulman, Y., Berdicevsky, I., 2004. The pathogenesis of dermatophyte infections in human skin sections. *J. Infect.* 48, 175–180. doi:10.1016/j.jinf.2003.09.008
- Elias, P.M., 1983. Epidermal lipids, barrier function, and desquamation. *J. Invest. Dermatol.* 80, 44s–9s. doi:10.1038/jid.1983.12
- Findley, K., Oh, J., Yang, J., Conlan, S., Deming, C., Meyer, J.A., Schoenfeld, D., Nomicos, E., Park, M., NIH Intramural Sequencing Center Comparative Sequencing Program, Kong, H.H., Segre, J.A., 2013. Topographic diversity of fungal and bacterial communities in

- human skin. *Nature* 498, 367–370. doi:10.1038/nature12171
- Friedrich, R.B., Kann, B., Coradini, K., Offerhaus, H.L., Beck, R.C.R., Windbergs, M., 2015. Skin penetration behavior of lipid-core nanocapsules for simultaneous delivery of resveratrol and curcumin. *Eur J Pharm Sci* 78, 204–213. doi:10.1016/j.ejps.2015.07.018
- Gaspar, R.B., Nele, M., Ferraz, H.C., 2017. Encapsulation of  $\alpha$ -tocopherol and  $\beta$ -carotene in concentrated oil-in-water beverage emulsions stabilized with whey protein isolate. *J Dispers Sci Technol* 38, 89–95. doi:10.1080/01932691.2016.1144196
- Goates, C.Y., Knutson, K., 1994. Enhanced permeation of polar compounds through human epidermis. I. Permeability and membrane structural changes in the presence of short chain alcohols. *Biochimica et Biophysica Acta (BBA) - Biomembranes* 1195, 169–179. doi:10.1016/0005-2736(94)90024-8
- Godin, B., Touitou, E., 2007. Transdermal skin delivery: predictions for humans from in vivo, ex vivo and animal models. *Adv. Drug Deliv. Rev.* 59, 1152–1161. doi:10.1016/j.addr.2007.07.004
- Grice, E.A., Segre, J.A., 2011. The skin microbiome. *Nat. Rev. Microbiol.* 9, 244–253. doi:10.1038/nrmicro2537
- Griesser, M., Pistis, V., Suzuki, T., Tejera, N., Pratt, D.A., Schneider, C., 2011. Autoxidative and cyclooxygenase-2 catalyzed transformation of the dietary chemopreventive agent curcumin. *J. Biol. Chem.* 286, 1114–1124. doi:10.1074/jbc.M110.178806
- Hansen, S., Lehr, C.-M., Schaefer, U.F., 2013. Improved input parameters for diffusion models of skin absorption. *Adv. Drug Deliv. Rev.* 65, 251–264. doi:10.1016/j.addr.2012.04.011
- Heng, M.C., Song, M.K., Harker, J., Heng, M.K., 2000. Drug-induced suppression of phosphorylase kinase activity correlates with resolution of psoriasis as assessed by clinical, histological and immunohistochemical parameters. *Br. J. Dermatol.* 143, 937–

949. doi:10.1046/j.1365-2133.2000.03767.x
- Heukelem, L., Lewitus, A.J., Kana, T.M., Craft, N.E., 1992. High-performance liquid chromatography of phytoplankton pigments using a polymeric reversed-phase c18 column1. *J Phycol* 28, 867–872. doi:10.1111/j.0022-3646.1992.00867.x
- Hua, L., Weisan, P., Jiayu, L., Ying, Z., 2004. Preparation, evaluation, and NMR characterization of vinpocetine microemulsion for transdermal delivery. *Drug Dev Ind Pharm* 30, 657–666. doi:10.1081/ddc-120039183
- Jacobi, U., Waibler, E., Sterry, W., Lademann, J., 2005. In vivo determination of the long-term reservoir of the horny layer using laser scanning microscopy. *Laser Physics* 15, 565–569.
- Karande, P., Mitragotri, S., 2009. Enhancement of transdermal drug delivery via synergistic action of chemicals. *Biochim. Biophys. Acta* 1788, 2362–2373. doi:10.1016/j.bbamem.2009.08.015
- Kim, W.J., Yockman, J.W., Lee, M., Jeong, J.H., Kim, Y.-H., Kim, S.W., 2005. Soluble Flt-1 gene delivery using PEI-g-PEG-RGD conjugate for anti-angiogenesis. *J. Control. Release* 106, 224–234. doi:10.1016/j.jconrel.2005.04.016
- Kitano, Y., Okada, N., 1983. Separation of the epidermal sheet by dispase. *Br. J. Dermatol.* 108, 555–560. doi:10.1111/j.1365-2133.1983.tb01056.x
- Kollár, R., Reinhold, B.B., Petráková, E., Yeh, H.J., Ashwell, G., Drgonová, J., Kapteyn, J.C., Klis, F.M., Cabib, E., 1997. Architecture of the yeast cell wall. Beta(1-->6)-glucan interconnects mannoprotein, beta(1-->)3-glucan, and chitin. *J. Biol. Chem.* 272, 17762–17775. doi:10.1074/jbc.272.28.17762
- Krausz, A.E., Adler, B.L., Cabral, V., Navati, M., Doerner, J., Charafeddine, R.A., Chandra, D., Liang, H., Gunther, L., Clendaniel, A., Harper, S., Friedman, J.M., Nosanchuk, J.D., Friedman, A.J., 2015. Curcumin-encapsulated nanoparticles as innovative antimicrobial

- and wound healing agent. *Nanomedicine* 11, 195–206. doi:10.1016/j.nano.2014.09.004
- Larese Filon, F., Mauro, M., Adami, G., Bovenzi, M., Crosera, M., 2015. Nanoparticles skin absorption: New aspects for a safety profile evaluation. *Regul Toxicol Pharmacol* 72, 310–322. doi:10.1016/j.yrtph.2015.05.005
- Law, S., Fotos, P.G., Wertz, P.W., 1997. Skin surface lipids inhibit adherence of *Candida albicans* to stratum corneum. *Dermatology (Basel)* 195, 220–223. doi:10.1159/000245946
- Lei, M., Wang, J., Ma, M., Yu, M., Tan, F., Li, N., 2015. Dual drug encapsulation in a novel nano-vesicular carrier for the treatment of cutaneous melanoma: characterization and in vitro/in vivo evaluation. *RSC Adv.* 5, 20467–20478. doi:10.1039/C4RA16306K
- Liu, C.-H., Chang, F.-Y., Hung, D.-K., 2011. Terpene microemulsions for transdermal curcumin delivery: effects of terpenes and cosurfactants. *Colloids Surf. B, Biointerfaces* 82, 63–70. doi:10.1016/j.colsurfb.2010.08.018
- Margalit, R., Okon, M., Yerushalmi, N., Avidor, E., 1992. Bioadhesive liposomes as topical drug delivery systems: molecular and cellular studies. *J. Control. Release* 19, 275–287. doi:10.1016/0168-3659(92)90083-4
- Mazzarino, L., Travelet, C., Ortega-Murillo, S., Otsuka, I., Pignot-Paintrand, I., Lemos-Senna, E., Borsali, R., 2012. Elaboration of chitosan-coated nanoparticles loaded with curcumin for mucoadhesive applications. *J. Colloid Interface Sci.* 370, 58–66. doi:10.1016/j.jcis.2011.12.063
- Mitragotri, S., 2003. Modeling skin permeability to hydrophilic and hydrophobic solutes based on four permeation pathways. *J. Control. Release* 86, 69–92. doi:10.1016/s0168-3659(02)00321-8
- Modrzyński, J.J., Christensen, J.H., Brandt, K.K., 2019. Evaluation of dimethyl sulfoxide



- (DMSO) as a co-solvent for toxicity testing of hydrophobic organic compounds. *Ecotoxicology* 28, 1136–1141. doi:10.1007/s10646-019-02107-0
- Mukerjee, A., Vishwanatha, J.K., 2009. Formulation, characterization and evaluation of curcumin-loaded PLGA nanospheres for cancer therapy. *Anticancer Res.* 29, 3867–3875.
- Nagelreiter, C., Mahrhauser, D., Wiatschka, K., Skipiol, S., Valenta, C., 2015. Importance of a suitable working protocol for tape stripping experiments on porcine ear skin: Influence of lipophilic formulations and strip adhesion impairment. *Int. J. Pharm.* 491, 162–169. doi:10.1016/j.ijpharm.2015.06.031
- Naz, Z., Ahmad, F.J., 2015. Curcumin-loaded colloidal carrier system: formulation optimization, mechanistic insight, ex vivo and in vivo evaluation. *Int. J. Nanomedicine* 10, 4293–4307. doi:10.2147/IJN.S82788
- Nelson, G., Duckham, S.C., Crothers, M.E.D., 2006. Microencapsulation in yeast cells and applications in drug delivery, in: Svenson, S. (Ed.), *Polymeric Drug Delivery I: Particulate Drug Carriers*, ACS Symposium Series. American Chemical Society, Washington, DC, pp. 268–281. doi:10.1021/bk-2006-0923.ch019
- O’neill, C., McBAIN, A., 2013. Probiotic bacteria. WO2013153358 A1.
- Panuszko, A., Bruździak, P., Śmiechowski, M., Stasiulewicz, M., Stefaniak, J., Stangret, J., 2019. DMSO hydration redefined: Unraveling the hydrophobic hydration of solutes with a mixed hydrophilic–hydrophobic characteristic. *J Mol Liq* 294, 111661. doi:10.1016/j.molliq.2019.111661
- Paramera, E.I., Konteles, S.J., Karathanos, V.T., 2011. Microencapsulation of curcumin in cells of *Saccharomyces cerevisiae*. *Food Chem.* 125, 892–902. doi:10.1016/j.foodchem.2010.09.063
- Parente, M.E., Ochoa Andrade, A., Ares, G., Russo, F., Jiménez-Kairuz, Á., 2015. Bioadhesive

- hydrogels for cosmetic applications. *Int J Cosmet Sci* 37, 511–518.  
doi:10.1111/ics.12227
- Patel, N.A., Patel, N.J., Patel, R.P., 2009. Formulation and evaluation of curcumin gel for topical application. *Pharm Dev Technol* 14, 80–89. doi:10.1080/10837450802409438
- Rachmawati, H., Edityaningrum, C.A., Mauludin, R., 2013. Molecular inclusion complex of curcumin- $\beta$ -cyclodextrin nanoparticle to enhance curcumin skin permeability from hydrophilic matrix gel. *AAPS PharmSciTech* 14, 1303–1312. doi:10.1208/s12249-013-0023-5
- Ramezanli, T., Kilfoyle, B.E., Zhang, Z., Michniak-Kohn, B.B., 2017. Polymeric nanospheres for topical delivery of vitamin D3. *Int. J. Pharm.* 516, 196–203.  
doi:10.1016/j.ijpharm.2016.10.072
- Rawal, R.C., Shah, B.J., Jayaraaman, A.M., Jaiswal, V., 2009. Clinical evaluation of an Indian polyherbal topical formulation in the management of eczema. *J. Altern. Complement. Med.* 15, 669–672. doi:10.1089/acm.2008.0508
- Romero-Steiner, S., Witek, T., Balish, E., 1990. Adherence of skin bacteria to human epithelial cells. *J. Clin. Microbiol.* 28, 27–31. doi:10.1128/jcm.28.1.27-31.1990
- Salari, R., Rajabi, O., Khashyarmanesh, Z., Fathi Najafi, M., Fazly Bazzaz, B.S., 2015. Characterization of Encapsulated Berberine in Yeast Cells of *Saccharomyces cerevisiae*. *Iran J Pharm Res* 14, 1247–1256.
- Shalaby, T.I., El-Refaie, W.M., 2018. Bioadhesive Chitosan-Coated Cationic Nanoliposomes With Improved Insulin Encapsulation and Prolonged Oral Hypoglycemic Effect in Diabetic Mice. *J. Pharm. Sci.* 107, 2136–2143. doi:10.1016/j.xphs.2018.04.011
- Shi, G., Rao, L., Yu, H., Xiang, H., Yang, H., Ji, R., 2008. Stabilization and encapsulation of photosensitive resveratrol within yeast cell. *Int. J. Pharm.* 349, 83–93.

doi:10.1016/j.ijpharm.2007.07.044

Sigurdsson, H.H., Kirch, J., Lehr, C.-M., 2013. Mucus as a barrier to lipophilic drugs. *Int. J. Pharm.* 453, 56–64. doi:10.1016/j.ijpharm.2013.05.040

Silva, L.A.D., Andrade, L.M., de Sá, F.A.P., Marreto, R.N., Lima, E.M., Gratieri, T., Taveira, S.F., 2016. Clobetasol-loaded nanostructured lipid carriers for epidermal targeting. *J. Pharm. Pharmacol.* 68, 742–750. doi:10.1111/jphp.12543

Soto, E.R., Ostroff, G.R., 2008. Characterization of multilayered nanoparticles encapsulated in yeast cell wall particles for DNA delivery. *Bioconjug. Chem.* 19, 840–848. doi:10.1021/bc700329p

Srinivasarao, M., Low, P.S., 2017. Ligand-Targeted Drug Delivery. *Chem. Rev.* 117, 12133–12164. doi:10.1021/acs.chemrev.7b00013

Su, R., Fan, W., Yu, Q., Dong, X., Qi, J., Zhu, Q., Zhao, W., Wu, W., Chen, Z., Li, Y., Lu, Y., 2017. Size-dependent penetration of nanoemulsions into epidermis and hair follicles: implications for transdermal delivery and immunization. *Oncotarget* 8, 38214–38226. doi:10.18632/oncotarget.17130

Suh, H.-W., Lewis, J., Fong, L., Ramseier, J.Y., Carlson, K., Peng, Z.-H., Yin, E.S., Saltzman, W.M., Girardi, M., 2019. Biodegradable bioadhesive nanoparticle incorporation of broad-spectrum organic sunscreen agents. *Bioeng. Transl. Med.* 4, 129–140. doi:10.1002/btm2.10092

Teichmann, A., Heuschkel, S., Jacobi, U., Presse, G., Neubert, R.H.H., Sterry, W., Lademann, J., 2007. Comparison of stratum corneum penetration and localization of a lipophilic model drug applied in an o/w microemulsion and an amphiphilic cream. *Eur J Pharm Biopharm* 67, 699–706. doi:10.1016/j.ejpb.2007.04.006

Thomas, B.J., Finnin, B.C., 2004. The transdermal revolution. *Drug Discov. Today* 9, 697–703.

doi:10.1016/S1359-6446(04)03180-0

Todo, H., Oshizaka, T., Kadhum, W.R., Sugibayashi, K., 2013. Mathematical model to predict skin concentration after topical application of drugs. *Pharmaceutics* 5, 634–651.

doi:10.3390/pharmaceutics5040634

Tønnesen, H.H., Másson, M., Loftsson, T., 2002. Studies of curcumin and curcuminoids. XXVII. Cyclodextrin complexation: solubility, chemical and photochemical stability. *Int. J. Pharm.* 244, 127–135. doi:10.1016/s0378-5173(02)00323-x

doi:10.1016/s0378-5173(02)00323-x

Trommer, H., Neubert, R.H.H., 2006. Overcoming the stratum corneum: the modulation of skin penetration. A review. *Skin Pharmacol. Physiol.* 19, 106–121. doi:10.1159/000091978

US5288632A - Encapsulation of material in microbial cells - Google Patents [WWW

Document], n.d. URL <https://patents.google.com/patent/US5288632A/en> (accessed 6.28.21).

van der Maaden, K., Jiskoot, W., Bouwstra, J., 2012. Microneedle technologies for (trans)dermal drug and vaccine delivery. *J. Control. Release* 161, 645–655.

doi:10.1016/j.jconrel.2012.01.042

Vaughn, A.R., Branum, A., Sivamani, R.K., 2016. Effects of Turmeric (*Curcuma longa*) on Skin Health: A Systematic Review of the Clinical Evidence. *Phytother Res* 30, 1243–1264.

doi:10.1002/ptr.5640

Verma, D.D., Verma, S., Blume, G., Fahr, A., 2003. Particle size of liposomes influences dermal delivery of substances into skin. *Int. J. Pharm.* 258, 141–151. doi:10.1016/s0378-

5173(03)00183-2

Vollono, L., Falconi, M., Gaziano, R., Iacovelli, F., Dika, E., Terracciano, C., Bianchi, L., Campione, E., 2019. Potential of curcumin in skin disorders. *Nutrients* 11.

doi:10.3390/nu11092169

- Yamashita, F., Hashida, M., 2003. Mechanistic and empirical modeling of skin permeation of drugs. *Adv. Drug Deliv. Rev.* 55, 1185–1199. doi:10.1016/S0169-409X(03)00118-2
- Young, S., Dea, S., Nitin, N., 2017. Vacuum facilitated infusion of bioactives into yeast microcarriers: Evaluation of a novel encapsulation approach. *Food Res. Int.* 100, 100–112. doi:10.1016/j.foodres.2017.07.067
- Young, S., Nitin, N., 2019. Thermal and oxidative stability of curcumin encapsulated in yeast microcarriers. *Food Chem.* 275, 1–7. doi:10.1016/j.foodchem.2018.08.121
- Young, S., Rai, R., Nitin, N., 2020. Bioaccessibility of curcumin encapsulated in yeast cells and yeast cell wall particles. *Food Chem.* 309, 125700. doi:10.1016/j.foodchem.2019.125700
- Zhao, Y.-Z., Lu, C.-T., Zhang, Y., Xiao, J., Zhao, Y.-P., Tian, J.-L., Xu, Y.-Y., Feng, Z.-G., Xu, C.-Y., 2013. Selection of high efficient transdermal lipid vesicle for curcumin skin delivery. *Int. J. Pharm.* 454, 302–309. doi:10.1016/j.ijpharm.2013.06.052
- Zillich, O.V., Schweiggert-Weisz, U., Hasenkopf, K., Eisner, P., Kersch, M., 2013. Release and in vitro skin permeation of polyphenols from cosmetic emulsions. *Int J Cosmet Sci* 35, 491–501. doi:10.1111/ics.12072

## Chapter 4

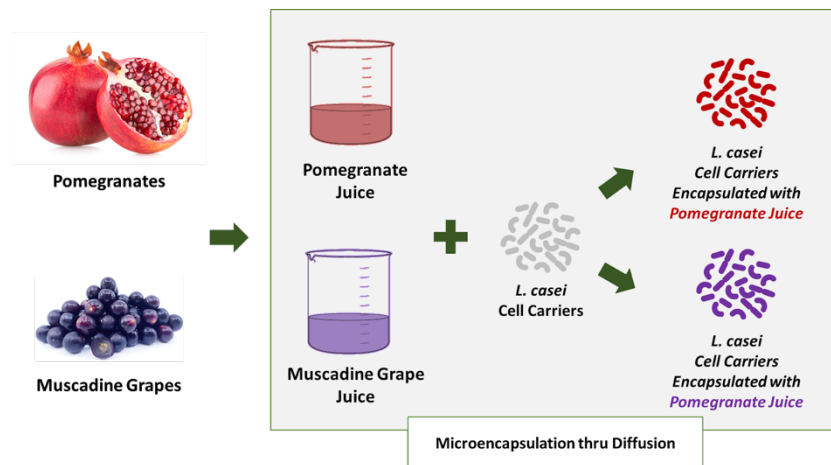
### Encapsulation of polyphenolics from pomegranate and grape juices in a model lactic acid bacterium

#### Abstract

This study was aimed at developing an innovative cell-based carrier to encapsulate phytochemicals from complex plant sources. The overall objective was to evaluate the encapsulation of a diverse range of phytochemicals directly from fruit juices using inactivated probiotic bacteria *Lactobacillus casei* as a model microcarrier. Muscadine grape (MG) juice and pomegranate (Pom) juice were prepared from fresh fruit and used as sample juices. After incubation with inactivated bacterial cells, 64.36 % and 66.97 % of the total anthocyanins, and 60.81 % and 72.67 % of the total antioxidant compounds, were encapsulated in the microcarrier from Pom and MG juices respectively. Confocal images illustrated a uniform localization of the encapsulated material in the cell carrier. The spectral emission scans indicated the presence of a diverse class of polyphenolic compounds, which was then characterized using high performance liquid chromatography (HPLC). Using HPLC, diverse phytochemical compound classes were analyzed, including flavanols (catechin and epicatechin), phenolic acid (gallic acid and caffeic acid) and hydroxycinnamic acid (coumaric acid), flavonols (quercetin and glycosylated myricetin), and polymeric polyphenols. The analysis validated that the cell carrier could encapsulate a broad profile of bioactive compounds from fruit juice, and the encapsulated content and efficiencies

varied by the chemical class, compound and the juice matrix. In addition, after a heat treatment at 90 °C for 60 min, more than 87 % total antioxidant capacity and 90 % anthocyanin content were recovered from both encapsulated MG and Pom. In summary, these results highlight significant potential of a selected bacterial strain for simultaneous encapsulation of diverse phenolic compounds from fruit juice and thereby improving their process stability.

### Graphical Abstract



#### 4.1. Introduction

Plants produce a wide variety of human health-benefiting compounds (Craig, 1999). Numerous studies have shown that plants contain rich and complex profiles of phytochemicals, including anthocyanins and other polyphenols.(Alu'datt et al., 2017; Lätti et al., 2008) The bioactive functionalities of these compounds, such as anti-oxidant, anti-inflammatory, anti-carcinogen and maltase inhibition, may deter or prevent chronic diseases such as cancer (Dai and Mumper, 2010), cardiovascular diseases (Morton et al., 2000) and diabetes (Asgar, 2013). Therefore, there is an increasing demand by consumers and the industry for the isolation, and their integration of these bioactive compounds with food. The challenges, however, lie in the complex chemical profile of the plant-based materials and the lack of stability under processing and storage conditions of bioactive compounds (Chang et al., 2006; Laine et al., 2008; Wang and Xu, 2007).

Several extraction techniques have been developed for separating these polyphenolic compounds from plant materials, such as absorption and ion-exchange technologies with microporous resins (Basafa and Hawboldt, 2021; Kammerer et al., 2019), liquid-liquid extraction (Mantilla et al., 2015), and membrane filtration (Sygouni et al., 2019). Some of the key limitations of these approaches include inefficient extraction of a large diversity of polyphenolic compounds, labor intensive processes using high volumes of organic solvent, and limited protections for the sensitive compounds against degradation after extraction (Basafa and Hawboldt, 2021; Lavelli et al., 2017). Thus, there is a significant need to develop environmentally and economically friendly approaches to efficiently separate and stabilize the high-value bioactive compounds from plant sources and deliver their health-promoting functionalities. Furthermore, these solutions may also need to address the sensory challenges with some of the plant bioactives.

Microencapsulation processes have been applied to concentrate, protect and facilitate the incorporation of the polyphenolic compounds from plant extracts into food and pharmaceutical



matrices (Borrmann et al., 2013; Kuck and Noreña, 2016). By definition, microencapsulation refers to technologies of formulating solids, liquids or gaseous materials into microparticles or dispersion, with diameters typically ranging between 0.1-1000  $\mu\text{m}$  (Desai and Park, 2005; Singh et al., 2010). In industrial applications, the microencapsulation process offers a wide array of advantages in delivering polyphenolics, such as protecting encapsulated phyto-active compounds from degradation during processing and storage (Ersus and Yurdagel, 2007; Laine et al., 2008), controlling and targeting the release of the encapsulated compounds, and masking the undesirable physical characteristics of the polyphenolic compounds, such as solubility, smell and taste (Al-kasmi et al., 2017; Zhao et al., 2020) etc. The most common coating materials in microcapsules are polymers, which include natural (e.g. polysaccharides, proteins and lipids) and synthetic polymers (e.g. poly (lactic acid), poly (glycolic acid) and copolymers (Pall Magnusson et al., 2011)). The shell for these microparticles is often formed using both physical and chemical processes, such as spray drying and coacervation (Borrmann et al., 2013; Ersus and Yurdagel, 2007). Encapsulation systems can provide protection for the bioactive compounds using a combination of exogenous preservatives and coating materials. However, conventional encapsulation systems lack mechanisms to selectively bind phytochemicals from plant extracts and to protect these health-promoting phytochemicals often without exogenous preservatives (Matos et al., 2018; Tikekar et al., 2013).

Biological microscale structures, such as microbial cells, have emerged as promising encapsulation carriers for bioactive compounds. The results of these prior studies illustrate that microbial cells such as yeast cells can bind and encapsulate purified phytochemicals and protect them from oxidative and thermal stresses (Young and Nitin, 2019). These pre-existing cell-based microstructures eliminate the need for expensive processes used for creating these microstructures from biopolymers, eliminate or reduce the exposure of phytochemicals to heat, oxygen and other

physical factors that may deteriorate the encapsulated compounds, and thus reduce/eliminate the need of exogenous preservatives and antioxidants (Belščak-Cvitanović et al., 2011; Tikekar et al., 2013; Young and Nitin, 2019). Current studies using microbial cells have focused on purified plant derived compounds, and to the best of our knowledge no study has evaluated the role of microbial carriers for binding and encapsulation of diverse phytochemicals from plant juices or concentrations. Furthermore, most of the studies using microbial cells have focused on yeast cells as a model system, with limited emphasis on bacterial cells for the binding and encapsulation of complex polyphenolic compounds.

Thus, the focus of this study was to evaluate binding and encapsulation of phytochemicals from two diverse fruit juices using inactivated probiotic bacteria *Lactobacillus casei*. Muscadine grapes (MG) juice and pomegranates (Pom) juice were selected in this study since these are popular and highly valued fruits with rich phytochemical profiles and antioxidant properties (Martino et al., 2013; Wu and Tian, 2017). Inactivated probiotic bacteria *L. casei* was selected as it is a widely used probiotic strain from a *Lactobacillus* family and thus is widely accepted as a beneficial ingredient in food systems (Forestier et al., 2001; Galdeano and Perdigón, 2006). Heat inactivated cells were selected for the encapsulation to limit metabolism of the encapsulated compounds as well as to increase permeability of the cells for the fruit phytochemicals. Furthermore, inactivated probiotic cells retain some of the beneficial probiotic functions as illustrated by recent studies (Adams, 2010; Lopez et al., 2008). To develop a simple approach that can be adapted by other researchers, an incubation process was utilized to bind and encapsulate phytochemicals from the juice matrix of MG and Pom using bacterial cells in this study. To characterize the binding and encapsulation efficiency, the anthocyanin content and antioxidant properties of the juice matrix before and after incubation was measured. To further characterize binding and localization of phytochemicals to bacterial cell matrix, multispectral fluorescence

confocal imaging data was acquired. The binding and encapsulation yield of key phytochemical compounds from MG and Pom matrices was also quantified using a high-performance liquid chromatography (HPLC). The effectiveness of the selected bacterial carrier to protect encapsulated phytochemical compounds was also assessed based on thermal treatment of both the encapsulated phytochemicals and the phytochemicals in a control juice matrix.

In summary, this study demonstrates the potential of using an inactivated probiotic bacterial cell carrier for binding and encapsulation of phytochemicals from a complex composition of two different juice matrices. Results are presented to characterize the binding and encapsulation process and stability of encapsulated compounds in bacterial carriers, using a combination of chemical analysis, spectral imaging and antioxidant properties.

## **4.2. Material and Method**

### **4.2.1. Plant material**

Fresh SweetHeart Pomegranates grown in Madera, CA, U.S.A. were procured from a local fresh fruit market. Muscadine grapes were obtained from the Coca-Cola Company, Atlanta, GA. Both cultivars are predominant varieties in the United States. Fruits were stored at 4 °C until juice processing.

### **4.2.2. Reagents and standards**

Phenolic standards (gallic acid, catechin, epicatechin, caffeic acid, coumaric acid, quercetin and myricetin glycosides) were obtained from Sigma Chemical Co. (St. Louis, Mo., U.S.A.). Keracyanin chloride were obtained from Sigma Chemical Co. as the anthocyanin standard. For the HPLC analysis, phosphoric acid (85 wt. % in H<sub>2</sub>O) was obtained from Signal Chemical Co. TPTZ (2, 4, 6-tripyridyl-s-triazine) and FeCl<sub>3</sub>·6H<sub>2</sub>O used for the FRAP assay were obtained from Thermo Fisher Scientific Inc. All solvents used in this study are HPLC grade.

#### **4.2.3. Juice processing**

A slow masticating juicer (KOIOS, Model SHA1066) was used to prepare the fresh fruit juice from grapes and pomegranates. The fruits were rinsed with deionized water and air dried before juice processing. Pomegranates were cut prior to juicing. Juice and pomace samples were collected separately from the juicer. The mass of fruit and produced juice were recorded, and the juice yield was calculated as a ratio of the mass of juice to the total fruit mass. Fresh juice was then divided into 5 ml aliquots and freeze-dried overnight. The dried juice powder was then reconstituted with 5 ml of DI water and centrifuged to remove any insoluble plant material.

#### **4.2.4. Bacterial strains and cell preparation**

*Lactobacillus casei* (ATCC 393) was selected as a model for human probiotic bacteria. The stock strain is stored in liquid nitrogen. MRS agar and broth were used to culture this strain according to the ATCC protocol. Before experiments, the stock strain was streaked onto MRS agar plates and incubated overnight at 37 °C. A single colony from the agar plate was then used to inoculate liquid medium, which was then incubated at 37 °C without agitation to achieve the stationary phase of bacterial culture. After centrifugal separation, the bacteria were inactivated using 70 % ethanol for 30 min and washed with sterile Phosphate Buffered Saline (PBS). The bacteria were then suspended in sterile PBS at a concentration of approximately  $10^{10}$  CFU/mL.

#### **4.2.5. Encapsulation in inactivated cell carriers**

Bacteria pellet was collected after centrifugation (11,000 rpm for 5 min) and mixed with the reconstituted Pomegranate or muscadine grape juice. The encapsulation process was carried out in a 4°C cold room for 24 hours with mild agitation. After encapsulation, the aqueous juice matrix and cell carriers were separated by centrifugation (11,000 rpm for 5 min) and collected separately. The cells were washed once using sterile PBS buffer.

#### **4.2.6. Confocal fluorescence imaging**

Confocal Laser Scanning Microscopy (CLSM) images of bacterial cells after encapsulation, with and without incubation with pomegranate or muscadine juice samples, were collected using a Zeiss LSM 510 upright microscope (Carl Zeiss AG) with 40x/1.1 water objective. Each sample was excited at 405 nm using an argon diode laser. Emission (xyz) scans were acquired using a 500-550 nm bandpass emission filter. Lambda (xy $\lambda$ ) scans of each sample were collected over a range of 470-670 nm with 20 nm step size. Average intensity of the images acquired at different wavelengths during the lambda scan was measured using ImageJ software and plotted using an Origin 8.0.

#### **4.2.7. Phenolic extraction and HPLC analysis**

Phenolic compounds were extracted by mixing 2 ml of the reconstituted juice sample with 13 ml of acidified methanol (with 1 % HCl). After mixing using a vortexer, the mixture was sonicated using a bath sonicator for 10 min and the extract was separated from the remaining juice solids by centrifugation at 5500 rpm for 5 min. Samples was then diluted 10-fold with milliQ water for HPLC analysis. To assess encapsulation efficiency and yield in cell-based carriers, phenolic content in the aqueous phase before and after encapsulation process was quantified.

Chromatographic separation and detection of phenolic compounds were performed on an Agilent 1260 Infinity reverse phase HPLC (RP-HPLC) system (Santa Clara, CA) equipped with a thermostatic autosampler, thermostatic column compartment and a diode array detector (DAD) according to a method adapted from Oberholster et al. (Hirzel et al., 2017) An Agilent PLRP-S 100 Å (4.6 × 150 mm, 3 μm) column with an Agilent 3 × 5 mm guard column (PL1310-0016; Santa Clara, CA) was used at a temperature of 35°C for all analyses. Two solvents were used in this analysis, solvent A with 1.5 % phosphoric acid solution, and solvent B with acetonitrile containing 20 % (v/v) solvent A. The protocol establishes a gradient as follows: 0 min, 94% solvent A; 73 min, 69% A; 78 min, 38% A; and 90 min, 94 % A. The flow rate was 1 mL/min and the

injection volume for all samples was 10  $\mu$ L. Samples were filtered through 0.45  $\mu$ m type HA Millipore filters (Millipore Corp., Bedford, Mass., U.S.A.) prior to injection.

Phenols were monitored at multiple wavelengths, including 280 nm for gallic acid, and flavan-3-ols, 320 nm for hydroxycinnamates, 360 nm for flavonols, and 520 nm for anthocyanins, using the DAD detector. Absorbance spectra was recorded from 250 nm to 600 nm. External calibration curves were prepared with standards of HPLC grade purity and used for quantification of the target compounds. Polymeric phenols were quantified as catechin equivalents. Chromatograms were integrated using the Agilent CDSChemStation Software.

#### **4.2.8. Heat treatment and extraction**

Thermal stabilities of the encapsulated bioactive compounds were evaluated using a thermostatic water bath at 90 °C for up to 60 min. 1 mL suspension of encapsulated cells were added to the prewarmed 20 mL glass vials (Thermo Scientific™ B780020) and incubated in the dark for 1, 2, 5, 10, 20, 40, 60 min. After the treatment, 1 mL acidified methanol was added to each vial. Bead-beating at 6.0 m/s for 30 s for 3 times (FastPrep-24™ 5G Instrument, MP Biomedicals) was then carried out to facilitate thorough extraction. Finally, the homogenized samples were sonicated using a bath sonication device (Branson 2510 Ultrasonic Cleaner, Branson Ultrasonics Corp., Danbury, CT, USA) for 10 min. The methanolic extract was then centrifuged to remove cell debris and the supernatant was used for subsequent anthocyanin measurement and total antioxidant capacity quantification.

#### **4.2.9. Colored pigment measurements**

Anthocyanin content in juice and encapsulation matrix was measured using a UV-Vis spectrometry. Absorbance value of the clarified samples were scanned from 250 nm to 500 nm, and a peak intensity was recorded at 530 nm for all the samples. Samples were diluted accordingly to avoid saturation in the absorbance signal.

#### **4.2.10. Total antioxidant capacity measurements**

The total antioxidant capacity of the juice matrix was quantified using the Ferric Reducing Antioxidant Power (FRAP) assay. The protocol was adapted from Benzie and Strain (1996). The stock solutions included 300 mM acetate buffer (pH 3.6), 10 mM TPTZ solution in 40 mM HCl, and 20 mM  $\text{FeCl}_3 \cdot 6\text{H}_2\text{O}$  solution. The fresh working solution was prepared by mixing 25 mL acetate buffer, 2.5 mL TPTZ solution, and 2.5 mL  $\text{FeCl}_3 \cdot 6\text{H}_2\text{O}$  solution and then warming the mixture at 37 °C before using. Fruit extracts (150  $\mu\text{L}$ ) were allowed to react with 2850  $\mu\text{L}$  of the FRAP solution for 30 min in the dark. Changes in color of the solution (indicating the presence of ferrous tripyridyltriazine complex) were quantified using a UV-Vis measurement at 593 nm using a spectrometer. The standard curve was generated using a range of Trolox solutions between 25 and 800  $\mu\text{M}$ . Results were expressed in  $\mu\text{M}$  TE/ml fresh juice. The samples were diluted in case the absorbance value measured for the samples was over the linear range of the standard curve.

#### **4.2.11. Statistical analysis**

Statistical analysis was performed using the GraphPad Prism software V.7.0a (Graphpad Software, Inc., La Jolla, CA). All experiments were performed in triplicates. The significant differences between the treatments were determined through one-way ANOVA with a significance level at  $p < 0.05$ . Multiple comparison was then carried out using the Holm-Šídák test with a significance level at 0.05.

### 4.3. Results and Discussion

#### 4.3.1. Total antioxidant capacity and anthocyanin content in juice matrices and encapsulated cell carriers

**Table 4.1** Characterization of Pom and MG juice matrix (A) and the encapsulation efficiency of the polyphenolics from the juice using *L. casei* cell carrier (B). Antioxidant activity of the juice before and after encapsulation was quantified for this characterization.

A	Pom juice matrix	MG juice matrix
Total antioxidant capacity (FRAP assay, T.E. $\mu\text{M}/\text{mL}$ )	509.12 ( $\pm 1.49$ )	3436.43 ( $\pm 40.41$ )
Total antioxidant capacity of encapsulated juice content in <i>L. casei</i> cell carriers	60.81% ( $\pm 0.86\%$ )	72.67% ( $\pm 0.70\%$ )

B	Pom juice matrix	MG juice matrix
Juice matrix anthocyanin ( $\mu\text{M}/\text{ml}$ )	3.37 ( $\pm 0.13$ )	9.12 ( $\pm 0.10$ )
Encapsulation efficiency of anthocyanin content in <i>L. casei</i> cell carriers	64.36% ( $\pm 2.63\%$ )	66.97% ( $\pm 1.68\%$ )

Pom and MG both contain a variety of phytochemicals, which in general can be classified into alkaloids, carotenoids, nitrogen-containing compounds, organosulfur compounds, and phenolics. (Yang and Xiao, 2013, p. 201) Many *in vitro* and *in vivo* studies support that antioxidant property of the phytochemicals' plays a major role in their essential health benefits such as anti-inflammation and anti-carcinogen. (Magrone et al., 2020; Speciale et al., 2010) Therefore, in this study, the total antioxidant capacities of the juice samples obtained from fresh fruits and of the encapsulated compositions in cell-based carriers were assessed. Furthermore, anthocyanin content was quantified as one of the major water-soluble polyphenolics present in both fruits.



To characterize the overall efficiency of encapsulating complex profiles of phytochemicals using the bacteria cell carriers, the encapsulation efficiency was measured based on the difference in antioxidant concentration of the juice sample before and after incubation with cells. To quantify this ratio, antioxidant concentrations in juice samples and in juice residue after the encapsulation process were measured using the FRAP assay. These differences in the FRAP values before and after encapsulation reflect the relative amount of phenolics infused or bound to a selected cell based micro-carrier. Table 1A showed the total antioxidant capacity of Pom and MG juice samples measured using the FRAP assay. The results indicated that the MG juice sample has substantially higher antioxidant concentration compared to the same volume of a Pom juice. The encapsulation efficiency in the selected bacterial carrier were 60.81 % and 72.67 % for Pom and MG, respectively. These percentage values indicate the total fraction of antioxidant compounds bound and encapsulated in a bacterial cell carrier with respect to total antioxidant content in the individual juice samples. These results suggest that a simple incubation method allows phytochemicals to passively diffuse from a juice matrix to inactivated *L. casei* cells and results in an efficient binding and encapsulation of the antioxidant compounds in the cell carrier.

In addition to characterizing the encapsulated antioxidant content, encapsulation efficiencies of the anthocyanin pigments from the juices to the cells were evaluated. Anthocyanins, being water soluble, are one of the major polyphenolic fractions in fruit juices and have significant contributions to its antioxidant properties. In order to assess the anthocyanin content in the juice before and after encapsulation, the juice matrix was extracted using methanol as described in the materials and methods section, and the total anthocyanin content in the extract before and after incubation with cells was measured using an UV-Vis spectrophotometry. The measured absorbance at 530 nm was converted to an equivalent cyanidin chloride concentration (an anthocyanin standard) using a standard curve. The results show that Pom and MG juice had

approximately 3.37  $\mu\text{M}/\text{mL}$  and 9.12  $\mu\text{M}/\text{mL}$  of the equivalent keracyanin content. Similar to the total antioxidant activity results, the total anthocyanin concentration in the MG juice was higher than the anthocyanins in the Pom juice. After incubation with inactivated bacterial cells, 64.36 % and 66.97 % of the total anthocyanins from the Pom and MG juices were encapsulated or bound to the cell carriers respectively. In summary, these results highlight a significant potential of the selected bacterial strain for encapsulating phenolic compounds from complex juice samples.

#### 4.3.2. Confocal images and lambda scans of encapsulated cells

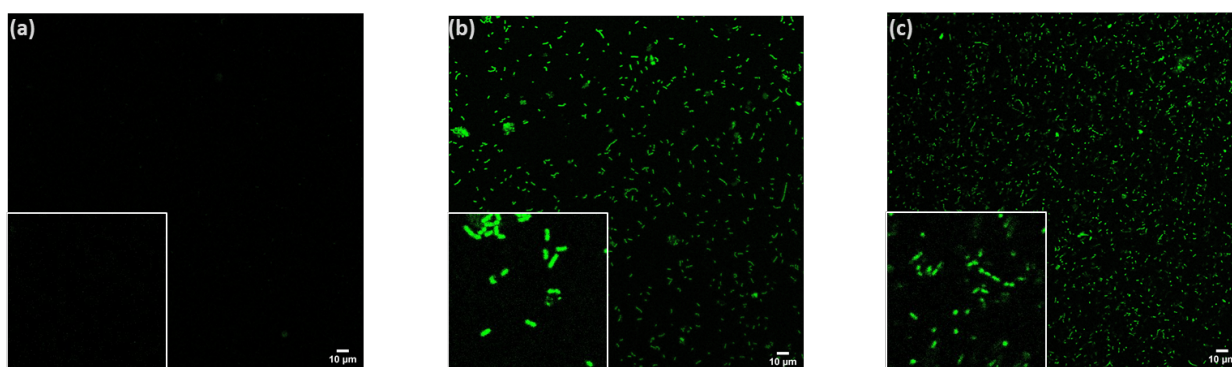


**Fig. 4.1.** Confocal fluorescence microscopy of juice encapsulated cells with a 405 nm excitation, and 500-550 nm emission; (a) *L. casei* control cells; (b) *L. casei* cells encapsulated with Pom juice; (c) *L. casei* cells encapsulated with MG juice. At lower left is the zoomed-in view of the same image; zoomed-in views in (b) and (c) demonstrate the uniform intracellular localization of polyphenolic compounds in the cell carriers.

To help visualize the encapsulated compounds and their intracellular distribution in the cell carriers, confocal multispectral fluorescence images were acquired based on the endogenous fluorescence signals of phytochemicals. The images were collected with a 405 nm excitation and an emission in the FITC channel from 500-550 nm. The fluorescence intensity of cells in each image was quantified by randomly selecting 20 regions of cells (eliminating the background

region) and measuring the mean pixel intensity using the ImageJ software. The mean background intensity was subtracted from the cell signals to remove the background signal.

As shown in Fig. 1, the signal intensity of *L. casei* carriers increased by approximately 26-fold following an incubation of cells with Pom juice (Fig. 1b), and a 24-fold increase upon incubation with a MG juice (Fig. 1c) as compared to the auto-fluorescence signal from the control cells (Fig.1a.) Differences in the fluorescence signal intensity between the controls and the modified cells with juice phenolics were statistically significant with a p-value  $\leq 0.05$ . The zoomed-in views in Fig. 1b and 1c indicated that the cell carriers retained their cellular structure after the encapsulation process, and the encapsulated material was localized uniformly across the intracellular compartment.

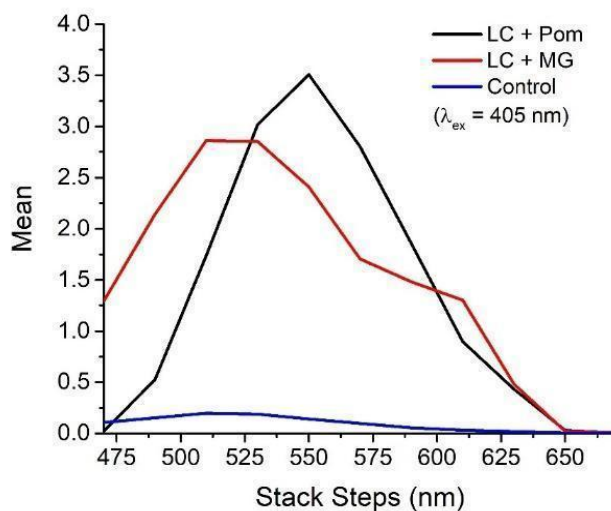


**Fig. 4.2.** Mean intensity of confocal lambda-scans over the range of 470-670 nm with a 405 nm excitation.

Further, lambda emission scans (Fig. 2) were collected in the range from 470-670 nm with a 20 nm step size with an excitation wavelength at 405 nm. The results in Fig. 2 revealed the fluorescence spectral profile of phenolic compounds encapsulated in the *L. casei* cells. Cells

incubated with Pom juice showed a broad fluorescence intensity distribution from 500 nm-600 nm with a peak maximum at around 550 nm. Cells encapsulated with MG juice also showed a broad emission distribution over a range of 450-630 nm with a peak maximum around 515 nm and a secondary peak around 590 nm.

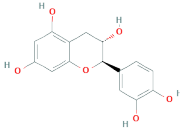
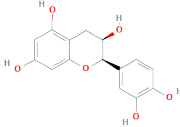
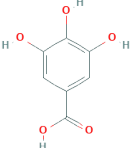
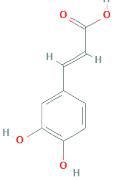
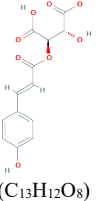
A broad emission range is usually associated with the presence of a diverse class of polyphenolic compounds. Based on the previous literature related to fluorescence properties of polyphenolics,(Agati et al., 2013; Iriel and Gabriela Lagorio, 2009; Singh and Mishra, 2015) the emission band between 533 nm to 595 nm mostly corresponds to anthocyanin content. The Pom spectra with the emission peak centered around 550 nm and the MG spectra with the secondary emission around 590 nm indicates the presence of anthocyanin compounds in the cell carriers from both juice matrixes. In addition, the major peak in the MG spectra around 515 nm suggests possible encapsulation of other phenolic compounds. Plant phenolics such as ferulic acid are known to have fluorescence emission centered around 520 nm - 530 nm.(Drabent et al., 1999; Lichtenthaler and Schweiger, 1998; Maurya et al., 2008)

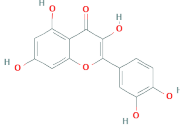
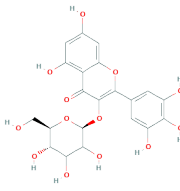
The broadening of the peaks observed in Fig. 2 could be attributed to other photoactive compounds present in the complex juice matrix. The shift in the emission range compared to the peaks observed from prior literature could also be caused by multiple factors. Anthocyanin polymerization during the juice processing and storage process could cause the emission to shift towards shorter wavelengths (Agati et al., 2013). In addition, fluorescence emission spectrums are known to be sensitive to environmental factors, including the excitation wavelength, medium pH and polarity, present macromolecules, etc.(Lakowicz, 2006) and these factors may contribute to the shifts observed in Fig. 2. In our measurements, phenolic compounds that emit blue fluorescence (400 nm - 470 nm) were not captured in Fig. 2 due to the limitation of the available wavelength range in this imaging systems. To address these gaps in the compositional analysis of encapsulated

compounds, analytical measurements using a HPLC method with known standards were conducted.

### 4.3.3. Phenolic profile of the juice matrix and encapsulated cell carrier

**Table 4.2.** Phenolic profile of Pom and MG juice and encapsulated compounds in *L. casei* cell carrier

Analyzed polyphenols					Pom			MG		
Class	Compound	Molecular structure	Molecular weight (g/mol)	Log P value	Content in 20% juice matrix (µg/ml)	Encapsulation efficiency	Statistical significance (p < 0.05)	Content in 20% juice matrix (µg/ml)	Encapsulation efficiency	Statistical significance (p < 0.05)
Flavanol	(+)-Catechin	 (C <sub>15</sub> H <sub>14</sub> O <sub>6</sub> )	290.27	0.41 (Poaty, 2009)	11.30	84.29% (±3.84%)	*	16.78	17.40% (±14.12%)	-
	(-)-Epicatechin	 (C <sub>15</sub> H <sub>14</sub> O <sub>6</sub> )	290.27	1.8	247.14	68.75% (±6.72%)	*	3.18	18.77% (±9.08%)	*
Phenolic acid	Gallic Acid	 (C <sub>7</sub> H <sub>6</sub> O <sub>5</sub> )	170.12	0.7	0.13	8.06% (±5.14%)	*	1.69	18.43% (±1.95%)	*
	Caffeic Acid	 (C <sub>9</sub> H <sub>8</sub> O <sub>4</sub> )	180.16	1.15	3.24	87.50% (±4.30%)	*	0	-	-
	Coutaric Acid	 (C <sub>13</sub> H <sub>12</sub> O <sub>8</sub> )	296.23	-1.32 (Jana, 2017)	1.71	73.21% (±8.27%)	*	0.07	10.24% (±6.06%)	-

Flavonol and derivatives	 Quercetin <chem>O=C1C(=C(O)C(=C(O)C1=O)C2=CC(=C(O)C=C2)O</chem> (C <sub>15</sub> H <sub>10</sub> O <sub>7</sub> )	302.23	1.48	20.93	1.20% (±6.20%)	-	21.70	2.83% (±3.75%)	
	 Myricetin 3-glycosides <chem>O=C1C(=C(O)C(=C(O)C1=O)C2=CC(=C(O)C=C2)OC3OC(O)C(O)C3O</chem> (C <sub>21</sub> H <sub>20</sub> O <sub>13</sub> )	480.40	-0.45	0.72	48.61% (±9.46%)	*	3.53	69.85% (±3.03%)	*
Polymeric poly-phenols	- Polymeric polyphenols (a mixture of polymeric pigments)	-	-	14.19	12.94% (±3.61%)	*	26.09	97.97% (±2.53%)	*

Among the diverse groups of bioactive compounds present in the fruit and fruit juices, polyphenolics constitute one of the largest and most diverse groups of phytochemicals (Abbas et al., 2017). To characterize the polyphenolic profile of the juices and the encapsulation efficiency, the samples of juice before and after incubation with cells were analyzed using HPLC, and based on these measurements, encapsulation efficiency of selected polyphenolics was quantified. As shown in Table 2, the target compound classes and compounds included in this study were flavanols including catechin and epicatechin, phenolic acid including gallic acid, caffeic acid and a hydroxycinnamic acid, coumaric acid, flavonols including quercetin and glycosylated myricetin, and polymeric polyphenols.

As observed from Table 2, most of the investigated compounds were present in both Pom and MG juice at different concentrations and had different levels of encapsulation efficiency. For flavanols, catechin and epicatechin were present in both the samples, while Pom juice contains significantly higher level of epicatechin (247.14  $\mu\text{g/mL}$ ) than MG juice (3.18  $\mu\text{g/mL}$ ). Catechin concentrations in Pom and MG juice were 11.30  $\mu\text{g/mL}$  and 16.78  $\mu\text{g/mL}$ , respectively. The

encapsulation efficiencies of both the selected flavanols in *L. casei* cells were consistently higher from Pom juice than from MG juice. 84.29 % of catechin and 68.75 % of epicatechin were encapsulated in cells incubated with Pom juice, and only 17.40 % of catechin and 18.77 % of epicatechin were encapsulated upon incubation of cells with MG juice.

In terms of the phenolic acids, both the amounts of phenolic acids in the selected juice products and their encapsulation efficiencies in *L. casei* also varied with the fruit source. In the case of Pom juice, caffeic acid (3.24  $\mu\text{g/mL}$  in juice) had the highest encapsulation efficiency in cells at 87.50 %, followed by coumaric acid (1.71  $\mu\text{g/mL}$  in juice) with an encapsulation efficiency of 73.21 %. In contrast, only 8.06 % of gallic acid content from Pom juice was encapsulated in the cell carriers. In the case of MG juice with a gallic acid content of 1.69  $\mu\text{g/mL}$ , encapsulation efficiency was 18.43 %. In MG juice, a relatively lower amount of coumaric acid (0.07  $\mu\text{g/mL}$ ) was measured and the encapsulation efficiency was also relatively lower at 10.24 % compared to Pom juice. Caffeic acid was below the detection limit in the MG samples.

Among flavonols, both Pom and MG juices contain similar levels of quercetin. Pom juice contains 20.93  $\mu\text{g/mL}$  quercetin and MG contains 21.70  $\mu\text{g/mL}$ . The encapsulation efficiencies of quercetin were however consistently low from both fruit juices, which is 1.20 % and 2.83 % from Pom and MG respectively. Glucoside derivatives are commonly found in grapes and wines, particularly delphinidin-3-glucoside, petunidin-3-glucoside and malvidin-3-glucoside (Revilla, 1999). In the juice samples obtained in this study, MG contains 3.53  $\mu\text{g/mL}$  myricetin 3-glycosides and a high encapsulation efficiency of 69.85 % was observed upon incubation of cells with MG juice, whereas Pom juice contains only 0.72  $\mu\text{g/mL}$  and the encapsulation efficiency from Pom juice samples was 48.61 %.

Another commonly abundant group of compounds in juice samples from these two fruits is polymeric polyphenols. Pom juice contains 14.19  $\mu\text{g/mL}$  polymeric phenol, and MG contains

26.09  $\mu\text{g/mL}$  polymeric phenol. The polymeric phenol identified using this protocol represents a mixture of polymeric pigments, which are formed based on reactions between grape anthocyanins and other components in the juice such as tannin, catechins and proanthocyanidins.(Peng et al., 2002; Remy et al., 2000) The encapsulation efficiencies of polymeric polyphenols in this study varied significantly with the fruit source of the juice. 97.97 % of the polymeric phenol was captured by the cell carriers upon incubation with MG juice, whereas in the case of Pom juice only 12.94 % was encapsulated in the cell carriers.

Taken together, the imaging and HPLC measurement results illustrate that cell carriers can simultaneously encapsulate a diversity of bioactive compounds from a complex juice matrix. Compared to previous studies that have predominantly focused on yeast cells for the encapsulation of purified hydrophobic polyphenolic compounds,(Ciamponi et al., 2012; Young et al., 2017) the results of this study suggest the potential of diverse cell carriers, including bacterial cell carriers, to simultaneously encapsulate multiple compounds from mixtures. Furthermore, since the encapsulation process was conducted using water soluble compounds in fruit juices, this study demonstrates that bacterial cell carriers can bind and encapsulate compounds from hydrophilic extracts and juices. Together with prior studies, the results of this study illustrate the potential of cell carriers to encapsulate both hydrophobic and hydrophilic bioactives.

The encapsulation process of these compounds from cell carriers can be attributed to both composition and structure of cell carriers. Besides the structural integrity that withstood the encapsulation process as shown in Fig 1, bacterial and yeast cell carriers have a relatively high fraction of protein content on a dry basis. In the case of *L. casei* cells, the protein content can be as high as 80% or higher on a dry basis. Similarly, the protein content in yeast cells can range from 25-60% on a dry basis.(Górska et al., 2016; Pacheco et al., 1997) In addition, cell carriers also express both soluble and structural proteins including membrane associated proteins. In previous



studies, protein-polyphenolic interactions have been explored and the binding between protein isolates and polyphenolic compounds from juice or other plant extracts has been demonstrated.(de Morais et al., 2020; Milani et al., 2017; T. Diaz et al., 2020) Thus, it is likely that a relatively high concentration and diversity of proteins in micro-scale cell carriers significantly promote the binding of diverse polyphenols from a juice matrix.

In addition to proteins, bacteria and yeast cells also contain a diversity of carbohydrate biopolymers mostly concentrated in cell walls and lipids that are integral parts of the cell membranes. Prior studies have shown interactions between polyphenols and cellular polysaccharides,(Pekkinen et al., 2014; Rosa et al., 2013) and the binding mechanism could be attributed to a range of physical and chemical interactions.(Jakobek, 2015) The complex and porous structures and surface properties of the cell wall has also been proposed to be important for the binding process.(Fernandes et al., 2014; Le Bourvellec et al., 2005; Saura-Calixto, 2011) These compositions and cellular structures can provide a rich environment for partitioning and compartmentalization of diverse compounds in cell-based carriers.

The results illustrate that the encapsulated content and efficiencies varied by the chemical class, compound and the juice matrix. Quercetin as a monomeric flavonol showed consistently low incorporation rate from both juices, while the glycosylated myricetin has significantly higher encapsulation efficiencies (48.61 % and 69.5 % from Pom and MG juice, respectively). In contrast, polymeric polyphenols yielded the highest encapsulation efficiency among all compounds tested from MG juice (at approximately 97 %), while the same class of compounds from Pom juice showed a significantly lower encapsulation efficiency (~ 12 %). This trend of differences in encapsulation efficiency based on differences in the composition of juice matrix was also observed in the case of flavonols and phenolic acids. Furthermore, no clear correlation between encapsulation efficiency and relative hydrophilicity of the compounds was observed based on

these measurements. These observations suggest that the partitioning of the compounds in cells from a juice matrix significantly depends on the interactions among the polyphenolic compounds and also other components of the juice. Characterization of these interactions is beyond the scope of this study, but these results suggest that it may be possible to select cellular compositions among the diverse class of microbes that may promote binding of selective polyphenols from a given plant extract and juice.

#### 4.3.4. Stabilization of bioactive compounds against heat treatment

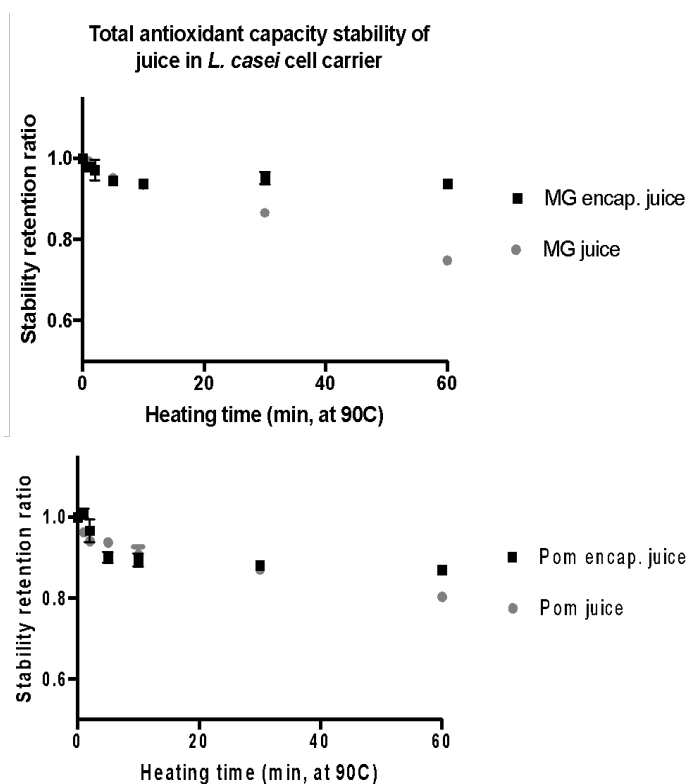


**Fig. 4.3.** Retention of antioxidant content of phenolic bioactives from grape and pomegranate juice samples upon selected heat treatment both with and without encapsulation in the selected cell-carrier. After treatment juice samples were extracted with 85 % methanol and quantified using the FRAP assay.

One of the important functionalities of encapsulation carriers is to protect the bioactive compounds from adverse environmental factors and food processing conditions. In order to evaluate the effectiveness of the selected bacterial carrier in protecting and stabilizing the encapsulated juice polyphenols, the encapsulated cells were heat-treated at 90 °C for 1, 2, 5, 10, 20, 40, 60 min in a temperature-controlled water bath. The heating conditions were selected based on prior studies.(Fischer et al., 2013, p. 201; Wang and Xu, 2007) After the heat treatment, the cell encapsulated polyphenolics were extracted using the methods described in section 2.8 of the Material and Methods section. The total antioxidant concentration of the extract was then measured using the FRAP assay. The control group of cells with encapsulated compounds but without the heat treatment were also extracted using the same approach and used for calculating the retention ratio during the treatment. The results in Fig. 3 illustrate the percentage of total antioxidant capacity retained at each time point during the heating process. As observed in Fig. 3, the bacterial carrier effectively protected encapsulated compounds during thermal treatment. Approximately 93% of the antioxidant capacity for the encapsulated MG juice was retained after 1 hour of heat treatment, whereas only 74% of the initial antioxidants were preserved without using encapsulation after the heat treatment of juice for 1 hour. Pom juice showed higher resistance against heating, where 80% of the antioxidant activity still persisted after the heat treatment for 1 hour. Upon encapsulation in the cell carriers, 87% of the total antioxidant capacity was retained in the encapsulated Pom juice content. Overall, these observations indicated that cell carriers can effectively protect encapsulated antioxidant compounds against thermal stress.

In addition to the total antioxidant capacity, the retention of anthocyanins was also monitored during the heating process at 90 °C. Cells encapsulated with polyphenols from the juice matrix were sampled at 1, 2, 5, 10, 20, 40, 60 min, and compared to the non-heated polyphenols encapsulated in cells from the juices. As described previously, the anthocyanin content retained in

the cells was extracted using methanol and measured using a UV-Vis spectrometer. Fig. 6 shows similar patterns of enhanced stability of anthocyanin compounds on cell carriers similar to the results in Fig. 5. Despite the fact that the MG juice contains more colored pigments (Fig. 2B), these

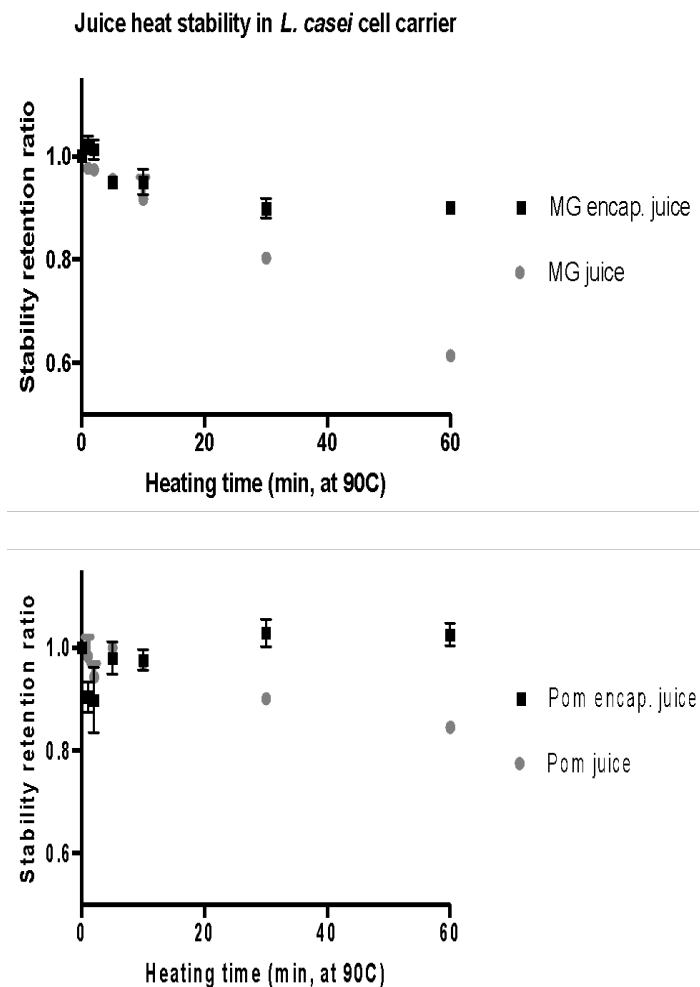


**Fig. 4.4.** Stability of juice pigments with and without encapsulation under heat treatment. After treatment, the juice samples were extracted with 85 % methanol and quantified using UV-Vis measurements at 530 nm.

compounds seemed to be more susceptible to heat when compared to the pigments from Pom juice. Only 61 % of the anthocyanin pigments in the MG juice were retained after 60 min of heat

treatment. In contrast, 90 % of the encapsulated anthocyanin pigments were preserved in the cell carriers. In terms of the Pom matrix, 84 % of the anthocyanins survived the heating of the juice, and nearly 100 % of the encapsulated pigments were preserved in the cell microcarriers. These results demonstrated that the bacterial cell carriers effectively protected encapsulated anthocyanins from degradation caused by the thermal treatment, and the protective effect was more significant for anthocyanins from MG than Pom.

Overall, the results demonstrated that, after 60 min of heat treatment at 90 °C, more than 87 % total antioxidant capacity and 90 % anthocyanin content were recovered from both encapsulated MG and Pom as compared to the respective juices without encapsulation. The degradation of juices' phenolics content including anthocyanin from heating were comparable with previous studies (between 15 % - 30 %).(Fischer et al., 2013; Wang and Xu, 2007) Additionally, in terms of the Pom juice, the loss of antioxidants was higher than the percentage of anthocyanin degradation. This might indicate that while pigment was better retained by the cell carriers, colorless phenols might be more heat labile and more susceptible to degradation.(Fischer et al., 2013; Martino et al., 2013; Nayak et al., 2011)

The thermal stability of encapsulated active compounds was statistically significantly higher than non-encapsulated juice of both fruits. This protective effect of microcarriers has been observed in a range of encapsulation systems such as spray-drying particles(Robert et al., 2010) and emulsions(Zaidel et al., 2014). However, a comparable or higher percentage of antioxidant capacity and pigment content retention was observed using the cell carriers compared to the synthetic encapsulation carriers. For instance, losses of more than 20% were observed for anthocyanins encapsulated in polymer matrices such as maltodextrin, a mixture of maltodextrin and gum arabic, or soluble starch, after treatment at 98 °C for 30 min,(Idham et al., 2012) whereas cell carriers reduced the loss to less than 10 % after heating of the encapsulated samples at 90 °C

for 60 min. The advantage of the cell carriers might be largely attributed to the physical cellular structure as well as its complex chemical composition. As shown in Fig. 1, the cell structures persisted through the encapsulation process, and literature has shown that some of the *Lactobacillus* strains can maintain structural integrity at elevated temperature around 100-120 °C, for 30-60 min.(Klaenhammer et al., 1993) The robust structure is essential for protecting encapsulated bioactives, whereas colloidal encapsulation systems tend to destabilize both physically and chemically during encapsulation or in adverse environmental conditions.(McClements, 2015) Besides the physical structure, the antioxidant property of intracellular content of *L. casei* has also been reported.(Aguilar-Toalá et al., 2019) Aguilar-Toalá *et al.* suggested that glutathione and other intracellular lipid and protein components might be involved in the antioxidant activities, which might in turn help stabilize and protect bioactive compounds encapsulated within the cell carrier. Therefore, cell carriers are effective encapsulation materials for preserving the bioactive functions of extracted polyphenolics during thermal processing.

In addition, encapsulation using cell carriers exhibits certain advantages in terms of the manufacturing process. In this study, we used *L. casei* cells to encapsulate a composite profile of polyphenolics with a basic temperature-controlled incubation. Currently, spray-drying and freeze-drying are the most commonly applied industrial techniques for microencapsulation and stabilization of plant polyphenolics from natural sources. Spray drying is a unit operation where liquid is atomized in a hot gas current to obtain a powder.(Phisut, 2012) Freeze-drying is an alternative drying method but less utilized due to the higher operational cost. While spray-drying is more prevalent due to its low cost, its limitations have also been extensively discussed. We observed 4-5 times higher anthocyanin content encapsulated in the cell carrier in this study when compared to spray-dried powder.(Yousefi et al., 2011) Despite variations in the raw material, loss

of heat sensitive compounds during spray-drying might be due to the exposure to oxygen (Yousefi et al., 2011) and the thermal treatment (with typical inlet air temperature around 150 – 220 °C, albeit with a short contact time) (Patil et al., 2014; Phisut, 2012). In addition, the drying process may cause loss of dried material due to wall deposition, low thermal efficiency,(Shishir and Chen, 2017) broad size distribution and irregular microstructures.(Dalmoro et al., 2012) Encapsulation using the preformed cellular structure of probiotic bacteria and passive incubation, on the other hand, significantly simplified the process with more uniform cellular size and microcellular structure.

## **Conclusion**

In summary, microencapsulation that leveraged inactivated probiotic cells (*L. casei*) as the preformed microcarrier, could separate and enhance the stability of antioxidant compounds of composite profiles from crude fruit juice material. As identified in this study, the profiles included anthocyanins and a variety of phenolic compounds, depending on the source fruit of the juice. Compared to the original MG and Pom fruit juice used in this study, the cell carriers contained more than 60% of the antioxidant capacity and anthocyanin content using the simple incubation protocol. After heat treatment at 90 °C for 60 min, more than 87 % of encapsulated antioxidant capacity and more than 90 % of the anthocyanin content were preserved within the cell carriers. This approach presents an economic and scalable technique to better utilize waste and by-products of the food processing industry. Future studies could be carried out to assess the potential of encapsulating phytochemicals of other plant sources, modification of the cell carrier structures and encapsulation protocol to further enhance the encapsulation efficiency, and any additional probiotic benefits that the bacterial carrier might have.

## **Conflict of interest**

There are no conflicts of interest to declare.

## **Acknowledgement**

This research was supported by funding from USDA-NIFA research awards (grant number 2018-67017-27563).

## **References**

- Abbas, M., Saeed, F., Anjum, F.M., Afzaal, M., Tufail, T., Bashir, M.S., Ishtiaq, A., Hussain, S., Suleria, H.A.R., 2017. Natural polyphenols: An overview. *International Journal of Food Properties* 20, 1689–1699. <https://doi.org/10.1080/10942912.2016.1220393>
- Adams, C.A., 2010. The probiotic paradox: live and dead cells are biological response modifiers. *Nutrition Research Reviews* 23, 37–46. <https://doi.org/10.1017/S0954422410000090>
- Agati, G., Matteini, P., Oliveira, J., de Freitas, V., Mateus, N., 2013. Fluorescence Approach for Measuring Anthocyanins and Derived Pigments in Red Wine. *J. Agric. Food Chem.* 61, 10156–10162. <https://doi.org/10.1021/jf402398a>
- Aguilar-Toalá, J.E., Estrada-Montoya, M.C., Liceaga, A.M., Garcia, H.S., González-Aguilar, G.A., Vallejo-Cordoba, B., González-Córdova, A.F., Hernández-Mendoza, A., 2019. An insight on antioxidant properties of the intracellular content of *Lactobacillus casei* CRL-431. *LWT* 102, 58–63. <https://doi.org/10.1016/j.lwt.2018.12.015>
- Al-kasmi, B., Alsirawan, M.H.D.B., Bashimam, M., El-zein, H., 2017. Mechanical microencapsulation: The best technique in taste masking for the manufacturing scale - Effect of polymer encapsulation on drug targeting. *Journal of Controlled Release* 260, 134–141. <https://doi.org/10.1016/j.jconrel.2017.06.002>



- Alu'datt, M.H., Rababah, T., Alhamad, M.N., Al-Mahasneh, M.A., Ereifej, K., Al-Karaki, G., Al-Duais, M., Andrade, J.E., Tranchant, C.C., Kubow, S., Ghozlan, K.A., 2017. Profiles of free and bound phenolics extracted from Citrus fruits and their roles in biological systems: content, and antioxidant, anti-diabetic and anti-hypertensive properties. *Food Funct.* 8, 3187–3197. <https://doi.org/10.1039/C7FO00212B>
- Asgar, M.A., 2013. Anti-Diabetic Potential of Phenolic Compounds: A Review. *International Journal of Food Properties* 16, 91–103. <https://doi.org/10.1080/10942912.2011.595864>
- Basafa, M., Hawboldt, K., 2021. A review on sources and extraction of phenolic compounds as precursors for bio-based phenolic resins. *Biomass Conv. Bioref.* <https://doi.org/10.1007/s13399-021-01408-x>
- Belščak-Cvitanović, A., Stojanović, R., Manojlović, V., Komes, D., Cindrić, I.J., Nedović, V., Bugarski, B., 2011. Encapsulation of polyphenolic antioxidants from medicinal plant extracts in alginate–chitosan system enhanced with ascorbic acid by electrostatic extrusion. *Food Research International* 44, 1094–1101. <https://doi.org/10.1016/j.foodres.2011.03.030>
- Borrmann, D., Pierucci, A.P.T.R., Leite, S.G.F., Leão, M.H.M. da R., 2013. Microencapsulation of passion fruit (*Passiflora*) juice with n-octenylsuccinate-derivatised starch using spray-drying. *Food and Bioproducts Processing* 91, 23–27. <https://doi.org/10.1016/j.fbp.2012.08.001>
- Chang, Q., Zuo, Z., Chow, M.S.S., Ho, W.K.K., 2006. Effect of storage temperature on phenolics stability in hawthorn (*Crataegus pinnatifida* var. *major*) fruits and a hawthorn drink. *Food Chemistry* 98, 426–430. <https://doi.org/10.1016/j.foodchem.2005.06.015>
- Ciamponi, F., Duckham, C., Tirelli, N., 2012. Yeast cells as microcapsules. Analytical tools and process variables in the encapsulation of hydrophobes in *S. cerevisiae*. *Applied*

- Microbiology and Biotechnology 95, 1445–1456. <https://doi.org/10.1007/s00253-012-4127-8>
- Craig, W.J., 1999. Health-promoting properties of common herbs. *The American Journal of Clinical Nutrition* 70, 491s–499s. <https://doi.org/10.1093/ajcn/70.3.491s>
- Dai, J., Mumper, R.J., 2010. Plant Phenolics: Extraction, Analysis and Their Antioxidant and Anticancer Properties. *Molecules* 15, 7313–7352.  
<https://doi.org/10.3390/molecules15107313>
- Dalmoro, A., Barba, A.A., Lamberti, G., d'Amore, M., 2012. Intensifying the microencapsulation process: Ultrasonic atomization as an innovative approach. *European Journal of Pharmaceutics and Biopharmaceutics* 80, 471–477.  
<https://doi.org/10.1016/j.ejpb.2012.01.006>
- de Morais, F.P.R., Pessato, T.B., Rodrigues, E., Peixoto Mallmann, L., Mariutti, L.R.B., Netto, F.M., 2020. Whey protein and phenolic compound complexation: Effects on antioxidant capacity before and after in vitro digestion. *Food Research International* 133, 109104.  
<https://doi.org/10.1016/j.foodres.2020.109104>
- Desai, K.G.H., Park, H.J., 2005. Recent Developments in Microencapsulation of Food Ingredients. *Drying Technology* 23, 1361–1394. <https://doi.org/10.1081/DRT-200063478>
- Drabent, R., Pliszka, B., Olszewska, T., 1999. Fluorescence properties of plant anthocyanin pigments. I. Fluorescence of anthocyanins in *Brassica oleracea* L. extracts. *Journal of Photochemistry and Photobiology B: Biology* 50, 53–58. [https://doi.org/10.1016/S1011-1344\(99\)00070-6](https://doi.org/10.1016/S1011-1344(99)00070-6)
- Ersus, S., Yurdagel, U., 2007. Microencapsulation of anthocyanin pigments of black carrot (*Daucus carota* L.) by spray drier. *Journal of Food Engineering* 80, 805–812.  
<https://doi.org/10.1016/j.jfoodeng.2006.07.009>

- Fernandes, A., Ivanova, G., Brás, N.F., Mateus, N., Ramos, M.J., Rangel, M., de Freitas, V.,  
2014. Structural characterization of inclusion complexes between cyanidin-3-O-glucoside  
and  $\beta$ -cyclodextrin. *Carbohydrate Polymers* 102, 269–277.  
<https://doi.org/10.1016/j.carbpol.2013.11.037>
- Fischer, U.A., Carle, R., Kammerer, D.R., 2013. Thermal stability of anthocyanins and  
colourless phenolics in pomegranate (*Punica granatum* L.) juices and model solutions.  
*Food Chemistry* 138, 1800–1809. <https://doi.org/10.1016/j.foodchem.2012.10.072>
- Forestier, C., De Champs, C., Vatoux, C., Joly, B., 2001. Probiotic activities of *Lactobacillus*  
*casei rhamnosus*: in vitro adherence to intestinal cells and antimicrobial properties.  
*Research in Microbiology* 152, 167–173. [https://doi.org/10.1016/S0923-2508\(01\)01188-3](https://doi.org/10.1016/S0923-2508(01)01188-3)
- Galdeano, C.M., Perdigón, G., 2006. The Probiotic Bacterium *Lactobacillus casei* Induces  
Activation of the Gut Mucosal Immune System through Innate Immunity. *Clinical and  
Vaccine Immunology* 13, 219–226. <https://doi.org/10.1128/CVI.13.2.219-226.2006>
- Górska, S., Buda, B., Brzozowska, E., Schwarzer, M., Srutkova, D., Kozakova, H., Gamian, A.,  
2016. Identification of *Lactobacillus* proteins with different recognition patterns between  
immune rabbit sera and nonimmune mice or human sera. *BMC Microbiology* 16.  
<https://doi.org/10.1186/s12866-016-0631-9>
- Hirzel, D.R., Steenwerth, K., Parikh, S.J., Oberholster, A., 2017. Impact of winery wastewater  
irrigation on soil, grape and wine composition. *Agricultural Water Management* 180,  
178–189. <https://doi.org/10.1016/j.agwat.2016.10.019>
- Idham, Z., Muhamad, I.I., Setapar, S.H.M., Sarmidi, M.R., 2012. Effect of Thermal Processes on  
Roselle Anthocyanins Encapsulated in Different Polymer Matrices. *Journal of Food*

- Processing and Preservation 36, 176–184. <https://doi.org/10.1111/j.1745-4549.2011.00572.x>
- Iriel, A., Gabriela Lagorio, M., 2009. Biospectroscopy of *Rhododendron indicum* flowers. Non-destructive assessment of anthocyanins in petals using a reflectance-based method. *Photochemical & Photobiological Sciences* 8, 337–344. <https://doi.org/10.1039/B814461C>
- Jakobek, L., 2015. Interactions of polyphenols with carbohydrates, lipids and proteins. *Food Chemistry* 175, 556–567. <https://doi.org/10.1016/j.foodchem.2014.12.013>
- Kammerer, D.R., Kammerer, J., Carle, R., 2019. Chapter 19 - Adsorption and Ion Exchange for the Recovery and Fractionation of Polyphenols: Principles and Applications, in: Watson, R.R. (Ed.), *Polyphenols in Plants (Second Edition)*. Academic Press, pp. 327–339. <https://doi.org/10.1016/B978-0-12-813768-0.00018-9>
- Klaenhammer, T.R., Fremaux, C., Ahn, C., Milton, K., 1993. CHAPTER 7 - Molecular Biology of Bacteriocins Produced by *Lactobacillus*, in: Hoover, D.G., Steenson, L.R. (Eds.), *Bacteriocins of Lactic Acid Bacteria*. Academic Press, pp. 151–180. <https://doi.org/10.1016/B978-0-12-355510-6.50015-4>
- Kuck, L.S., Noreña, C.P.Z., 2016. Microencapsulation of grape (*Vitis labrusca* var. Bordo) skin phenolic extract using gum Arabic, polydextrose, and partially hydrolyzed guar gum as encapsulating agents. *Food Chemistry* 194, 569–576. <https://doi.org/10.1016/j.foodchem.2015.08.066>
- Laine, P., Kylli, P., Heinonen, M., Jouppila, K., 2008. Storage Stability of Microencapsulated Cloudberry (*Rubus chamaemorus*) Phenolics. *J. Agric. Food Chem.* 56, 11251–11261. <https://doi.org/10.1021/jf801868h>

- Lakowicz, J.R. (Ed.), 2006. Solvent and Environmental Effects, in: Principles of Fluorescence Spectroscopy. Springer US, Boston, MA, pp. 205–235. [https://doi.org/10.1007/978-0-387-46312-4\\_6](https://doi.org/10.1007/978-0-387-46312-4_6)
- Lätti, A.K., Riihinen, K.R., Kainulainen, P.S., 2008. Analysis of Anthocyanin Variation in Wild Populations of Bilberry ( *Vaccinium myrtillus* L.) in Finland. *J. Agric. Food Chem.* 56, 190–196. <https://doi.org/10.1021/jf072857m>
- Lavelli, V., Sri Harsha, P.S.C., Laureati, M., Pagliarini, E., 2017. Degradation kinetics of encapsulated grape skin phenolics and micronized grape skins in various water activity environments and criteria to develop wide-ranging and tailor-made food applications. *Innovative Food Science & Emerging Technologies* 39, 156–164. <https://doi.org/10.1016/j.ifset.2016.12.006>
- Le Bourvellec, C., Bouchet, B., Renard, C.M.G.C., 2005. Non-covalent interaction between procyanidins and apple cell wall material. Part III: Study on model polysaccharides. *Biochimica et Biophysica Acta (BBA) - General Subjects* 1725, 10–18. <https://doi.org/10.1016/j.bbagen.2005.06.004>
- Lichtenthaler, H.K., Schweiger, J., 1998. Cell wall bound ferulic acid, the major substance of the blue-green fluorescence emission of plants. *Journal of Plant Physiology* 152, 272–282. [https://doi.org/10.1016/S0176-1617\(98\)80142-9](https://doi.org/10.1016/S0176-1617(98)80142-9)
- Lopez, M., Li, N., Kataria, J., Russell, M., Neu, J., 2008. Live and Ultraviolet-Inactivated *Lactobacillus Rhamnosus* GG Decrease Flagellin-Induced Interleukin-8 Production in Caco-2 Cells. *The Journal of Nutrition* 138, 2264–2268. <https://doi.org/10.3945/jn.108.093658>

- Magrone, T., Magrone, M., Russo, M.A., Jirillo, E., 2020. Recent Advances on the Anti-Inflammatory and Antioxidant Properties of Red Grape Polyphenols: In Vitro and In Vivo Studies. *Antioxidants* 9, 35. <https://doi.org/10.3390/antiox9010035>
- Mantilla, S.V., Manrique, A.M., Gauthier-Maradei, P., 2015. Methodology for Extraction of Phenolic Compounds of Bio-oil from Agricultural Biomass Wastes. *Waste Biomass Valor* 6, 371–383. <https://doi.org/10.1007/s12649-015-9361-8>
- Martino, K.G., Paul, M.S., Pegg, R.B., Kerr, W.L., 2013. Effect of time–temperature conditions and clarification on the total phenolics and antioxidant constituents of muscadine grape juice. *LWT - Food Science and Technology* 53, 327–330. <https://doi.org/10.1016/j.lwt.2013.03.001>
- Matos, M., Gutiérrez, G., Martínez-Rey, L., Iglesias, O., Pazos, C., 2018. Encapsulation of resveratrol using food-grade concentrated double emulsions: Emulsion characterization and rheological behaviour. *Journal of Food Engineering* 226, 73–81. <https://doi.org/10.1016/j.jfoodeng.2018.01.007>
- Maurya, R., Prasad, S.M., Gopal, R., 2008. LIF technique offers the potential for the detection of cadmium-induced alteration in photosynthetic activities of Zea Mays L. *Journal of Photochemistry and Photobiology C: Photochemistry Reviews* 9, 29–35. <https://doi.org/10.1016/j.jphotochemrev.2008.03.001>
- McClements, D.J., 2015. Encapsulation, protection, and release of hydrophilic active components: Potential and limitations of colloidal delivery systems. *Advances in Colloid and Interface Science* 219, 27–53. <https://doi.org/10.1016/j.cis.2015.02.002>
- Milani, P.G., Formigoni, M., Lima, Y.C., Piovan, S., Peixoto, G.M.L., Camparsi, D.M., da Silva Rodrigues, W. do N., da Silva, J.Q.P., da Silva Avincola, A., Pilau, E.J., da Costa, C.E.M., da Costa, S.C., 2017. Fortification of the whey protein isolate antioxidant and

- antidiabetic activity with fraction rich in phenolic compounds obtained from *Stevia rebaudiana* (Bert.) Berton leaves. *J Food Sci Technol* 54, 2020–2029.  
<https://doi.org/10.1007/s13197-017-2638-0>
- Morton, L.W., Caccetta, R.A.-A., Puddey, I.B., Croft, K.D., 2000. Chemistry And Biological Effects Of Dietary Phenolic Compounds: Relevance To Cardiovascular Disease. *Clinical and Experimental Pharmacology and Physiology* 27, 152–159.  
<https://doi.org/10.1046/j.1440-1681.2000.03214.x>
- Nayak, B., Berrios, J.D.J., Powers, J.R., Tang, J., 2011. Thermal Degradation of Anthocyanins from Purple Potato (Cv. Purple Majesty) and Impact on Antioxidant Capacity. *J. Agric. Food Chem.* 59, 11040–11049. <https://doi.org/10.1021/jf201923a>
- Pacheco, M.T.B., Caballero-Córdoba, G.M., Sgarbieri, V.C., 1997. Composition and Nutritive Value of Yeast Biomass and Yeast Protein Concentrates. *Journal of Nutritional Science and Vitaminology* 43, 601–612. <https://doi.org/10.3177/jnsv.43.601>
- Pall Magnusson, J., Omer Saeed, A., Fernández-Trillo, F., Alexander, C., 2011. Synthetic polymers for biopharmaceutical delivery. *Polymer Chemistry* 2, 48–59.  
<https://doi.org/10.1039/C0PY00210K>
- Patil, V., Chauhan, A.K., Singh, R.P., 2014. Optimization of the spray-drying process for developing guava powder using response surface methodology. *Powder Technology* 253, 230–236. <https://doi.org/10.1016/j.powtec.2013.11.033>
- Pekkinen, J., Rosa, N.N., Savolainen, O.-I., Keski-Rahkonen, P., Mykkänen, H., Poutanen, K., Micard, V., Hanhineva, K., 2014. Disintegration of wheat aleurone structure has an impact on the bioavailability of phenolic compounds and other phytochemicals as evidenced by altered urinary metabolite profile of diet-induced obese mice. *Nutrition & Metabolism* 11, 1. <https://doi.org/10.1186/1743-7075-11-1>

- Peng, Z., Iland, P.G., Oberholster, A., Sefton, M.A., Waters, E.J., 2002. Analysis of pigmented polymers in red wine by reverse phase HPLC. *Australian Journal of Grape and Wine Research* 8, 70–75. <https://doi.org/10.1111/j.1755-0238.2002.tb00213.x>
- Phisut, N., 2012. Spray drying technique of fruit juice powder: some factors influencing the properties of product. *International Food Research Journal* 19, 1297–1306.
- Remy, S., Fulcrand, H., Labarbe, B., Cheynier, V., Moutounet, M., 2000. First confirmation in red wine of products resulting from direct anthocyanin–tannin reactions. *Journal of the Science of Food and Agriculture* 80, 745–751. [https://doi.org/10.1002/\(SICI\)1097-0010\(20000501\)80:6<745::AID-JSFA611>3.0.CO;2-4](https://doi.org/10.1002/(SICI)1097-0010(20000501)80:6<745::AID-JSFA611>3.0.CO;2-4)
- Robert, P., Gorena, T., Romero, N., Sepulveda, E., Chavez, J., Saenz, C., 2010. Encapsulation of polyphenols and anthocyanins from pomegranate (*Punica granatum*) by spray drying. *International Journal of Food Science & Technology* 45, 1386–1394. <https://doi.org/10.1111/j.1365-2621.2010.02270.x>
- Rosa, N.N., Dufour, C., Lullien-Pellerin, V., Micard, V., 2013. Exposure or release of ferulic acid from wheat aleurone: Impact on its antioxidant capacity. *Food Chemistry* 141, 2355–2362. <https://doi.org/10.1016/j.foodchem.2013.04.132>
- Saura-Calixto, F., 2011. Dietary Fiber as a Carrier of Dietary Antioxidants: An Essential Physiological Function. *J. Agric. Food Chem.* 59, 43–49. <https://doi.org/10.1021/jf1036596>
- Shishir, M.R.I., Chen, W., 2017. Trends of spray drying: A critical review on drying of fruit and vegetable juices. *Trends in Food Science & Technology* 65, 49–67. <https://doi.org/10.1016/j.tifs.2017.05.006>
- Singh, M.N., Hemant, K.S.Y., Ram, M., Shivakumar, H.G., 2010. Microencapsulation: A promising technique for controlled drug delivery. *Res Pharm Sci* 5, 65–77.



- Singh, V., Mishra, A.K., 2015. White Light Emission from Vegetable Extracts. *Sci Rep* 5, 1–9.  
<https://doi.org/10.1038/srep11118>
- Speciale, A., Canali, R., Chirafisi, J., Saija, A., Virgili, F., Cimino, F., 2010. Cyanidin-3-O-glucoside Protection against TNF- $\alpha$ -Induced Endothelial Dysfunction: Involvement of Nuclear Factor- $\kappa$ B Signaling. *J. Agric. Food Chem.* 58, 12048–12054.  
<https://doi.org/10.1021/jf1029515>
- Sygouni, V., Pantziaros, A.G., Iakovides, I.C., Sfetsa, E., Bogdou, P.I., Christoforou, E.A., Paraskeva, C.A., 2019. Treatment of Two-Phase Olive Mill Wastewater and Recovery of Phenolic Compounds Using Membrane Technology. *Membranes* 9, 27.  
<https://doi.org/10.3390/membranes9020027>
- T. Diaz, J., Allen Foegeding, E., Ann Lila, M., 2020. Formulation of protein–polyphenol particles for applications in food systems. *Food & Function* 11, 5091–5104.  
<https://doi.org/10.1039/D0FO00186D>
- Tikekar, R.V., Pan, Y., Nitin, N., 2013. Fate of curcumin encapsulated in silica nanoparticle stabilized Pickering emulsion during storage and simulated digestion. *Food Research International* 51, 370–377. <https://doi.org/10.1016/j.foodres.2012.12.027>
- Wang, W.-D., Xu, S.-Y., 2007. Degradation kinetics of anthocyanins in blackberry juice and concentrate. *Journal of Food Engineering* 82, 271–275.  
<https://doi.org/10.1016/j.jfoodeng.2007.01.018>
- Wu, S., Tian, L., 2017. Diverse Phytochemicals and Bioactivities in the Ancient Fruit and Modern Functional Food Pomegranate (*Punica granatum*). *Molecules* 22, 1606.  
<https://doi.org/10.3390/molecules22101606>

- Yang, J., Xiao, Y.-Y., 2013. Grape Phytochemicals and Associated Health Benefits. *Critical Reviews in Food Science and Nutrition* 53, 1202–1225.  
<https://doi.org/10.1080/10408398.2012.692408>
- Young, S., Dea, S., Nitin, N., 2017. Vacuum facilitated infusion of bioactives into yeast microcarriers: Evaluation of a novel encapsulation approach. *Food Research International* 100, 100–112. <https://doi.org/10.1016/j.foodres.2017.07.067>
- Young, S., Nitin, N., 2019. Thermal and oxidative stability of curcumin encapsulated in yeast microcarriers. *Food Chemistry* 275, 1–7. <https://doi.org/10.1016/j.foodchem.2018.08.121>
- Yousefi, S., Emam-Djomeh, Z., Mousavi, S.M., 2011. Effect of carrier type and spray drying on the physicochemical properties of powdered and reconstituted pomegranate juice (*Punica Granatum L.*). *J Food Sci Technol* 48, 677–684. <https://doi.org/10.1007/s13197-010-0195-x>
- Zaidel, D.N.A., Sahat, N.S., Jusoh, Y.M.M., Muhamad, I.I., 2014. Encapsulation of Anthocyanin from Roselle and Red Cabbage for Stabilization of Water-in-Oil Emulsion. *Agriculture and Agricultural Science Procedia*, 2nd International Conference on Agricultural and Food Engineering (CAFE 2014) - New Trends Forward 2, 82–89.  
<https://doi.org/10.1016/j.aaspro.2014.11.012>
- Zhao, X., Ai, Y., Hu, Y., Wang, Y., Zhao, L., Yang, D., Chen, F., Wu, X., Li, Y., Liao, X., 2020. Masking the Perceived Astringency of Proanthocyanidins in Beverages Using Oxidized Starch Hydrogel Microencapsulation. *Foods* 9, 756.  
<https://doi.org/10.3390/foods9060756>

## Chapter 5

# Feasibility of encapsulating phenolic bioactive compounds in live cell carriers and characterization of microbial metabolism of encapsulated bioactive

### Abstract

This study aimed to develop an innovative encapsulation carrier based on live microbial cells to encapsulate bioactive compounds, convert the target compounds into active metabolites and release *in situ*. Overall, this study evaluated the encapsulation and biotransformation of bioactive compounds leveraging the intrinsic metabolic activities of microbial cells. Gram-positive skin commensal bacteria *Staphylococcus epidermidis* was studied as the model microcarrier to encapsulate curcumin as the model phenolic compound. Curcumin was encapsulated into live *S. epidermidis* cells via a pressure-facilitated process. The impact of the encapsulation process on the live cell carriers' viability and metabolomics profile was characterized by standard plate counting method and a metabolic capability measurement assay. The subsequent long-term growth of the cell carrier was also monitored using the same viable cell count and metabolic activity measurements. To better understand the physiological responses of cells to the intracellularly encapsulated curcumin, live cells exposed to extracellular curcumin (dispersed in the culture media) and deactivated cell carriers were also measured as control groups. In addition, representative metabolites of curcumin and the cell carriers' metabolomic profiles after encapsulation were identified

using HPLC-MS/MS. After encapsulation, 42% and 39% reduction of colony forming units and metabolic activities of the live cell carriers were observed. Cell carriers recovered and resumed growth after 2 hours of incubation when compared to control cells that did not go through the encapsulation process. This was further validated with growth curves monitored and measured in the span of 10 hours, which indicated that cells exposed to extracellular curcumin exhibited the longest lag time before reaching exponential growth and lowest maximum growth rate. The encapsulated curcumin content in live cell carriers decreased overtime, which, we hypothesized, was partially due to metabolism since the content in deactivated cell carriers remained constant. The hypothesis was validated with our tandem mass-spectrometry analysis, from which we detected intracellular as well as released extracellular curcumin metabolites. Different metabolomic profiles of cells depending on the localization of the phenolic compound were also observed. In conclusion, the results of this study signified the potential of leveraging microbial cells as a novel active encapsulation carrier to 1) convert target compounds into bioactive metabolites, and 2) release the functional metabolites *in situ*. Future studies might be conducted to validate the additional health benefits that the microcarrier may deliver.

## 5.1. Introduction

The skin microbiome has diverse class of microbes including bacteria, viruses and fungi (Grice and Segre, 2011). Together this complex community of microbes influences both the dermatological health and the immune status (Belkaid and Tamoutounour, 2016; Kali, 2015). Some of the microbes on a skin surface generate beneficial products such as antimicrobial peptides and immune modulating metabolites that attenuate skin disorders and deliver health benefits (Kali, 2015). As one of the most predominant and innocuous commensal species, *Staphylococcus epidermidis* has also been proposed to function as a probiotic bacterium on the skin (Keshari et al., 2019; Negari et al., 2021). For instance, some of the metabolites and peptides generated by *S. epidermidis* on the skin surface are known to benefit skin immune function as well as inhibit the growth of pathogens. *S. epidermidis* can metabolize carbon-rich molecules as prebiotics to yield short-chain fatty acids that can inhibit growth of pathogens such as *Staphylococcus aureus* (Huang et al., 2020), *Propionibacterium acne* (Wang et al., 2014) and *Cutibacterium acnes* (Yang et al., 2019). Similarly, 6-N-hydroxyaminopurine, a metabolite from *S. epidermidis*, was shown to selectively inhibit UV induced skin tumors in an animal model system (Nakatsuji et al., 2018).

The biological activity of a probiotic bacteria can be significantly influenced by prebiotic compounds that can be delivered by exogenous or endogenous sources (Grimoud et al., 2010; Krutmann, 2009). In general, the prebiotics compounds are metabolized by the probiotic bacteria and transformed into bioactive metabolites that are beneficial to the host (Krutmann, 2009). Delivery and co-localization of the prebiotic with the target bacteria are prerequisite conditions for the biochemical transformation of the prebiotic compounds by the target bacteria. To date, most of the research studies evaluating potential interactions between prebiotic and probiotic interactions often incubate the bacteria cells at a relatively high concentration with compounds of

interest under controlled and nutrient rich conditions (Gopal et al., 2001; Grimoud et al., 2010). These conditions do not resemble the physiological environment on the skin surface i.e. naturally dry, salty, acidic and nutrient-poor conditions and do not address the challenges with co-localization of the prebiotics with probiotic bacteria on a skin surface or other target anatomical sites.

One possible solution is to physically combine the selected compound and the bacteria into a single formulation, which can be delivered to the target site and promote generation of the desirable metabolites. Infusion or incorporation of exogenous compounds in bacterial cells can be an approach to develop a formulation that combines bacteria and target compounds. Related to this concept, prior studies have demonstrated encapsulation of bioactive compounds in inactivated microbial cells and cell lysates (Pham-Hoang et al., 2013; Young et al., 2020). However, to the best of our knowledge none of the prior studies have demonstrated infusion or encapsulation of exogenous in live bacterial cells and generation of metabolites based on the metabolic activity of cells.

The current study explored the potential of live microbial cells as encapsulation carriers to leverage their inherent functionalities in metabolizing intracellular compounds into bioavailable and functional metabolites. Thus, this study was aimed to evaluate microencapsulation and metabolism of a model phenolic compound in a live bacterial carrier. *Staphylococcus epidermidis* was selected as a live cell carrier. *S. epidermidis* is known as a Gram-positive staphylococcus and is one of the five significant microorganisms that are located on human skin and mucosal surfaces (Namvar et al., 2014). This strain was chosen to mimic the application of bioactive compounds on skin and their subsequent bioconversion by skin microflora *in-vitro*. Live cell carriers could potentially overcome challenges associated with the lack of specific microflora, or the physico-biochemical constraints that may interaction between the microflora

and the target compounds. Curcumin was selected in this study for its topical functionalities such as anti-inflammatory (Agrawal et al., 2014) and anti-microbial activities (Liu and Huang, 2012). In addition, the biotransformation of curcumin has been proposed to be crucial for curcumin bioactivities (Scazzocchio et al., 2020). A vacuum-facilitated process was applied to encapsulate curcumin in the *S. epidermidis* cells (Young et al., 2017). To characterize the impact of encapsulation on the live cell carriers' viability and metabolism level, microbial population and metabolic capacity were measured based on the standard plate counting and the established MTT assay respectively. The long-term impact on the cell carrier growth was also monitored and measured using the same plate counting and MTT protocols. Two control groups were included in this study and compared to live cells with intracellularly encapsulated curcumin: 1) live cells exposed to extracellular curcumin dispersed in a culture media, and 2) deactivated cell carriers (to control for potential degradation of curcumin under the incubation conditions). Furthermore, representative metabolites of curcumin and the cell carriers' metabolomic profiles after encapsulation were identified using HPLC-MS/MS. To the best of our knowledge, no prior study has evaluated live cells as active encapsulation carriers. The metabolomic response and *in-situ* release of produced metabolites when the commensal cells are exposed to extracellular vs. intracellular (encapsulated) bioactive compounds have not previously been studied.

## **5.2. Material and Method**

### **5.2.1. Material**

Curcumin derived from *Curcuma longa* (Turmeric) ( $\geq 65\%$ , HPLC grade from Sigma), Tryptic Soy Agar/Broth (TSA/TSB), phosphate buffered saline (PBS, Fisher BioReagents), Thiazolyl Blue Tetrazolium Bromide (MTT; Sigma, M2128)

### **5.2.2. Bacterial strains and growth**

The Gram-positive bacterium *S. epidermidis* (ATCC 35984) was selected as the model human skin commensal bacteria. The liquid nitrogen stock was streaked onto TSA plates and incubated at 37°C overnight. Before experiments, single colonies were picked from the plate, cultured in TSB and incubated at 37°C aerobically with agitation at 250 rpm overnight. The cell density of the overnight culture was around 10<sup>9</sup> cfu/ml. To prepare inactivated cells as control groups, bacteria cells were incubated with 70% ethanol for 30 min and immediately centrifuged after to remove the ethanol. The pellet was then reconstituted using PBS to original volume.

### **5.2.3. Encapsulation of curcumin into bacterial carriers via vacuum infusion**

After being centrifuged and washed with sterile PBS once, the overnight culture was resuspended in 4.75 ml PBS and combined with 0.25 ml curcumin solution in ethanol. Encapsulation was performed by using a patent pending pressure facilitated infusion approach. The vacuum infusion takes around 5 min, followed by a 10-min incubation in dark. The cell pellet was then centrifuged at 11,000 rpm for 10 min to remove excess compound and washed using sterile PBS for 3 times.

### **5.2.4. Incubation of encapsulated bacterial carriers**

To measure growth curves and curcumin content, 250 ml culture flasks containing 100 ml TSB was incubated with the prepared overnight culture or encapsulated cells with the initial OD<sub>600</sub> around 0.07. The flasks were incubated aerobically at 37°C with agitation at 250 rpm. 1ml samples were taken every 1 hr for a period of up to 12 hr and the cell pellet was collected by centrifuge 11,000 rpm for 2 min.

Growth curve fitting of viable count data was performed using DMFit (the same model also available via <https://www.combase.cc>) to measure growth parameters including lag time and the maximum growth rate (Baranyi and Roberts, 1994). When using DMFit to fit the growth curve,



late-stationary phase time points after 10 hr incubation were excluded to prevent model distortion (Rolfe et al., 2012).

#### 5.2.4.1. Characterization of encapsulated curcumin

Curcumin in the cell pellet was extracted using methanol with bead beating at 6.0 m/s, 40 s for 3 cycles (FastPrep-24™ 5G Instrument, MP Biomedicals). The curcumin absorption was measured using the UV spectrometry (Genesys™ 10 UV-Vis Spectrophotometer, Thermo Scientific) at 425 nm and quantified through a standard curve prepared from curcumin methanol solution ( $R^2 = 0.99$ ).

#### 5.2.4.2. Metabolic activity assay

The metabolic activity of the bacteria encapsulation carriers was measured using MTT assay. The protocol was adopted from previous studies with slight modifications (Tada et al., 1986). 5 mg/mL Thiazolyl Blue Tetrazolium Bromide was dissolved in 1x PBS with vigorous vortex. The solution was then filtered through 0.2  $\mu$ m sterile filters to remove crystals and sterilize. The solution was made fresh before experiments. For measurements, 100  $\mu$ L cell suspension of samples were added to 96-well plates. 20  $\mu$ L MTT solution was added to each well and the plate was incubated at room temperature for 4 hours. 10 % SDS solution was then added and incubate o/n at 37 °C to dissolve the crystals. The absorbance was read at 570 nm, the background absorbance at 690 nm was read and subtracted.

### 5.2.5. Metabolomics analyses

#### 5.2.5.1. Sample preparation

The overnight *S. epidermidis* culture was prepared according to the protocol described in section 1.2. After centrifuged at 11,000 rpm for 5 min to remove the overnight media, the culture was reconstituted to original volume with new culture media and used in following analyses. Samples of the control group was kept at 37°C. For the first experiment group, the bacteria cells

were encapsulated with curcumin and incubated for 3 hours to allow potential bacterial reaction and metabolization. For the second experiment group, extracellular curcumin was added to the culture medium and incubated for 3 hours. The concentration was calibrated to be consistent with the curcumin concentration of the suspension of encapsulated cells, which was calculated to be 0.0527 mg/ml in this experiment based on the quantified encapsulation efficiency. The samples were then collected in cryotubes at 1 mL and centrifuged at 11,000 rpm for 10 min. The cell and culture medium were then separated and snap frozen in liquid nitrogen for following analyses.

#### 5.2.5.2.HPLC-MS/MS analyses

An untargeted metabolomics analyses was carried out to understand the cell carrier's potential metabolization of encapsulated compound and the differences compared to extracellular presence of the compound. TripleTOF® 6500 Quadrupole Time-Of-Flight mass spectrometer (Sciex) coupled with Sciex MicroLC was used to identify the metabolite profile produced by cell carriers both intracellularly and extracellularly. MS detection was carried out in 6 replicates. A 200  $\mu\text{m}$  x 0.5 mm trap column and a 75  $\mu\text{m}$  x 15 cm analytical column (ChromXP C18-CL, 3  $\mu\text{m}$ , 120Å; Sciex) were used. The mobile phases were 0.1% formic acid in water (A) and 0.1% formic acid in acetonitrile (B). A flow rate was 300 nL/min. LC gradient elution condition was initially 5% B to 30% B (90 min) and 80% B (95–105 min). The electrospray ionization was performed in both positive and negative ion modes. The mass spectra were acquired from 1000-8000 m/z with an accumulation time of 0.1 s in high sensitivity mode. Exclusion time was 20 s. The injection volume was 0.4  $\mu\text{L}$  and the resuspension volume was set to 100  $\mu\text{L}$ . The source parameters were optimized to obtain reproducible mass data. The complete data processing was performed with MS-Dial 2.70 software.

#### 5.2.5.3.Partial least square discriminant analysis for HPLC-MS/MS results

HPLC-MS output of intracellular and extracellular metabolomics profiles was respectively processed using the open source package sklearn, PLSRegression in python (v3.6.3). The PLS-DA model were constructed using the in-house scripts. The covariance confidence ellipse was plotted using the open source package matplotlib (v3.3.2) with p-value  $\leq 0.05$ .

### 5.2.6. Other statistical analyses

ANOVA and the post-hoc Tukey's Honestly Significant Difference (HSD) tests were performed using the GraphPad Prism software V.7.0a (Graphpad Software, Inc., La Jolla, CA). Experiments were performed in triplicates. The significant differences between treatments were determined through one-way ANOVA with significance level at p-value  $< 0.05$  unless stated otherwise.

## 5.3. Result and Discussion

### 5.3.1. Effect of encapsulation on the metabolic activities of live cell carriers

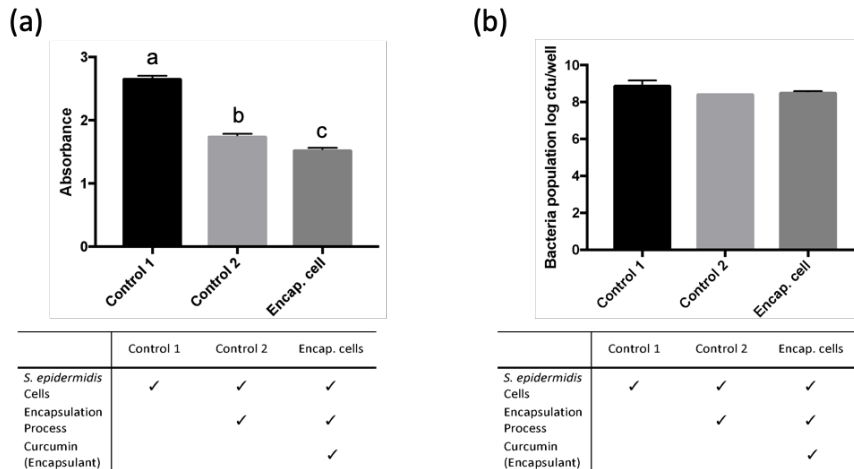


**Figure 5.1** (a) Metabolic activity and (b) bacterial population of control groups and encapsulated cells. Absorbance in (a) was measured at  $\lambda = 590$  nm as part of the MTT assay; letters indicate statistically significant difference among the groups ( $p < 0.05$ ) based on Tukey's test.

Both the viability and metabolic activity of live cells after the encapsulation of a target compound are essential for its function as a metabolically active encapsulation carrier. Curcumin, as a model polyphenolic compound in this study, was encapsulated into alive *S. epidermidis* cells with a pressure-assisted technique as we have demonstrated in a previous study (Young et al., 2017). In order to assess effect of the encapsulation process and the encapsulated compound on the selected cell carrier, microbial metabolic activity and viability were characterized using the MTT assay and the standard plate counting method respectively as described in the material and methods section. The MTT assay evaluates the metabolic activity of living cells (Chacon et al., 1997). In this assay tetrazolium component (MTT) is reduced into a colored and an insoluble formazan product by the mitochondria of viable cells (Mahajan et al., 2012). The plate counting method quantifies the total viable cell population including viable but metabolically-inhibited cells. Besides one-way ANOVA which reflects the overall significant differences among the treatments, Tukey's HSD test was carried out to enable pairwise comparisons.

As observed in Figure 1(a), the encapsulation process including brief exposure to negative pressure and 5% ethanol without the compound itself reduced the metabolic activity of bacterial cells (*control 2*) as compared to the *control 1* by approximately 34% (Tukey HSD p-value = 0.001). The cells encapsulated with curcumin (*Encap. cells*) exhibited the lowest metabolic activity among the samples, with an overall decrease in metabolic activity of approximately 42% compare to the *Control 1* (Tukey HSD p-value = 0.001). This decrease in metabolic activity of the Encap cells was also statistically significant compared to the *Control 2* (Tukey HSD p-value = 0.001). Consistent with the MTT assay results, around 32% and 39% of the cell carriers were not able to form colonies after encapsulation (*Control 2*) and after encapsulation with Curcumin (*Encap. cells*) (Figure 1(b)). On a log scale in Figure 1(b), the number of viable cells decreased

by less than 1 log CFU/sample due to the encapsulation process and encapsulation of curcumin using the vacuum infusion process. These results indicated that the inhibition of cellular activity was mainly caused by the negative pressure assisted encapsulation process and brief exposure to 5% ethanolic solution. Overall, Figure 1 demonstrated that the encapsulation process and the encapsulant curcumin reduced the metabolic activities and bacterial population counts but preserved viability of majority of the bacterial cells. To the best of our knowledge, none of the prior studies have evaluated potential of using live bacteria cells as an active encapsulation system that may generate metabolites from the encapsulated compounds. For achieving this goal, both the viability and metabolic activity of bacterial cells is critical. Using live microbial cells as encapsulation carrier can provide unique opportunities to enhance both the co- delivery of bioactives and bacterial cells as often both bacteria and compounds are needed to generate beneficial metabolites (Grimoud et al., 2010). This approach can also have potential applications as a pro-drug carrier. In this approach, pro-drug form of the compound is encapsulated in live cells and delivered to the target site with the bacteria, which then metabolizes and releases the active form of the drug.

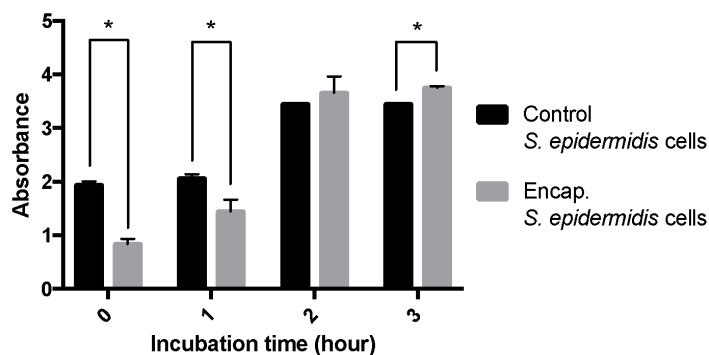


**Figure 5.2** Metabolic activity of encapsulated cell carriers and control groups measured at  $\lambda = 590$  nm as part of the MTT assay with 3 hours incubation at 37 °C. Within each

incubation time, the symbol \* indicates statistically significant differences between control and encap. cells ( $p < 0.05$ ).

In order to further examine the reduction of the cell carrier's metabolic activity after encapsulation, we incubated the encapsulated cells in fresh culture media for up to 3 hours and measured the metabolic activity with the MTT assay at an interval of one-hour. Cells without going through the encapsulation were used as the control and the OD<sub>600</sub> of the experiment and the control groups were calibrated to ensure the same level of cell density at the starting point ( $\sim 10^9$  cfu/ml). At the beginning of the incubation time with media, the encap. cells showed significantly lower metabolic activity compared to the control group (Figure 2), which is consistent with the observations from Figure 1. With an increase in incubation time, the cells with encapsulated curcumin showed gradually elevated metabolic activity and recovered their metabolic activity within 2 hours of incubation. This result further validated our prior observation and demonstrated that the encapsulation process and the encapsulated compound deterred the microbial metabolism and only partially decreased bacterial population for a short period of time ( $< 2$  hours), potentially due to a cellular damage resulting from the encapsulation process. After 2 hours of incubation the cells recovered from the stress and regained their metabolic activity.

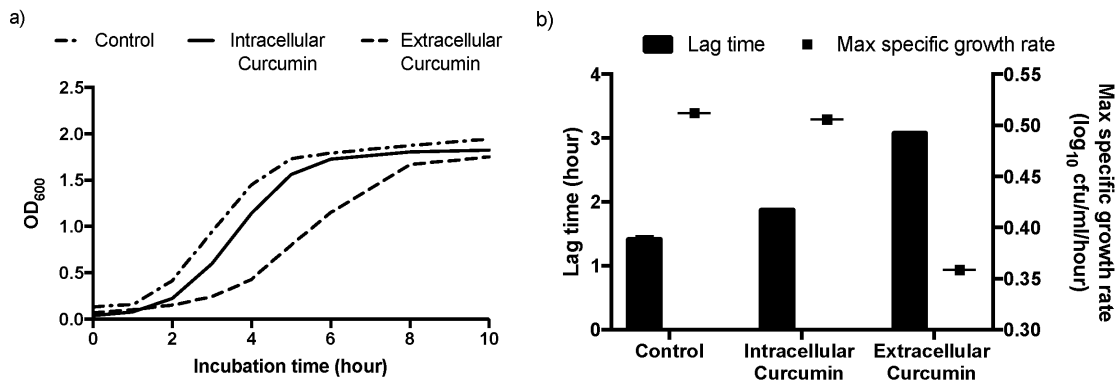


**Figure 5.3** a) Representative growth curves and b) the growth parameters obtained from the Baranyi growth model for: natural cells without encapsulation (*Control*), cell carriers encapsulated with curcumin (*Intracellular Curcumin*), and cell carriers incubated with extracellular curcumin (*Extracellular Curcumin*). The cell densities were measured by absorbance at  $\lambda = 600$  nm (OD<sub>600</sub>) through the 10-hour incubation at 37 °C with agitation.

To characterize growth potential of bacterial cells after encapsulation of curcumin and to compare the influence of localization of curcumin in bacterial cells, the growth of bacterial suspension cultures with and without encapsulated curcumin and with cells incubated with extracellular curcumin was measured. The growth parameters including the lag time and the maximum growth rate were obtained by fitting the growth curve in Figure 3b) using the well-established cell growth kinetic model as described in the Methods section (Baranyi and Roberts, 1994). The curve fit to the selected model had a R<sup>2</sup> greater than 0.99, indicating a good fit.

As observed in Figure 3, the control group had a lag time of 1.42 hours and the highest max specific growth rate at 0.51 log<sub>10</sub> CFU/mL/hour, consistent with prior observations that have reported a short lag time of less than 2 hours for *Staphylococci* (Jonas et al., 2018). Cells incubated with extracellular curcumin had the longest lag time of 3.09 hours before reaching an exponential growth phase, which is also reflected by the lowest maximum specific growth rate at

0.36 log<sub>10</sub> CFU/mL/hour. In comparison, the growth of cells with intracellular curcumin was only moderately inhibited, demonstrating an average lag time of 1.88 hour and maximum specific growth rate of 0.50 log<sub>10</sub> CFU/mL/hour. The lag times of the three groups and the maximum specific growth rates showed statistically significant variation with a confidence level at 0.99 (p-value < 0.01).

Influence of curcumin on microbial metabolism and viability has been evaluated in various previous studies and has been recently summarized in a review (Praditya et al., 2019). Based on the literature, diverse mechanisms have been proposed. For example, Tyagi et al. demonstrated that exposure to curcumin can cause membrane leakage in both the Gram-positive and Gram-negative bacteria and can inhibit the growth of bacteria (Tyagi et al., 2015). In the case of *Bacillus subtilis*, antibacterial activity of curcumin was attributed to inhibition of bacterial cell proliferation by blocking the assembly of FtsZ in the Z ring that has a vital role in cell division (Rai et al., 2008). Incubation with curcumin was also shown to influence virulence, quorum sensing and other infective activities of *Pseudomonas aeruginosa* (Rudrappa and Bais, 2008). Overall, these trends support the inhibitory activity of extracellular curcumin as observed in Figure 3.

However, the different patterns in the microbial growth and activities between cells loaded with intracellular curcumin and cells exposed to extracellular curcumin suggested that the encapsulation process might have affected and altered the interactions between the compound and the alive cell carriers, which dampened the antibacterial effect of the compound. This could be attributed to a range of factors. For example, Mun et al. previously confirmed the binding of curcumin with peptidoglycan, the key component of gram-positive bacteria's cell wall. The binding might cause interruption of cell wall and damage to the cytoplasmic membrane as illustrated by transmission electron microscopic images (Mun et al., 2014). Existing evidence



also suggested that curcumin's binding to lipid bi-layer, which changed the properties of host cell membranes (e.g. membrane-thinning effect) and might affect the functions of membrane proteins (Hung et al., 2008). The encapsulation process might have expedited the passing-through of the compounds through the cell wall and plasma membrane, reduced the time for curcumin to bind and disturb the cellular structure. Once localized within the cell, curcumin as a moderately hydrophobic compound might bind to intracellular compartments due to its affinity for lipid membranes. This might hinder normal growth of the cells imminently after the compounds were present within the cells, but curcumin's antibacterial actions against cell wall and plasma membrane might be attenuated by the pressure-facilitated encapsulation process, which led to a less-inhibited growth indicated by the Intracellular Curcumin curve in Figure 3. More comprehensive studies in the future are necessary to elucidate pathways for the uptake of encapsulated compound in active microbes, which is essential for future development of alive cell carriers for food and biomedical applications.

### 5.3.2. Fate of curcumin in live cell carriers

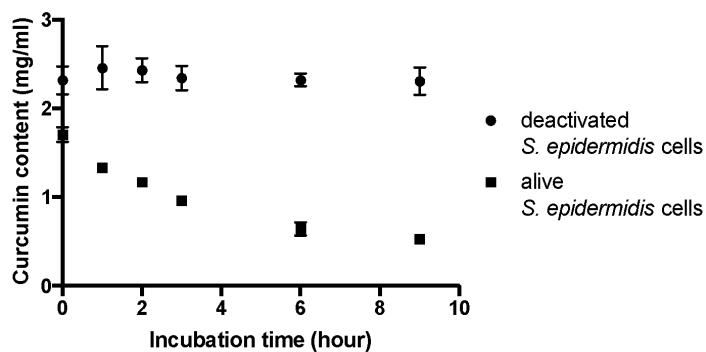


**Figure 5.4** The decay of intracellular curcumin occurred with alive cell carriers.

The intracellular curcumin content in cells as a function of incubation time in a cell culture media was quantified using UV-Vis spectrometry. Deactivated cells were used as the control

group to examine potential influence of chemical reactions such as degradation or hydrolysis of encapsulated curcumin in cells. Changes in the concentration of extracted curcumin from live cells and deactivated cells as a function of incubation time was measured using a UV-Vis spectrometer at a wavelength of 425 nm. The absorbance measurement was converted to an equivalent concentration of curcumin in the cell suspension based on a standard curve prepared with a curcumin standard in a methanolic solution. Results in Figure 4 show that only 31% of the encapsulated curcumin was remaining in the cells after 9-hour incubation in live cells, while around 90% of the original compound was retained in the deactivated cells.

### 5.3.3. Metabolomics analyses of the live cell carrier

Incubation Condition	Metabolite Localization	Curcumin	Tetrahydro-curcumin	Bisdemethoxy-curcumin
		Max – Min Spectrum Peak Height ( $\square 10^3$ Unit of Absorbance)		
Intracellular Curcumin	Intracellular	781 - 910	42 - 54	30 - 37
	Extracellular	7 - 52	-	-
Extracellular Curcumin	Intracellular	414 - 557	32 - 33	3 - 8
	Extracellular	-	34 - 45	-

**Table 5.1** Curcumin and representative metabolites identified in cell carriers exposed to either intracellular curcumin or extracellular curcumin using HPLC-MS/MS. The compounds were semi-quantified using the MS/MS spectrum peak height, and the ranges (min – max,  $10^3$  unit of absorbance) of triplicate measurements were shown in the table. The limit of detection (LOD) was calculated as three times the standard deviation of triplicate blank measurements, and the compounds with mean value below LOD were labeled as “-” in the table.

Metabolism and bio-transformation of the encapsulated compound in the live cell carriers can be one of the key reasons for the decay of encapsulated curcumin in cell-based carriers. The bio-transformation may be desired in certain applications as the metabolites generated by the bacterial cells can have enhanced bioactivities in some cases (Scazzocchio et al., 2020). For characterizing influence of the cellular metabolism on the fate of encapsulated compound in live cell carriers and influence of the encapsulated compound on the cells, an un-targeted metabolomic analysis approach using a high-performance liquid chromatography coupled with tandem mass spectrometry (HPLC-MS/MS) platform based on a described protocol in the Material and Method section. Curcumin metabolites were identified using a mass-based search followed by manual verification. The semi-quantitative comparison was achieved based on peak heights in the mass spectrograph. The control cells and cells incubated with the extracellular curcumin were analyzed using the same approach. The limit of detection (LOD) was calculated as three times the standard deviation of triplicated blank measurements. This is one of the common methods to determine the detection limit based on detector response of target compounds from blank samples (Indrayanto, 2018).

As illustrated in Table 1, the MS/MS analysis identified remaining curcumin and key curcumin metabolites produced by cell carriers. Cells encapsulated with curcumin maintained a higher intracellular concentration of curcumin than the cells incubated extracellularly with the same concentration of curcumin (52.7  $\mu\text{g/ml}$ ). This difference in the concentration may be

attributed to the efficiency of vacuum infusion process to rapidly (~5-10 s) infuse curcumin in cells compared to the passive binding and diffusion of curcumin during an extended incubation time for 3 hours. Low concentration (10-100 fold lower than the curcumin concentration in the cells) of extracellular curcumin was only observed for the cells encapsulated with curcumin. This suggest some passive release of curcumin from the cells during incubation. This release may result during cell division and other cellular process. However, in contrast to these results, there was no significant detection of extracellular curcumin in the samples of cells incubated with curcumin. This lack of detection could be due to hydrolysis of curcumin in the media during extended incubation. Curcumin is highly susceptible to hydrolysis at the pH of 7.2, with 90% decomposed in less than 30 min (Wang et al., 1997). This result also suggest that the sustained, low concentration of extracellular curcumin released from cells infused with curcumin is partially protected from hydrolysis. This could result due to complexation with cellular components such as proteins.

The other key curcumin metabolites identified in this study include tetrahydrocurcumin and bisdemethoxycurcumin. The pathways for synthesizing these metabolites have been identified and the reactions for their synthesis are mostly mediated by nicotinamide adenine dinucleotide phosphate (NADPH)-dependent curcumin/dihydrocurcumin reductase (Hassaninasab et al., 2011). The levels of these metabolites generated by bacterial cells were a function of the incubation condition, i.e. cells infused with curcumin vs. cell incubated with extracellular curcumin. Tetrahydrocurcumin was generated by both incubation conditions with encapsulated curcumin and cells incubated with extracellular curcumin. For the cells with encapsulated curcumin, the metabolite was localized mostly in the intracellular fraction, whereas cells incubated with extracellular curcumin showed existence of the compound both intracellularly and extracellularly. Bisdemethoxycurcumin was predominantly produced intracellularly by the

cells with encapsulated curcumin and was not detected in the extracellular media for both the incubation conditions. Overall, these observations suggested that the role of the localization of the bioactive compound in influencing the metabolism of the selected compound by bacterial cells. Future studies may be designed to link cellular metabolism with the intracellular localization of bioactive compounds and metabolic state of cells. These studies may also include comprehensive understanding of the metabolic pathways including the expression of key metabolic enzymes. The metabolic transformation of curcumin by human microbiota has been proposed to generate many active metabolites with properties such as anti-oxidation and anti-inflammation (Scazzocchio et al., 2020). For instance, as one of the major metabolites from curcumin, tetrahydrocurcumin has been extensively investigated for its bioactivity and compared with curcumin. Studies showed that tetrahydrocurcumin exhibits higher antioxidant activity than curcumin (Somparn et al., 2007), and has superior activity for suppressing lipid peroxidation (Pari and Murugan, 2007) and carcinogenesis (Lai et al., 2011). More importantly, these observations indicate the potential to produce target metabolites based on the interaction between the live cell carrier and the target compounds. Future studies could be carried out to further advance knowledge of the bio-transformation pathways and influence of the incubation environment.

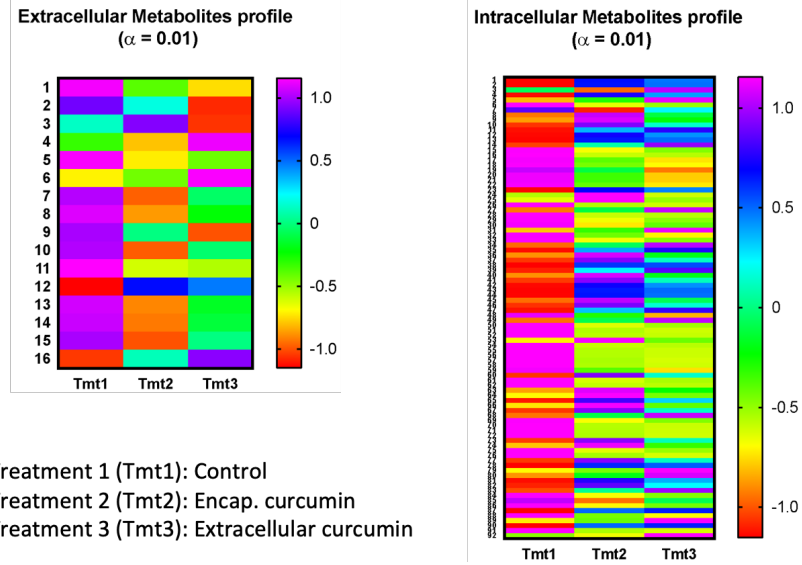


**Figure 5.5** 16 extracellular metabolites and 92 intracellular metabolites with concentrations that are statistically significantly different among the three treatments (p-value < 0.01), produced by the live *S. epidermidis* cells. The metabolites content was calculated as the mean of triplicated measurements and visualized after scaling normalization (subtracted with the mean content of all metabolites included in the figure within each treatment and divided by the maximum content of the most abundant metabolites within the treatment).

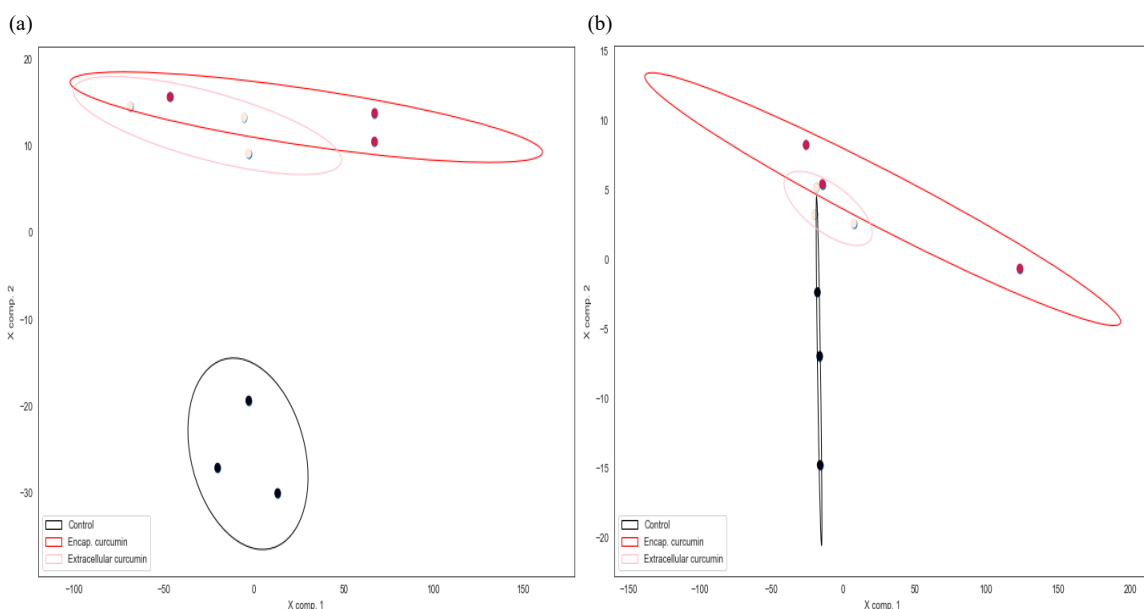


**Figure 5.6** Scatter plot of the overall (a) intracellular metabolomics and (b) extracellular metabolomics profile of live *S. epidermidis* cells encapsulated with curcumin (circles in red), in comparison with control groups (circles in black) and cells incubated with extracellular curcumin (circles in pink). Partial least square discriminant analysis was performed on a total of 3332 metabolites and 95% confidence ellipses were shown in the graph to investigate and visualize the profiles between treatments.

In addition to bio-transformation of curcumin by cells, curcumin and its metabolites can also significantly influence the overall metabolomic profiles of the cell carriers. Figure 5 illustrates 16 extracellular metabolites and 92 intracellular metabolites with concentrations that are statistically different among the three treatments ( $p$ -value  $< 0.01$ ): control cells (Tmt1), cells with encapsulated curcumin (Tmt2), and cells incubated with extracellular curcumin (Tmt3). In order to visualize the differences among the profiles, metabolite content (quantified using MS/MS spectrum peak height) was transformed using scaling normalization and plotted in the form of heatmaps. The scaling normalization was performed by subtracting each metabolite relative

concentration level from the mean concentration level of the selected metabolites included in Figure 5 for each of the treatments and dividing the resulting difference by the maximum relative concentration level for the selected metabolites. The results in the Figure 5 show that compared to the control group, treatment groups Tmt 2 and 3 have significantly reduced levels of metabolites in both the intracellular and extracellular compartments for majority of the compounds. The only exception was observed for few metabolites whose levels increased in the treatment groups compared to the controls. In those cases, the compounds were not expressed in control cells or at relatively low levels. This trend agrees with the reduction in metabolic activity of the cells in the presence of curcumin as measured using the MTT assay. This reduction may be induced by the growth inhibitory properties of curcumin (Liu and Huang, 2012).

Figure 6 presents the evaluation of the overall changes in the metabolic profile of cells induced by different treatments in this study. Partial least square discriminant analysis (PLS-DA) has been widely used to characterize and distinguish metabolic processes in metabolomics studies (Kalivodová et al., 2015; Worley and Powers, 2013). In this study, the comprehensive metabolic profile of more than 3300 identified as intracellular and extracellular metabolites for the Tmt1, Tmt2 and Tmt3 were respectively analyzed using the PLS-DA algorithm, and the relationships among the metabolic activities of the live cell carriers under different treatments were demonstrated with confidence ellipse plots in Figure 6.

Overall, Figure 6 (a) indicated that intracellular metabolite profile of the two treatment groups that were exposed to curcumin were statistically different compared to the control group ( $p$ -value  $< 0.05$ ). In addition, the profiles of the treatments overlapped and moved to the same direction in the graph as compared to the control group. These observations demonstrated that cell carriers with encapsulated curcumin and cell carriers incubated with extracellular curcumin induced similar metabolic responses in the cell carriers. Future research may be designed to



analyze and determine the intracellular and extracellular metabolic profile of different cell carriers under different environment, culture conditions and encapsulated compounds. Based on this understanding, genetic modifications might be applied to modify the cell carrier's metabolic properties and enable cell carriers to produce target molecules and their release *in-vivo*.

## **Conclusion**

In summary, this study demonstrated a novel encapsulation carrier - live bacterial microcarriers that could encapsulate bioactive compounds and remain viable, convert the compound into active metabolites in subsequent incubation and release the metabolites *in situ*. After the model phenolic compound curcumin was encapsulated into live *S. epidermidis* cells, the cells retained viability and metabolic activities, recovered and resumed growth after 2 hours from the encapsulation process. Curcumin encapsulated in live cells decreased overtime, and major metabolites of curcumin including tetrahydrocurcumin and bisdemethoxycurcumin were observed both intracellularly and extracellularly. The cell carrier also responded to intracellularly encapsulated curcumin versus extracellular curcumin with different metabolomic profiles. Overall, this study has shown the potential of live cell carriers as active encapsulation capsules that can convert encapsulated compounds and deliver the metabolites *in situ*. Future research could be carried out to: 1) selectively modify the metabolism with bioengineering techniques to achieve target transformation and 2) understand and utilize the additional health benefits of the live microcarrier.



## Reference

- Agrawal, R., Sandhu, S.K., Sharma, I., Kaur, I.P., 2014. Development and Evaluation of Curcumin-loaded Elastic Vesicles as an Effective Topical Anti-inflammatory Formulation. *AAPS PharmSciTech* 16, 364–374. <https://doi.org/10.1208/s12249-014-0232-6>
- Baranyi, J., Roberts, T.A., 1994. A dynamic approach to predicting bacterial growth in food. *International Journal of Food Microbiology, Special Issue Predictive Modelling* 23, 277–294. [https://doi.org/10.1016/0168-1605\(94\)90157-0](https://doi.org/10.1016/0168-1605(94)90157-0)
- Belkaid, Y., Tamoutounour, S., 2016. The influence of skin microorganisms on cutaneous immunity. *Nat Rev Immunol* 16, 353–366. <https://doi.org/10.1038/nri.2016.48>
- Chacon, E., Acosta, D., Lemasters, J.J., 1997. 9 - Primary Cultures of Cardiac Myocytes as In Vitro Models for Pharmacological and Toxicological Assessments, in: Castell, J.V., Gómez-Lechón, M.J. (Eds.), *In Vitro Methods in Pharmaceutical Research*. Academic Press, San Diego, pp. 209–223. <https://doi.org/10.1016/B978-012163390-5.50010-7>
- Choudhury, A.K., Raja, S., Mahapatra, S., Nagabhushanam, K., Majeed, M., 2015. Synthesis and Evaluation of the Anti-Oxidant Capacity of Curcumin Glucuronides, the Major Curcumin Metabolites. *Antioxidants* 4, 750–767. <https://doi.org/10.3390/antiox4040750>
- Gopal, P.K., Sullivan, P.A., Smart, J.B., 2001. Utilisation of galacto-oligosaccharides as selective substrates for growth by lactic acid bacteria including *Bifidobacterium lactis* DR10 and *Lactobacillus rhamnosus* DR20. *International Dairy Journal* 11, 19–25. [https://doi.org/10.1016/S0958-6946\(01\)00026-7](https://doi.org/10.1016/S0958-6946(01)00026-7)
- Grice, E.A., Segre, J.A., 2011. The skin microbiome. *Nature Reviews Microbiology* 9, 244–253. <https://doi.org/10.1038/nrmicro2537>

- Grimoud, J., Durand, H., Courtin, C., Monsan, P., Ouarné, F., Theodorou, V., Roques, C., 2010. In vitro screening of probiotic lactic acid bacteria and prebiotic glucooligosaccharides to select effective synbiotics. *Anaerobe* 16, 493–500.  
<https://doi.org/10.1016/j.anaerobe.2010.07.005>
- Hassaninasab, A., Hashimoto, Y., Tomita-Yokotani, K., Kobayashi, M., 2011. Discovery of the curcumin metabolic pathway involving a unique enzyme in an intestinal microorganism. *Proc Natl Acad Sci U S A* 108, 6615–6620. <https://doi.org/10.1073/pnas.1016217108>
- Huang, T.Y., Herr, D.R., Huang, C.-M., Jiang, Y., Huang, T.Y., Herr, D.R., Huang, C.-M., Jiang, Y., 2020. Amplification of probiotic bacteria in the skin microbiome to combat *Staphylococcus aureus* infection. *Microbiol. Aust.* 41, 61–64.  
<https://doi.org/10.1071/MA20018>
- Hung, W.-C., Chen, F.-Y., Lee, C.-C., Sun, Y., Lee, M.-T., Huang, H.W., 2008. Membrane-Thinning Effect of Curcumin. *Biophysical Journal* 94, 4331–4338.  
<https://doi.org/10.1529/biophysj.107.126888>
- Indrayanto, G., 2018. Chapter Five - Validation of Chromatographic Methods of Analysis: Application for Drugs That Derived From Herbs, in: Brittain, H.G. (Ed.), *Profiles of Drug Substances, Excipients and Related Methodology*. Academic Press, pp. 359–392.  
<https://doi.org/10.1016/bs.podrm.2018.01.003>
- Jonas, A.M., Glinel, K., Behrens, A., Anselmo, A.C., Langer, R.S., Jaklenec, A., 2018. Controlling the Growth of *Staphylococcus epidermidis* by Layer-By-Layer Encapsulation. *ACS Appl. Mater. Interfaces* 10, 16250–16259.  
<https://doi.org/10.1021/acsami.8b01988>
- Kali, A., 2015. Human Microbiome Engineering: The Future and Beyond. *J Clin Diagn Res* 9, DE01–DE04. <https://doi.org/10.7860/JCDR/2015/14946.6570>

- Kalivodová, A., Hron, K., Filzmoser, P., Najdekr, L., Janečková, H., Adam, T., 2015. PLS-DA for compositional data with application to metabolomics. *Journal of Chemometrics* 29, 21–28. <https://doi.org/10.1002/cem.2657>
- Keshari, S., Balasubramaniam, A., Myagmardoloonjin, B., Herr, D.R., Negari, I.P., Huang, C.-M., 2019. Butyric Acid from Probiotic *Staphylococcus epidermidis* in the Skin Microbiome Down-Regulates the Ultraviolet-Induced Pro-Inflammatory IL-6 Cytokine via Short-Chain Fatty Acid Receptor. *International Journal of Molecular Sciences* 20, 4477. <https://doi.org/10.3390/ijms20184477>
- Krutmann, J., 2009. Pre- and probiotics for human skin. *Journal of Dermatological Science* 54, 1–5. <https://doi.org/10.1016/j.jdermsci.2009.01.002>
- Lai, C.-S., Wu, J.-C., Yu, S.-F., Badmaev, V., Nagabhushanam, K., Ho, C.-T., Pan, M.-H., 2011. Tetrahydrocurcumin is more effective than curcumin in preventing azoxymethane-induced colon carcinogenesis. *Molecular Nutrition & Food Research* 55, 1819–1828. <https://doi.org/10.1002/mnfr.201100290>
- Liu, C.-H., Huang, H.-Y., 2012. Antimicrobial Activity of Curcumin-Loaded Myristic Acid Microemulsions against *Staphylococcus epidermidis*. *Chemical and Pharmaceutical Bulletin* 60, 1118–1124. <https://doi.org/10.1248/cpb.c12-00220>
- Mahajan, S.D., Law, W.-C., Aalinkeel, R., Reynolds, J., Nair, B.B., Yong, K.-T., Roy, I., Prasad, P.N., Schwartz, S.A., 2012. Chapter three - Nanoparticle-Mediated Targeted Delivery of Antiretrovirals to the Brain, in: Düzgüneş, N. (Ed.), *Methods in Enzymology, Nanomedicine*. Academic Press, pp. 41–60. <https://doi.org/10.1016/B978-0-12-391858-1.00003-4>

- Marczylo, T.H., Steward, W.P., Gescher, A.J., 2009. Rapid Analysis of Curcumin and Curcumin Metabolites in Rat Biomatrices Using a Novel Ultrapformance Liquid Chromatography (UPLC) Method. *J. Agric. Food Chem.* 57, 797–803. <https://doi.org/10.1021/jf803038f>
- Mun, S.-H., Kim, S.-B., Kong, R., Choi, J.-G., Kim, Y.-C., Shin, D.-W., Kang, O.-H., Kwon, D.-Y., 2014. Curcumin Reverse Methicillin Resistance in *Staphylococcus aureus*. *Molecules* 19, 18283–18295. <https://doi.org/10.3390/molecules191118283>
- Nakatsuji, T., Chen, T.H., Butcher, A.M., Trzoss, L.L., Nam, S.-J., Shirakawa, K.T., Zhou, W., Oh, J., Otto, M., Fenical, W., Gallo, R.L., 2018. A commensal strain of *Staphylococcus epidermidis* protects against skin neoplasia. *Science Advances* 4, eaao4502. <https://doi.org/10.1126/sciadv.aao4502>
- Namvar, A.E., Bastarahang, S., Abbasi, N., Ghehi, G.S., Farhadbakhtiarian, S., Arezi, P., Hosseini, M., Baravati, S.Z., Jokar, Z., Chermahin, S.G., 2014. Clinical characteristics of *Staphylococcus epidermidis*: a systematic review. *GMS Hyg Infect Control* 9. <https://doi.org/10.3205/dgkh000243>
- Negari, I.P., Keshari, S., Huang, C.-M., 2021. Probiotic Activity of *Staphylococcus epidermidis* Induces Collagen Type I Production through FFaR2/p-ERK Signaling. *International Journal of Molecular Sciences* 22, 1414. <https://doi.org/10.3390/ijms22031414>
- Pari, L., Murugan, P., 2007. Tetrahydrocurcumin prevents brain lipid peroxidation in streptozotocin-induced diabetic rats. *J Med Food* 10, 323–329. <https://doi.org/10.1089/jmf.2006.058>
- Pham-Hoang, B.N., Romero-Guido, C., Phan-Thi, H., Waché, Y., 2013. Encapsulation in a natural, preformed, multi-component and complex capsule: yeast cells. *Appl Microbiol Biotechnol* 97, 6635–6645. <https://doi.org/10.1007/s00253-013-5044-1>

- Praditya, D., Kirchoff, L., Brüning, J., Rachmawati, H., Steinmann, J., Steinmann, E., 2019. Anti-infective Properties of the Golden Spice Curcumin. *Front. Microbiol.* 10. <https://doi.org/10.3389/fmicb.2019.00912>
- Prasad, S., Tyagi, A.K., Aggarwal, B.B., 2014. Recent Developments in Delivery, Bioavailability, Absorption and Metabolism of Curcumin: the Golden Pigment from Golden Spice. *Cancer Res Treat* 46, 2–18. <https://doi.org/10.4143/crt.2014.46.1.2>
- Rai, D., Singh, J.K., Roy, N., Panda, D., 2008. Curcumin inhibits FtsZ assembly: an attractive mechanism for its antibacterial activity. *Biochemical Journal* 410, 147–155. <https://doi.org/10.1042/BJ20070891>
- Rolfe, M.D., Rice, C.J., Lucchini, S., Pin, C., Thompson, A., Cameron, A.D.S., Alston, M., Stringer, M.F., Betts, R.P., Baranyi, J., Peck, M.W., Hinton, J.C.D., 2012. Lag Phase Is a Distinct Growth Phase That Prepares Bacteria for Exponential Growth and Involves Transient Metal Accumulation. *Journal of Bacteriology* 194, 686–701. <https://doi.org/10.1128/JB.06112-11>
- Rudrappa, T., Bais, H.P., 2008. Curcumin, a Known Phenolic from *Curcuma longa*, Attenuates the Virulence of *Pseudomonas aeruginosa* PAO1 in Whole Plant and Animal Pathogenicity Models. *J. Agric. Food Chem.* 56, 1955–1962. <https://doi.org/10.1021/jf072591j>
- Scazzocchio, B., Minghetti, L., D'Archivio, M., 2020. Interaction between Gut Microbiota and Curcumin: A New Key of Understanding for the Health Effects of Curcumin. *Nutrients* 12, 2499. <https://doi.org/10.3390/nu12092499>
- Somporn, P., Phisalaphong, C., Nakornchai, S., Unchern, S., Morales, N.P., 2007. Comparative antioxidant activities of curcumin and its demethoxy and hydrogenated derivatives. *Biol Pharm Bull* 30, 74–78. <https://doi.org/10.1248/bpb.30.74>

- Tada, H., Shiho, O., Kuroshima, K. ichi, Koyama, M., Tsukamoto, K., 1986. An improved colorimetric assay for interleukin 2. *Journal of immunological methods* 93, 157–165. [https://doi.org/10.1016/0022-1759\(86\)90183-3](https://doi.org/10.1016/0022-1759(86)90183-3)
- Tyagi, P., Singh, M., Kumari, H., Kumari, A., Mukhopadhyay, K., 2015. Bactericidal Activity of Curcumin I Is Associated with Damaging of Bacterial Membrane. *PLoS One* 10. <https://doi.org/10.1371/journal.pone.0121313>
- Wang, Y., Kuo, S., Shu, M., Yu, J., Huang, S., Dai, A., Two, A., Gallo, R.L., Huang, C.-M., 2014. *Staphylococcus epidermidis* in the human skin microbiome mediates fermentation to inhibit the growth of *Propionibacterium acnes*: implications of probiotics in acne vulgaris. *Appl Microbiol Biotechnol* 98, 411–424. <https://doi.org/10.1007/s00253-013-5394-8>
- Wang, Y.-J., Pan, M.-H., Cheng, A.-L., Lin, L.-I., Ho, Y.-S., Hsieh, C.-Y., Lin, J.-K., 1997. Stability of curcumin in buffer solutions and characterization of its degradation products. *Journal of Pharmaceutical and Biomedical Analysis* 15, 1867–1876. [https://doi.org/10.1016/S0731-7085\(96\)02024-9](https://doi.org/10.1016/S0731-7085(96)02024-9)
- Worley, B., Powers, R., 2013. Multivariate Analysis in Metabolomics. *Curr Metabolomics* 1, 92–107. <https://doi.org/10.2174/2213235X11301010092>
- Yang, A.-J., Marito, S., Yang, J.-J., Keshari, S., Chew, C.-H., Chen, C.-C., Huang, C.-M., 2019. A Microtube Array Membrane (MTAM) Encapsulated Live Fermenting *Staphylococcus epidermidis* as a Skin Probiotic Patch against *Cutibacterium acnes*. *International Journal of Molecular Sciences* 20, 14. <https://doi.org/10.3390/ijms20010014>
- Young, S., Dea, S., Nitin, N., 2017. Vacuum facilitated infusion of bioactives into yeast microcarriers: Evaluation of a novel encapsulation approach. *Food Research International* 100, 100–112. <https://doi.org/10.1016/j.foodres.2017.07.067>



Young, S., Rai, R., Nitin, N., 2020. Bioaccessibility of curcumin encapsulated in yeast cells and yeast cell wall particles. *Food Chemistry* 309, 125700.

<https://doi.org/10.1016/j.foodchem.2019.125700>

Zhang, A., Sun, H., Wang, P., Han, Y., Wang, X., 2012. Modern analytical techniques in metabolomics analysis. *Analyst* 137, 293–300. <https://doi.org/10.1039/C1AN15605E>

Zhou, B., Xiao, J.F., Tuli, L., Resson, H.W., 2012. LC-MS-based metabolomics. *Mol Biosyst* 8, 470–481. <https://doi.org/10.1039/c1mb05350g>

## Chapter 6

### Conclusions and Future Studies

This research investigated the utilities of cell-based carriers for the encapsulation, delivery and transformation of bioactive compounds. Using yeast cell, yeast cell wall particle and bacterial cell as model encapsulation systems, the studies demonstrated the intrinsic functionalities of the cell carriers including encapsulation efficiencies, stabilization of bioactives under adverse conditions, and binding and controlled release at the target sites. Furthermore, a novel concept of live cell encapsulation carriers was developed for potential applications that requires *in situ* biotransformation of target compounds.

Based on the findings of this research, following research area and opportunities for future studies are warranted:

- Encapsulation of hydrophilic and hydrophobic compounds using cell carriers
  - Mechanistic understanding of the encapsulation and release process and key physico-chemical characteristics that influence the encapsulation process and efficiency with different cell carriers
  - Quantitative analysis and predictive modeling that predict the encapsulation process and efficiency using the microcapsules and optimize the encapsulation system and process for different target compounds and post-encapsulation applications

- *In vivo* studies of additional probiotic benefits of both inactive and active cell carriers and potential synergistic effects with the released encapsulated bioactives
- Encapsulation with live cell carriers
  - Targeted metabolomics studies that elucidate the synthesis pathway of target metabolites and incubation factors that impact the process
  - *In vivo* studies of the live carriers focusing on the production and delivery of target metabolites
  - Genetic modification of cell carriers to enable production of target molecules from the encapsulated compounds
  - Cell surface modifications that enabled additional functionalities including binding and homing properties with target cells or tissue
- Other application-based studies
  - Contextualized microencapsulation formulations and techniques for other compounds and cell carriers as part of other applications in food and biomedical industries